Anicet Pétillon

Sediment dynamics in the salt marshes of the Ria Formosa lagoon

2021

Anicet Pétillon

Sediment dynamics in the salt marshes of the Ria Formosa lagoon

Master in Marine and Coastal Systems

Work performed under the supervision of:

Dr. Ana Rita Zarco Carrasco
(Universidade do Algarve, CIMA)
And
Dr. Katerina Kompiadou
(Universidade do Algarve, CIMA)

UAlg FCT
UNIVERSIDADE DO ALGARVE
FACULDADE DE CIÊNCIAS E TECNOLOGIA

2021

Declaration of authorship of work

Sediment dynamics in the salt marshes of the Ria Formosa lagoon

Declaro ser o autor deste trabalho, que é original e inédito. Autores e trabalhos consultados estão devidamente citados no texto e constam da listagem de referências incluída.

I declare to be the author of this work, which is original and unpublished. Authors and works consulted are duly cited in the text and are included in the list of references.

Issy-les-Moulineaux (France), 28 de Outubro de 2021 _

Anicet Pétillon

Acknoledgement

First, I would like to thank my supervisors, Dr. Ana Rita Zarcos Carrasco and Dr. Katerina Kompiadou for allowing me to join this study. Thank you for your help, your patience, and your good humour during morning fieldwork.

I would also like to thank my professors from Marine and Coastal Systems for these two instructive years and the Centre for Marine and Environmental Research (CIMA) for hosting my internship and in particular Margarida da Conceição Pereira Ramires for the help during laboratory works.

My mother and my sister both deserve my gratitude for the unconditional support they showed until the end.

My roommates Gabrielle Descamps, Marius Bossard, Emile Guélard, Ruben Bao Gallien, Alexandre Paumier and Ruslan Sergueï also deserve special thanks for their support and help on the reflexion of this paper and in the identification of plant species present on the study site.

I would like to thank my fellow students of my master's degree for the two wonderful years spent in their company.

Finally, I would like to thank my friends from Paris, the "Bernards en vadrouille, the "Kayous de Jussieu" and those from my former association BAC BDE UPMC who came to visit me and to discover the Algarve.

Abstract

Salt marshes are transitional environments between the ocean and the land. They are home to numerous species and provide many ecosystem services. They are regulated by various geomorphological, hydrodynamic, and biological factors. To ensure their longevity, these environments require a substantial sediment supply to maintain themselves in the intertidal zone. The objective of the study was to characterize the sediment dynamics in a marsh platform of the Ria Formosa lagoon through field campaigns, and at distinct hydrodynamic conditions (spring tides and neap tides). Hydrodynamic conditions (tidal range, hydroperiod, tidal current direction, alongshore and cross-shore current velocities) were recorded at four sampling stations, placed from the Ramalhete Channel towards the intermediate/high marsh. Suspended sediment samples were collected at the sampling stations and at varying water column depths and analysed for suspended concentrations. The deposition rates at each sampling station were also determined.

The obtained results shows that dominant currents are alongshore though the cross-shore velocities become more important landward, toward the high marsh. The obtained total suspended sediment concentrations decrease along the studied transect. In contrast, sediment deposition rates increase along the transect, towards the mainland. Vegetation plays an important role in influencing hydrodynamics and sediment transport. *Zostera noltei* does not offer much resistance to hydrodynamic flow. During spring tides, *Spartina maritima* allows an increase in velocity in the lower marsh, which allows sediment to be brought into the upper marsh, which is only flooded during spring tides. *Sarcocornia sp.* reduces the velocity of the currents, which allows for lower energetic hydrodynamic conditions, favourable for sediment deposition. The tidal range seems to have no influence on the sediment dynamics on the tidal flat. But tidal conditions have a higher influence on the salt marsh (low marsh and high marsh).

Key words: Salt marsh; Suspended sediment concentration; Deposition rate; Hydrodynamic conditions; Vegetation.

Resumo

A zona húmida da Ria Formosa é uma laguna mesotidal localizada no sul de Portugal. É um ambiente de transição entre o oceano e a terra. As zonas húmidas fornecem muitos serviços ecossistémicos, tais como protecção contra inundações, atenuação de ondas, e são sumidouros de carbono . Além disso, estão entre os sistemas mais produtivos do mundo com elevadas taxas de produção primária. São, portanto, ambientes estratégicos e habitats prioritários para as espécies que neles vivem. Estes ambientes estão sob tensão crescente devido às actuais alterações climáticas e à actividade humana. A sua protecção deve, portanto, ser uma prioridade para assegurar a sua longevidade.

As zonas húmidas costeiras têm uma morfodinâmica complexa que depende de factores geofísicos, hidrodinâmicos e biológicos. Encontram-se em zonas entre marés, sujeitas a condições hidrodinâmicas de baixa energia e são colonizadas por vegetação halófita. As lagunas são constituídas por uma rede de canais e que recortam através as planícies de maré e os sapais. A entrada sedimentar nestes ambientes é sob a forma de sedimento suspenso na coluna de água.

A Ria Formosa está fortemente sujeita à influência das marés. O transporte de sedimentos para os sapais está pois sujeito às condições hidrodinâmicas do ambiente. Estes sedimentos comportam-se de forma coesa e estão sujeitos a diferentes processos (transporte, floculação, deposição, consolidação, erosão e ressuspensão) dentro da coluna de água. Assim, a taxa de deposição de sedimentos em diferentes ambientes húmidos depende da direcção e velocidade das correntes das marés e da concentração total de sedimentos em suspensão na coluna de água. A vegetação nos sapais também exerce um papel preponderante no aprisionamento e deposição sedimentar. Na Ria Formosa, as espécies características dos sapais são *Zostera noltei* (no plano da maré), *Spartina maritima* (no pântano baixo), e *Sarcocornia sp*. (no pântano alto)

Este estudo visa caracterizar os padrões de transporte sedimentar nos sapais da Ria Formosa. Para este efeito, foram colocadas quatro estações de monitorização sedimentar ao longo de um perfil perpendicular à entre à linha de costa continental, entre o canal do Ramalhete e o sapal médio /alto. As estações de monitorização sedimentar estão localizas nos diversos ambientes sedimentares: planície de maré (duas estações), baixo sapal (uma estação) e alto sapal (uma estação). Foram realizadas várias campanhas de campo durante

as quais foram colhidos dados de topografia ao longo do perfil, foram registadas as condições hidrodinâmicas tais como altura da água, período de inundação, e velocidades das correntes de maré nas estações de monitorização. Foram colhidas de amostras de sedimento em suspensão, a diferentes elevações na coluna de água e amostras de sedimento depositado junto ao fundo. Estas campanhas tiveram lugar em diferentes condições de amplitude de maré, isto é, durante as marés mortas e durante as marés vivas. Depois de processamento laboratorial, determinou a concentração de sedimento em suspensão na coluna de água, a taxa de deposição de sedimento, a quantidade de matéria orgânica no sedimento depositado e a granulometria do sedimento nos diferentes ambientes do perfil.

Os registos de hidrodinâmica foram processados para obter a direção das correntes de marés, nomeadamente a componentes da velocidade e a velocidade resultante, e o fluxo total de água que passa pelas estações de monitorização. Para a análise dos sedimentos, a concentração de sedimentos em suspensão em toda a coluna de água foi determinada através da filtração das amostras.

Os resultados de hidrodinâmica mostram que a direção dominante das correntes é maioritariamente longilitoral, perdendo, no entanto, expressão na estação de monitorização do alto sapal durante as marés vivas. O fluxo de água é mais significativo nas estações de monitorização mais próximas do canal (na planície de maré) do que nas estações de monitorização localizadas no sapal. Foram medidos maiores fluxos na morfologia do baixo sapal em condições de marés vivas.

A concentração total de sedimentos em suspensão é mais elevada na segunda estação da planície de maré, para ambas as amplitudes de maré. Quando comparadas com as medições efetuadas na planície de maré, as taxas de deposição sedimentar determinadas para o sapal são mais elevadas, especialmente para o alto sapal e durante marés vivas. Finalmente, a quantidade de matéria orgânica nas amostras de sedimentos depositados parece ser significativamente variável entre as marés amostradas. O tamanho dos grãos do sedimento aumenta ao longo do perfil, o que permite maiores taxas de deposição em ambientes com condições hidrodinâmicas menos energéticas.

As espécies vegetais presentes na área de estudo têm características morfométricas distinctas, dependendo da espécie e do ambiente em que se encontram. Influenciam a dinâmica das correntes de diferentes maneiras, potenciando o aprisionamento e deposição dos sedimentos em suspensão na coluna de água. A *Zostera noltei* tem uma influência menor na sedimentação da área de estudo, mas evita que o sedimento na planicei de maré entre facilmente em ressuspensão. Devido à sua maior rigidez, a *Spartina maritima* tem um efeito positivo sobre a velocidade da corrente e ajuda a aprisionar sedimentos no baixo sapal, especialmente durante condições de marés vivas. Durante condições de marés mortas, a velocidade das correntes diminui no baixo sapal, o que permite uma maior sedimentar. Ademais, a rigidez da *Sarcocornia sp.* e as condições hidrodinâmicas mais baixas (correntes de menor magnitude) permitem uma elevada taxa de deposição alto sapal.

Em sintese, na área de estudo, os sedimentos são predominantemente trazidos pelo canal do Ramalhete, através das correntes de maré marés e por um pequeno canal terciário que recorta a planície de maré. A velocidade mais reduzida das correntes no sapal permite uma maior deposição sedimentar.

Table of contents

List of figures

List of tables

List of abbreviations

TF1: Tidal Flat 1 station

TF2: Tidal Flat 2 station

LM: Low Marsh station

HM: High Marsh Station

SSC: Suspended Sediment Concentration

DR: Deposition Rate

MSL: Mean Sea Level

OM: Organic Matter

ST: Spring Tide

NT: Neap Tide

NMF: Net Momentum Flux of water

TSSC: Total of Suspended Sediment Concentration

MMLPSA: Malvern Mastersizer Laser Particle Size Analyzer

DGPS: Differential Global Positioning System

1. Introduction

1.1. Motivation

Salt marshes are transitional wetlands between land and sea. These coastal wetlands provide multiple ecosystem services such flooding protection, waves attenuation, and blue carbon sink (Chmura et al., 2003; Craft et al., 2009; Duarte et al., 2013; Fagherazzi et al., 2020; Garzon et al., 2019; Kumar et al., 2020; Ribeiro et al., 2008; Yang et al., 2008). These ecosystems are among the most productive ecosystems in the world with high rates of primary production (Gedan et al., 2009). Current climate change threatens salt marshes, as these regions are subject to natural disturbances, such as increase sea levels (Gedan et al., 2009; Raposa et al., 2016; van Regteren et al., 2020) and anthropogenic pressures (Carrasco et al., 2021; Samper-Villarreal et al., 2016). Depending on their morphodynamic, hydrodynamic and biological properties, each coastal wetland may evolve differently from the others. Their ecological services make salt marshes priority habitats (Evans, 2006; R. J. Johnston et al., 2002; McKinley et al., 2020; Neckles et al., 2015)

As salt marshes are subject to natural and anthropogenic disturbances, a better understanding of their evolution according to sedimentary inputs, physical characteristics, and the relationship between vegetation and sediments are necessary to better understand their development, and thus to ensure the longevity of these environments. Furthermore, this kind of coastal wetland characterization has never been performed in the Ria Formosa.

1.2. Main objectives

Objectives of this study are to characterize the sediment transport dynamics in the coastal wetlands in the Ria Formosa lagoon, and the associated drivers. For that, the suspended sediment concentration (SSC) and the sediment deposition rate (DR) will be determined based on fieldwork data collection and analysis. The data will be used to assess the sediment pathways and dynamics and the influence of vegetation along the tidal flat - marsh platform, to express the major interactions and processes that dominate hydrodynamics and sediment dynamics in these environments.

1.3. State of the art

Since the industrial era, emissions of greenhouse gases have been increasing, with consequences for the climate and the environment. Titus et al. (1991) showed that temperature increases due to greenhouse gas emissions and this have an impact on sea level. Indeed, with the increase in temperature, the ice at the poles melts and the water expands due to its thermal extension, which cause the sea level to rise. Salt marshes and tidal plains that make up the coastal wetland are ecosystems that develop in temperate zones, colonized by halophytic vegetation, and characterized by low hydrodynamic conditions and tidal flooding (Simas et al., 2001). These environments are used by many and diverse animal species as breeding and nursery grounds (Chmura et al., 2003; Craft et al., 2009; Duarte et al., 2013; Fagherazzi et al., 2020). In addition, coastal wetlands play an important role in soil carbon sequestration (Kumar et al., 2020; Ribeiro et al., 2008). In 2016, Samper-Villarreal et al., showed that turbidity, water depth, and vegetation type are the main factors influencing soil carbon content. These environments have a high ecological and economical importance (Carrasco et al., 2016). Because of their low altitude, these aquatic ecosystems are highly influenced by sea level rise and a large increase in sea level will have a significant impact on their survival (Carrasco et al., 2016; Simas et al., 2001). The balance between vertical marsh accretion and relative SLR is considered a key control on long-term marsh survival (Carrasco et al., 2021).

1.3.1. Geomorphology and hydrodynamic of coastal wetlands

The morphodynamic of coastal wetlands is complex since it depends on many physical, geophysical, hydrodynamic, and biological factors (D'Alpaos & Marani, 2016; Fagherazzi et al., 2005). Their formations require a sufficient supply of sediments, favorable conditions for the colonization of the environment by halophytic plants, but also to be located on a floodable platform with shallow water depth, protected from the swells (Fagherazzi et al., 2012). Wetland platforms are adapted to low hydrodynamic conditions. As they are located on a floodable platform, they are mainly influenced by tides and tidal amplitudes are a determining factor for the location of salt marshes (Simas et al., 2001). These coastal wetlands develop between mean sea level (MSL) and mean high tide level (Tiner, 2013).

Coastal wetlands can be found around the world in some different kind of environments: in front of the open ocean (Wang, 2010), bordering the mouth of an estuary (Ma et al.,

2018), or protected by a barrier system (Christiansen et al., 2000). They can be zoned into three distinct parts: the tidal channel network, the tidal flat, bordering the channels and located below MSL, and finally the salt marshes developing over a area that extends up to the highest tidal amplitudes (Taramelli et al., 2018). Water reaches the coastal wetlands through the network of tidal channels. Coastal wetlands are submerged when the tide rises, and fed by suspended sediments, transported by currents. As some creeks are located on the tidal flat or on marsh, they can bring water faster. On high marsh, it is possible to find ponds (Johnston et al., 2003). These ponds may always have water inside as they are deeper than the marsh, so, one part of the amount of water brought remains in them. Depending on environmental conditions, the net momentum flux of water (NMF) may be different during the flood phase and ebb phase of a tidal cycle (French & Stoddart, 1992). Vegetation plays an important role in the sediment deposition.

To maintain stability, the sediment supply must be sufficient to counter sea level rise (Arnaud-Fassetta et al., 2006; Carrasco et al., 2016; Raposa et al., 2016). Not all wetlands react in the same way to sea level rise, with macrotidal marshes showing a better adaptation to rising water levels than mesotidal or microtidal salt marshes (Friedrichs & Perry, 2001; Kirwan & Guntenspergen, 2010). Indeed, the frequency and duration of tidal flooding (hydroperiod) regulates the flow of sediments and their DRs (Fagherazzi et al., 2020; Pasternack et al., 2000). Several studies have shown the evolution of salt marshes in anticipation of a rise in MSL, showing that salt marshes can extend vertically (Kirwan & Guntenspergen, 2010; Ladd et al., 2019; Mariotti & Fagherazzi, 2013), but also laterally (Balke et al., 2016; Bouma et al., 2016; Ladd et al., 2019). More recent studies have shown the evolution of vertical accretion and seaward progradation of marshes under sea level rise conditions (Fagherazzi et al., 2020; van Regteren et al., 2020). On the other hand, if the sediment supply is not sufficient, sea level rise may lead to a transgression from the wetlands to the mainland (Fagherazzi et al., 2020). In addition, the importance of storms and sea level rise will likely lead to an increase in the intensity of waves and currents over tidal areas, which also contributes to the retrogression of coastal wetlands (Mariotti & Carr, 2014; Mariotti & Fagherazzi, 2010). With the increase of anthropic interventions occurring in these environments, there is an increase disturbance in the sediment stability by

blocking the expansion of wetlands or their sediment supply (Cui et al., 2016; Gedan et al., 2009; Raposa et al., 2016; van Regteren et al., 2020).

1.3.2. Sediment transport in coastal wetlands

The accumulation of sediment for the development of coastal wetlands comes from allochthonous sediment and organic matter (OM) produced by plant species living in these environments (Chmura & Hung, 2004; Moskalski & Sommerfield, 2012). The OM originates from the roots and leaf litter of the halophytic plants present and from microbial and algal primary production (Friedrichs & Perry, 2001), while its production is especially important for vertical accretion in wet coastal areas (Kirwan & Murray, 2007). Sediments are transported in suspension in the water column. SSC depends on their morphological properties (e.g. grain size) and the hydrodynamic conditions of the environment. Indeed, coarse particles are too heavy to be suspended in the water column and suspended sediments mainly consist of fine fraction ($D < 63$ µm). Moreover, sediments become finer and finer as it moves inland in tidal dominated coastal wetland (Christiansen et al., 2000; Strachan et al., 2016; Wiberg et al., 2015).

These sediments have a cohesive behaviour in the water column, it means they tend to bind together (Guillou et al., 2011; Winterwerp & van Kesteren, 2004). This kind of sediments are composed of water, a mix between fine sand, silt and clay, and OM. The “cohesive behavior” term refers to ductile behavior (Winterwerp & van Kesteren, 2004). Fine sediments can adopt this behavior thanks to their sizes and shapes, but also to electrical charge distribution (Guillou et al., 2011). Indeed, this kind of particle coagulate can form bonds due to attractive van der Waals or electrochemical forces (Guillou et al., 2011; Kombiadou & Krestenitis, 2013; Winterwerp & van Kesteren, 2004). The different processes to which cohesive sediments are subject are advection, dispersion, flocculation, deposition, consolidation, erosion, and resuspension (Guillou et al., 2011; Kombiadou & Krestenitis, 2013; Winterwerp & van Kesteren, 2004). These processes are resume in the Figure 1. The advection is the movement of sediments, at the same velocity of its surrounding environment. Dispersion occurs due to velocity gradients and results to an additional transport term that is stochastic in its nature. After they start to be transported, sediments are spread until they settle (Sly, 1989). The flocculation is a coagulation phenomenon that occurs when two or more particles come into contact and merge,

creating chemical or Van der Walls bonds to form a larger floc, increasing its weight, and making it more likely to sink and settle (Guillou et al., 2011). When sediments settle, it is the deposition, when they reach the bottom. After the particles have settled, they are gradually covered by other particles deposited above them, and their weight is causing the gradual loss of interstitial pore water (Guillou et al., 2011). This phenomenon is the consolidation, during which the strength of deposited sediment beds gradually increases. The turbulent motion of the flow over the ground creates shear stresses that can erode the bed or resuspend settled sediment, if they were not yet fully consolidated (Guillou et al., 2011; Sly, 1989)

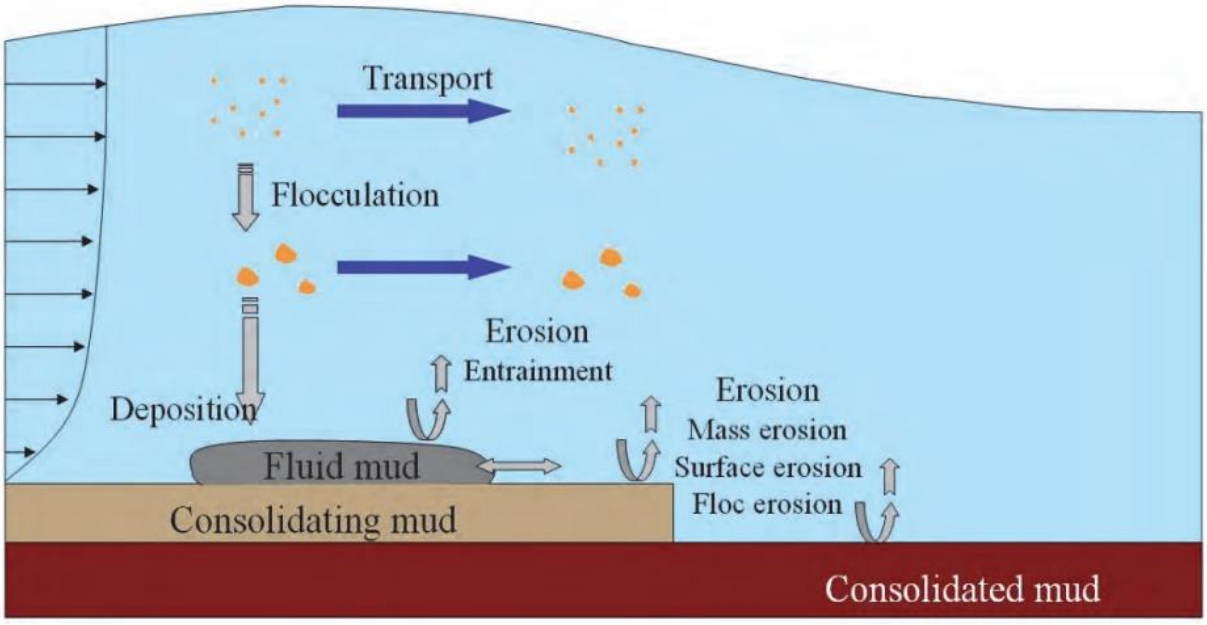

Figure 1: Macroscopic description of the cohesive sediment transport processes (figure source: Guillou et al., 2011)

The SSC in the water column controls the potential for sediment input to coastal wetlands (French, 1993; Reed et al., 1999). Reed, in 1990, showed that the hydroperiod, or flood period, is an important parameter for sediment deposition, since it determines the time during which sediment can deposit in each environment. Some studies have shown that the greater the distance from the channel or the creek, the lower the SSC and the DR are (Christiansen et al., 2000; Ma et al., 2018; Moskalski & Sommerfield, 2012). Areas located at higher elevations have lower DR than lower ones because of their shorter hydroperiod (Reed, 1990). Precipitation also has a direct impact on exposed sediments since it allows them to be resuspended and thus redistribute them (Mwamba & Torres, 2002). Storms and

the related terrestrial flows to a wetland must also be considered as a source of sediments, influencing their redistribution (Fagherazzi et al., 2020; Reed, 1989). Despite erosion of the marsh edges by the wave action, or sea level rise (Mariotti & Carr, 2014; Mariotti & Fagherazzi, 2010, 2013), eroded sediments can also serve as a source for vertical accretion of marshes (Mariotti & Carr, 2014; Schuerch et al., 2019). Benthic organisms can also have an impact on the resuspension of sediments, due to bioturbation, which erodes and resuspends them, and biostabilisation, which makes cohesive beds harder to erode (Bouma, et al., 2005).

1.3.2. Vegetation influence on sediment dynamic in coastal wetlands

Coastal wetlands can also be divided according to their vegetation, such as the work of Stock (2014) for wetlands near the Wadden Sea. The substrate and the hydrodynamic conditions acting at the different locations of the system are not the same, and therefore the lower parts of the coastal wetland do not shelter the same species as the higher parts and do not have the same effects on the platform vertical growth (Murray et al., 2008). Vegetation in coastal wetlands requires periods of exposure to open air and flooding by sea water and soil having suitable chemical properties and salinity (Elellterills et al., 1979). Multiple abiotic factors affect the colonization of the environment by vegetation, such as the anoxia of the high salinity soils of the tidal flat (van Regteren et al., 2020). Plant resistance to anoxic conditions is different for each specie (Davy et al., 2011). These stressful conditions increase with decreasing altitude (Bertness & Hacker, 1994). For the establishment of a good plant cover, stable soil conditions are necessary (Balke et al., 2016). For example, grain size influences soil stability: sandy soils are more susceptible to erosion than muddy soils, making the latter a favorable environment for species establishment (Houwing et al., 1999). A minimum soil elevation of 0.50 cm below MSL is required for seed establishment on the tidal flat (Wang & Temmerman, 2013). Vegetation growth can be stimulated by increasing submersion, which contributes to the accretion of organic sediments and the trapping of inorganic sediments (Morris et al., 2002; Mudd et al., 2010).

Regarding plant succession, the upper part of the marshes is characterized by dense vegetation, while the lower part of the marsh is characterized by a more diverse vegetation with less cover density (van der Wal et al., 2008). The boundary between the tidal flat and

the salt marshes is characterized by pioneer species that are essential for the development of salt marshes. Salt marsh vegetation provides hydraulic resistance to marine currents (Backhaus & Verduin, 2008) and waves (Garzon et al., 2019) and prevents deposited sediments from being resuspended (Boorman et al., 1998; Leonard & Luther, 1995).

Halophytic vegetation influences marsh hydrodynamics and sediment transport through increased inorganic sedimentation rates, due to an increased flow resistance and the reduction in turbulent kinetic energy, as well as through direct particle capture by plant stems (Leonard & Luther, 1995; Mudd et al., 2010; Temmerman et al., 2005; Vandenbruwaene et al., 2011). Plant canopies act as an obstacle to the current, which is deflected over and around them (Fonseca & Koehl, 2006; Ghisalberti, 2002; Ghisalberti & Nepf, 2009). Water passes over the canopies at a higher velocity than the portion of water passing in the center of the canopy (Boorman et al., 1998), resulting in the formations of a shear zone characterized by vortices at the interface between vegetation and the water column (Sánchez et al., 2001). The density of plant stems has been determined as one of the critical parameters in the control of sediment deposition (Temmerman et al., 2005). Pioneer species can spread over the tidal flat (Bouma et al., 2009; Temmerman et al., 2005), and thus allow for better sediment retention at this location (van Regteren et al., 2017). The deflection of the current around these scattered canopies of pioneer vegetation can also lead to erosion around them (van Regteren et al., 2017).

2. Study area

The Ria Formosa is a shallow coastal lagoon located in Algarve, in the South of Portugal (Figure 2A). This region has a Mediterranean climate, with wet winters and hot and dry summers. The lagoon extends for about 55 km between the peninsulas of Ancão (to the West) and Cacela (to the East). The Western part of the lagoon is much wider than the Eastern part, which extends Eastwards from Olhão. The lagoon covers an area of 18,400 ha and is bounded offshore by two peninsulas and five islands which are separated by six tidal inlets distributed from West to East as follows: Ancão inlet, Faro-Olhão inlet, Armona inlet, Fuseta inlet, Tavira inlet, and finally Lacem inlet. The western part of the Ria Formosa is presented in the Figure 2B, to the west the Ancão Peninsula (AP), the Barreta Islands (BI), the Culatra Island (CI) and the Tavira Island (TI), and three of the inlets of the ria in the ocean: Ancão Inlet (AI), Faro-Olhão Inlet (FOI), and Armona Inlet (AI), with location of the study area (red point).

Figure 2: Location of the study area, (A) in Portugal, (B) in the Ria Formosa

The lagoon is subject to a semi-diurnal mesotidal regime with a tidal range of 1.3 m and 2.8 m, respectively to neap tide (NT) and spring tide (ST) with highest amplitude of 3.5 m during some STs (Ferreira et al., 2016). The average depth is 2 m below MSL (Sousa et al., 2019). Water renewal in the lagoon is very high, with 50 to 70% of the water mass exchanged at each tide (Sousa et al., 2019).

The Ria Formosa consists of different geomorphological units: a complex network of tidal channels, salt marshes (Figure 3A and Figure 3B), tidal plains (Figure 3B and Figure 3C), lagoon beaches, creeks (Figure 3C), ponds (Figure 3D), and flood deltas (Arnaud-Fassetta et al., 2006; Sousa et al., 2019). Tidal channels can be divided into three sub-channels: deep and wide channels that are fully submerged in all tidal cycles, secondary channels that are active only during high tides and characterized by narrower and shallower channels and tertiary channels active only during STs. Salt marshes can be divided into three subsets: supratidal marshes, upper intertidal marshes, and lower intertidal marshes. The sediments in these environments are finer than those found in tidal channels, with the silt content over 50% and with coarse sand below 5%, with very few bioclasts (Arnaud-Fassetta et al., 2006; Sousa et al., 2019). Tidal flats are environments between channels and salt marshes, located below MSL. The sediments consist mainly of silt and clay but a coarser fraction with sometimes bioclasts is located at the lower part of the tidal flat, at the limit with the channels. The main sediment inputs belong to the class of clays and silts. The coarse fraction contribution from the river inflow is low compared to the contribution of fine sediments (Sousa et al., 2019). The tides carry these suspended sediments in the lagoon, and out during the ebb but some of them will be kept trapped in salt marshes and tidal flats (Andrade et al., 2004).

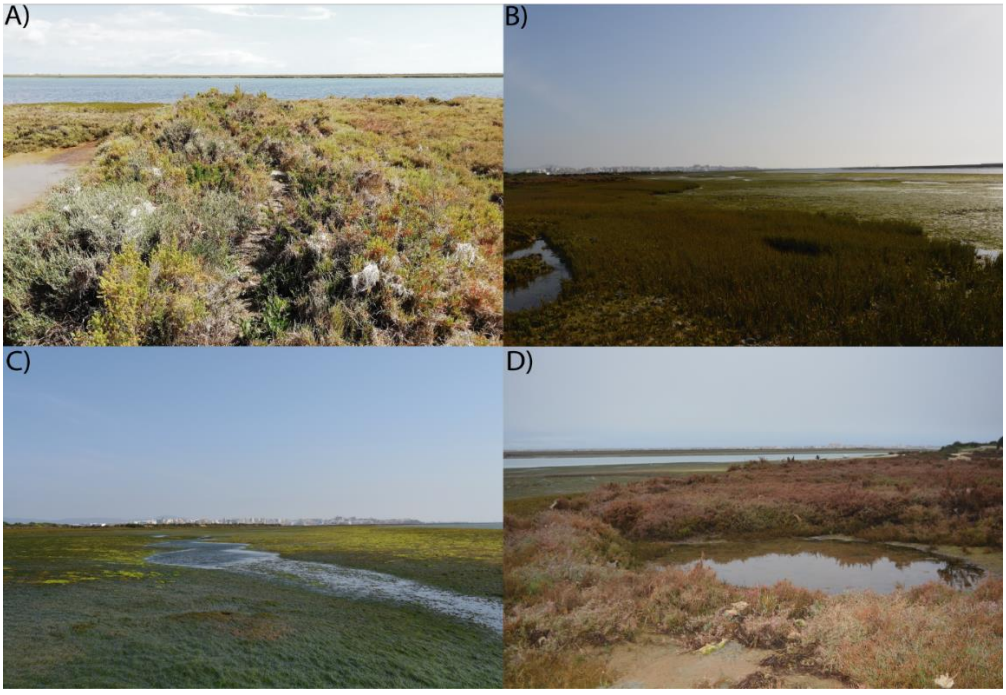

Figure 3: (A) photo of the high marsh with the channel in background; (B) low marsh and tidal flat; (C) creek located the tidal flat; (D) ponds located on the high marsh

Most of the dominant salt marsh plants are halophytic species that can develop in coastal wetland. The high and medium marsh are characterized by species such as *Sarcocornia sp.*, the low marsh is characterized by an abundance of the species *Spartina maritima*, while the tidal flat is characterized by the presence of *Zostera noltei* and finally the tidal channels are characterized by species *Cymodocea nodosa, Zostera marina* and *Zostera noltei* (Andrade et al., 2004; Kumar et al., 2020). This species association reflects the high salinity values (35‰) for the lagoon water (Andrade et al., 2004). A presentation of plants species is given in the Appendix 1.

Anthropogenic activities have strongly altered the sedimentary input in some parts of the lagoon, and with the rise in sea level, are endangering the future survival of the lagoon. The Ria Formosa became a Natural Reserve in 1978, and a Natural Park in 1987. In addition, it is part of the wetlands of the Ramsar Convention and belongs to the Natura 2000 sites of the European Union. Aside of being an ecosystem of great importance, the Ria Formosa is also an important resource for fishing, aquaculture, salt extraction and tourism (Newton & Mudge, 2003).

The studied wetland is located in the Western part of the Ria Formosa lagoon, close to the Ramalhete channel (Figure 2). This place presents the morphological units presented before, namely the tidal flat, traversed by a creek, a low marsh, and a high marsh (Figure 4). A creek is present downdrift, located on the tidal flat and ponds are scattered throughout the high marsh.

Figure 4: Studied transect on the study area during NT, close to Ramalhete Channel, the photo is taken from the high marsh on the 26th of January

3. Methodology

3.1. Fieldwork

3.1.1. Field campaigns and data collection

Fieldwork data collection included topographic data, water levels, hydroperiods, current velocities, and sediment transport (SSCs and deposited sediments). The bed elevation of the wetland with respected to the MSL, was measured across a transverse profile on 26th of January, using a Differential Global Positioning System (DGPS). Four monitoring stations, from the tidal flat towards the high marsh, were positioned across the topographic profile (oriented Northwest to Southeast, Figure 5), where sediment transport and hydrodynamic measurements were recorded. All stations were located with the DGPS. The lowest station, Tidal Flat 1 (TF1), is located on the lower part of the tidal flat, near the Ramalhete channel. Station Tidal Flat 2 (TF2) is also located on the tidal flat, but inland from the tidal channel. The two stations on the tidal flat, TF1 and TF2, are vegetated with *Zostera noltei* (dwarf seagrass). The third station, Low Marsh (LM), is located on the low salt marsh and is vegetated with *Spartina maritima* (small cordgrass). Finally, the highest station, High Marsh (HM), is mainly vegetated with *Sarcocornia sp*. (saltwarts).

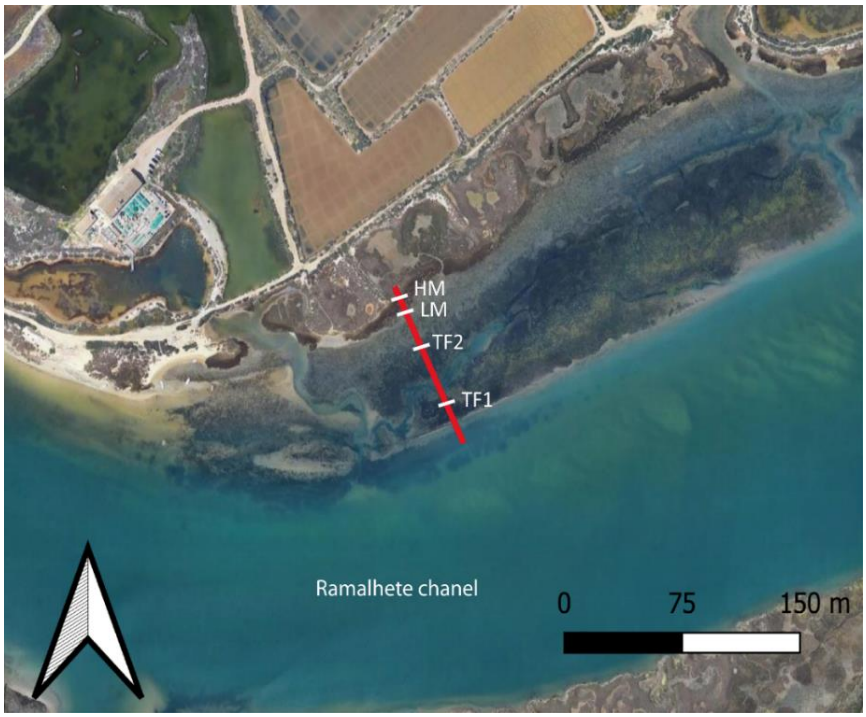

Figure 5: Studied transect with the location of the 4 monitoring stations

Sediment samples and hydrodynamic data were collected during the ST of the 28th of February and during the NT of the 6th of June. Moreover, two additional sets of samples for the DR were collected during the NT of the 26th of January and the ST of the 26th of April. The field survey data are summarized in the Table 1.

Table 1: Summary of sampling by campaign, green means data collection and red means no data collection

		Topography	Hydroperiod and water level	Current velocities	SSC	Deposited sediment	Organic matter content
NT	26th Jan.	Yes	Yes	No	No	Yes	Yes
	6th Jun.	No	Yes	Yes	Yes	Yes	Yes
ST	28th Feb.	No	Yes	Yes	Yes	Yes	Yes
	26th Apr.	No	Yes	No	No	Yes	Yes

During NTs, the maximum water level is not high enough to reach the last station (HM) and therefore no samples and data were collected there. Data collection for NT and ST were used to quantify Total Suspended Sediment Concentration (TSSC) for varying minimum and maximum tidal range amplitudes, respectively. Tidal range calendar tables are given in the Appendix 2. The experimental transect in NT and ST conditions, with the distance from the channel and the topography of the study area are summarized in Figure 6. Informations on how the samples were collected, the methodology of the laboratory work and the data processing are given in the following parts of this chapter.

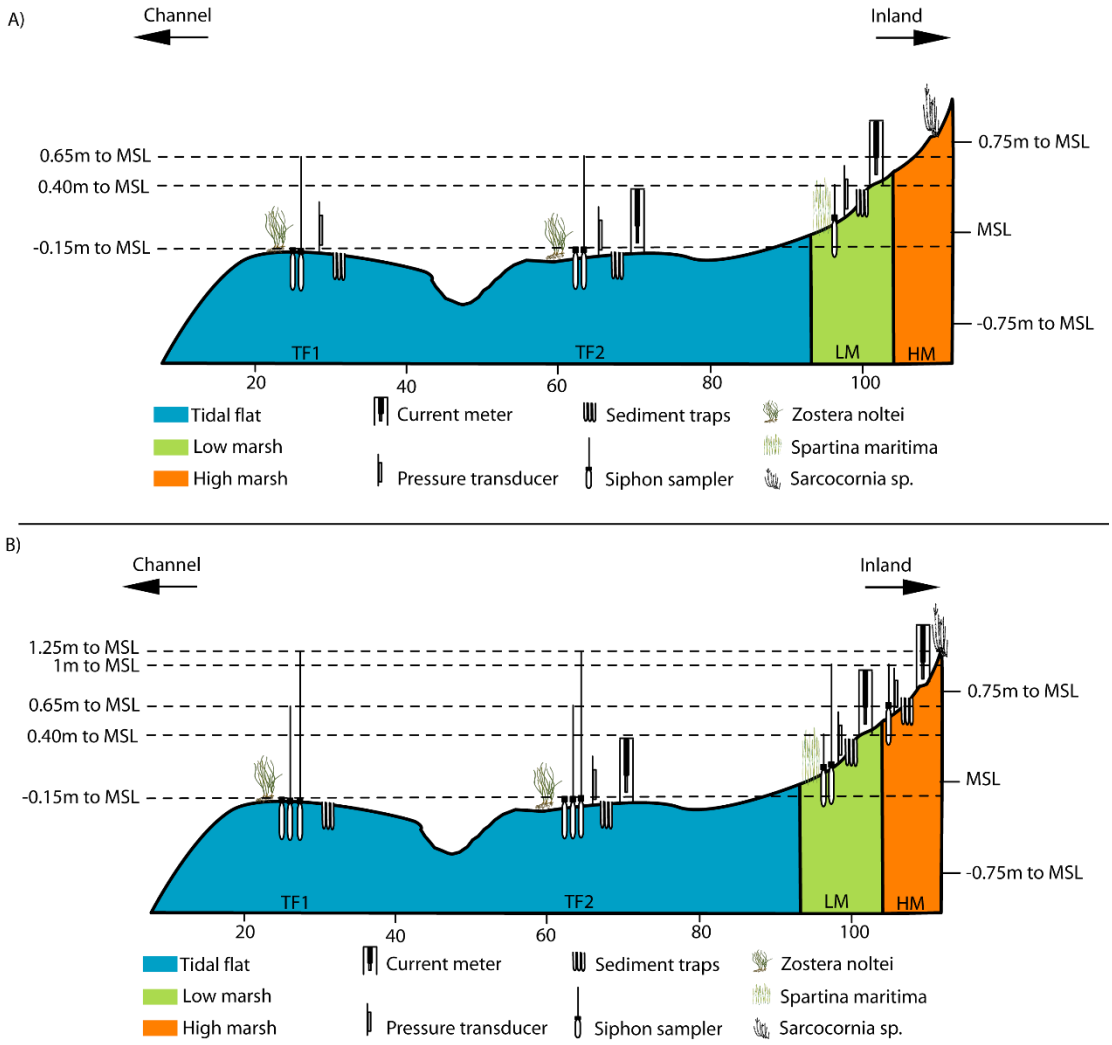

Figure 6: Experimental transect during NT (A) and ST (B) conditions, with SSC sampler intake elevations

3.1.2. Hydrodynamic conditions

Pressure transducers (ESI PR3420; PTs) were placed in all flooded stations during NTs and at TF2, LM and HM during STs, at an elevation of ~2 cm above ground level, to record the time of tide immersion at each morphology. PTs were calibrated at the atmosphere level. The hydroperiod is obtained based on the water column pressure exerted on the sensor. Data were recorded at a frequency of 1 record every minute.

An electromagnetic current meter (Valeport 801; EMCM) was used to record current velocities along and across the axes of the instrument (X and Y directions). The placement of the EMCM in the field was such, that X corresponded to the alongshore direction and Y corresponded to the cross-shore direction. Data were recorded at a rate of 2 records per

minute. During the fieldwork, the EMCM was placed at stations TF2 and LM for the NT campaign. For the ST survey, velocities were recorded at stations TF2, LM and HM.

Data were collected during a complete tidal cycle, placing the instruments on each station at low tide and recovering them at the following low tide. PT and the EMCM placement on the field are shown in the Figure 7. The EMCM is fixed on a metal bar which is held in place by two wooden poles sunk into the ground. During the ST campaign, data for TF2 were recorded during the first tide of 28th of February, for HM during the night between 28th of February and 1st of March and for LM data were recorded on 1st of March. For the NT, data for TF2 were recorded during the first tide of 6th of June and for LM were recorded during the second tide of that day.

Figure 7: Photo of the EMCM in the field (mounted on a support structure; EMCM is in the middle of the horizontal steel bar), and PT (next to the structure, on the left) at the TF2 station during the 28th of February campaign

3.1.3. Sediment transport

To collect the suspended sediment during the flood tide, siphon samplers (Figure 6) were placed at each station. The samplers consist of a 0.5 l bottle with a cap pierced with two holes, each with a nozzle and a sealing ring, to which two pipes were attached. These two pipes have different lengths to attach them at different height. The lower attached pipe allows the water and suspended sediment to be sampled when the flood water reaches the height of the sampler intake. The second, higher attached pipe allows the air in the bottle

to be evacuated when the water fills the siphon sampler in the form of bubbles, replicating the method of a siphon (Bouma et al., 2005; Ma et al., 2018).

Samples were collected at fixed elevation for both tidal conditions (Figure 6). On the tidal flat and at LM, the siphon samplers are fixed at ground level. At HM, the siphon sampler is sunk into the ground to ensure that the sampler is not higher than the intake. For ST at TF1 and TF2, the intake pipes were set at elevations of -0.15 m, 0.65 m and 1.25 m with siphon elevations of 0.75 m for the first two intakes and 1.35 m for the highest siphon corresponding to the third intake. At LM, intakes were set at 0.4 m and 1 m and siphons were set at 0.5 m and 1.1 m respectively. Finally at HM, only one siphon sampler was installed, with an intake at 1 m for a siphon elevated to 1.1 m. During the NT, only two siphon samplers were used at TF1 and TF2 with intakes at -0.15 m and 0.65 m and for siphons elevated to 0.75 m for both. Finally, at LM under the same tidal conditions, only one sampler was deployed for an intake set at 0.4 m with a siphon set at 0.5 m. All these elevations are with respect to MSL.

To quantify the rate of sediment deposition on the bed, a set of three sediment traps (Figure 6) were installed at TF1, TF2, LM, and HM. The traps consisted of simple falcon tubes (Falcon® tubes, 11.5 cm long, 50 ml of capacity, opening of 1.5 cm of radius) pushed in the soil so that the opening of the falcon is elevated with bed-level. The sediment DR was defined as the total sediment particles deposited on the bed, without considering resuspension (Gacia et al., 1999). During the 28th of February fieldwork, 3 additional sediment traps were placed at stations LM and HM. During the fieldwork of the 26th of April, 6 additional sediment traps were placed on HM. These traps were placed not far from the transect, 3 of them few meters from the transect, orientated North-East, and the others at the same distance, orientated South-West. These additional 6 traps allowed to assess potential differences in DR along the high marsh and identify any 2D patterns of sedimentation.

As for PTs and EMCM, siphon samplers and sediment traps (Figure 8)were installed during the low tide and recovered at the next low tide.

Figure 8: Sediment traps (on the bottom left corner) and siphon sampler (in the middle) at TF1 on the 28th of February

3.2. Laboratory analysis

The collected sediments from traps and the SSC samples were transported to the laboratory and stored under cool, dark conditions on arrival, until further processing. Laboratory analysis concerns sediment granulometry and assessment of suspended and deposited sediment mass.

3.2.1. Grain size

To determine the size of the sediment grains, an analysis with a Malvern Mastersizer Laser Particle Size Analyzer (MMLPSA) was performed. The device uses a small amount of solution to make the measurements using laser diffraction. It measures the angular variation of the laser light intensity. Water solution was used to calibrate the MMLPSA. Once the calibration was complete, drops of sediment-containing solution were added, and the MMLPSA measured the size of the grains collected.

3.2.2. Suspended sediment concentration

The samples contained in the siphon samplers were filtered to collect the sediment suspended in the water. To do this, a filtration ramp (Figure 9) was connected to a compressor and a water outlet to create suction. Prior to filtration, the weights of the 0.45 µm pore-size filters (Gelman Sciences, Sterilized membrane, GN-6 Metricel®, diameter

47 mm) to be used were measured, as well as the volume of each sample, using a balance and test tubes. Filters were placed on the filtration ramp, allowing for the retention of all sediment contained in the sample. Each test tube was washed with deoxygenated water and added to the filtration, to avoid losing sediments from samples. Between each filtration, all cups and tubes were washed with deoxygenated water to avoid sample contamination. After filtration, the filters were placed in the oven to dry, at a temperature of 45°C for 24 to 48 hours. Once the filters were dry, their weight was measured again.

Figure 9: Filtration of suspended sediments

3.2.3. Deposition rate

The falcon tubes containing the deposited sediment samples were shaken, to resuspend the sediment, washed to remove salt contained in samples, and the contents of the tubes were poured into pre-weighed beakers. These samples were then weighed and placed in the oven for 24 to 48 hours at a temperature of 45°C, to allow the water in the sample to evaporate. Once the water had fully evaporated, the samples were weighed again. Afterwards, hydrogen peroxide (H_2O_2) was added to the samples, to destroy the OM content. The reaction occurs when brown foam forms and ends when the foam changes from brown to white. To catalyze the reaction of OM destruction, the samples were placed

on a hot plate (Figure 10A). Once the OM had been destroyed, the samples were returned to the oven for a second time (24-48 hours, 45°C; Figure 10B), to allow the liquids in the samples to evaporate and destroy the remaining OM. Once the samples were dry, their weights were measured again. The difference between the samples before (Figure 10C) and after (Figure 10D) the destruction of the OM is illustrated in the following figures.

Figure 10: Laboratory work for the DR estimation, (A) reaction of the OM with the H2O2; (B) samples in the oven; (C) samples before the destruction of the OM; (D) samples after the destruction of the OM

3.3. Data analysis

3.3.1. Hydrodynamic data

Records from PTs were used to compute the hydroperiod using the EXCEL software and considering the time the instrument recorded column heights over 2 cm.

The data recorded by the EMCM were analysed using EXCEL software. To the alongshore and cross-shore velocities was applied a 10-minute moving average. Figures without apply of the moving average are presented in the Appendix 3. On alongshore and cross-shore velocity graphics the first part (mainly positive values) corresponds to the flood phase of the tide and the second part (mainly negative values) illustrates the ebb phase of the tide.

Having the alongshore and cross-shore velocities, it was possible to calculate the direction of the resultant tidal current velocity using the following formula:

$$D = \text{atan} \left| \frac{v_x}{v_y} \right| \quad (1)$$

Where D is the direction of the tidal current (angle relative to the cross-shore direction), v_x is the alongshore velocity and v_y is the cross-shore velocity. The graphical representation of this equation shows the direction of the current velocity, ranging from 0° to 90° (that is from fully cross-shore to fully along-shore direction, respectively).

Moreover, to quantify the NMF of water that crossed through the station during an entire tide, the resultant velocity V_R was calculated for all stations using the formula:

$$V_R = \sqrt{{v_x}^2 + {v_y}^2} \quad (2)$$

Results obtained by equation (2) were integrated with time, to calculate the NMF (m^3/m^2) that passes by the location of the EMCM sensor. NMF during flood and ebb phase were calculated separately.

3.3.2. Grain size

The data obtained with the MMLPSA were analyzed with the Gradistat software. This software is based on the statistical particle size analysis of Folk and Ward (1957). The results obtained represent the median value of the diameter sizes (in µm) of the particles contained in the analyzed samples. The size of the sediment grains provides information on the sedimentary class to which they belong.

3.3.3. Suspended sediment concentration

To determine the SSC, the weight of sediment in each siphon sampler after filtration is determined by the following equation:

$$SSC = \frac{(w_{f+s} - w_f)}{V} \quad (3)$$

Where SSC is the concentration of suspended sediment, w_{f+s} is the weight of the dried filter containing the sediment, w_f is the weight of the filter, and V is the volume contained

in the siphon sampler. Values from the same station were integrated to have the TSSC (in g/m^2) that passed by the station.

3.3.4. Sediment deposition rate

An average of the weights of the collected sediments, the hydroperiod, and the OM content was made per station for each campaign. To determine the DR (in g/cm^2/hr), the following formula was applied:

$$DR = \frac{\frac{W_s}{A}}{T} \tag{4}$$

where W_s is the amount of deposited sediment (gr), A is the opening area of the sediment trap (cm^2), and T is the hydroperiod of the sediment trap (hr). W_s is determined by the difference between the weight of the sample before it goes into the oven for the first time (w_{s0}) and the weight of the sample once it is taken out of the oven for the second time (w_{s2}):

$$W_s = w_{s0} - w_{s2} \tag{5}$$

The OM content in the samples was obtained by the following equation, where w_{s1} is the weight of the sample after the first time it went in the oven:

$$OM = \frac{(w_{s2} - w_{s1}) * 100}{w_{s1}} \tag{6}$$

4. Results

4.1. Topography and grain size distribution along the profile

4.1.1. Topography and station characteristics

The studied transect is ~115 m long, starting from the Ramalhete channel, with elevation fluctuating between -1.11 m and more than 1.15 m, with reference to MSL (Figure 11). The tidal flat begins near 18 m and goes until 97 m from the channel. TF1 and TF2 are located at 18.05 m and at 59.35 m from the channel with an elevation of -0.25 m compared to MSL. A small creek, of ~0.58 m depth, is located on the tidal flat between TF1 and TF2 (at around 48 m from the Ramalhete Channel, Figure 11). This creek joins the channel to the Southwest of the transect and flows inland on the tidal flat to the Northeast. The delimitation between the tidal flat and the marsh is the position where elevation reaches the MSL. The low marsh is located between 93.03 m to 100 m with an increase since 0 m to 0.5 m of elevation (Figure 11). Over this elevation it is the high marsh. The LM station is located at an elevation of 0 m MSL and at a distance of ~93 m from the channel, while HM is the highest station, with an elevation of 0.71 m, located at 107.94 m inland from the Ramalhete Channel (Figure 11).

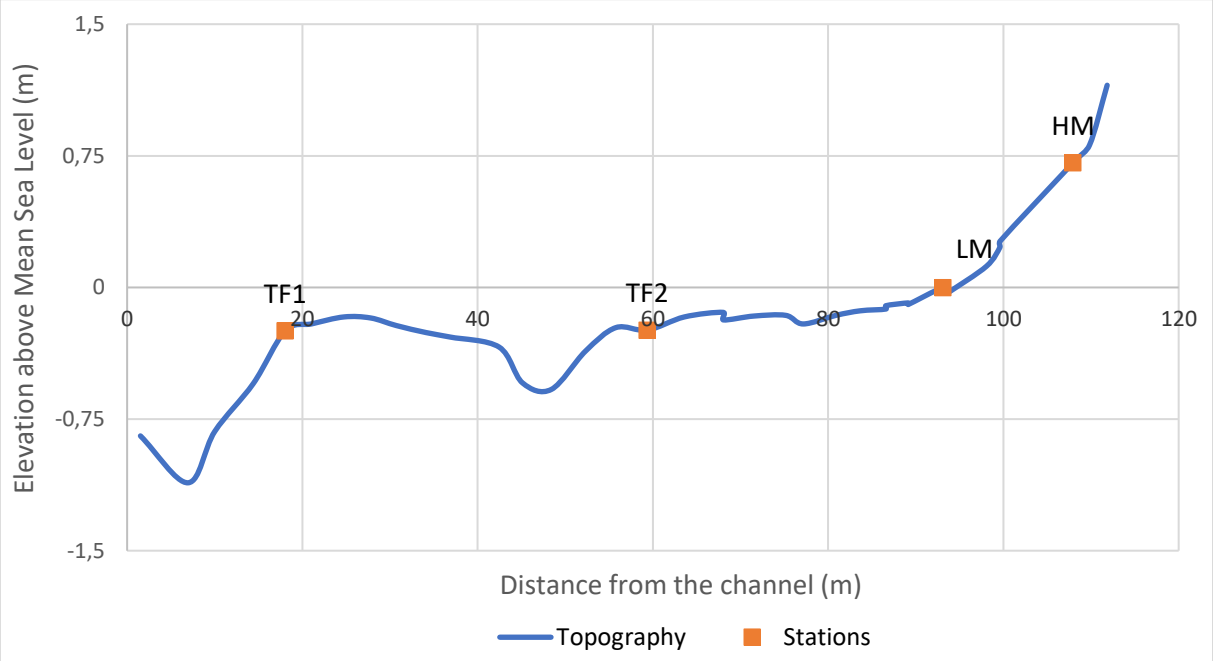

Figure 11: Topography along the studied transect and location of the surveyed stations

4.1.2. Grain size distribution

The grain size characteristics of each station are presented in Table 2. These results were obtained with Gradistat software, where d50 is the particle size corresponding to cumulative percentage of 50%. An increase of sediment grain size is observed along the transect (towards the HM; Table 2). TF1 is the morphology showing the lowest median grain diameter of 5.02 µm. Samples from TF2 have almost the same grain size, with a d50 equal to 5.14 µm. Sediment from tidal flat (TF1 and TF2) can be classified in the very fine silt category. Above the tidal flat, on the low marsh (LM), d50 is equal to 8.64 µm and on the high marsh (HM), d50 is equal to 8.15 µm. Both LM and HM belong to the fine silt class.

Table 2: Grain size distribution per surveyed station

Station	Tidal Flat 1 (TF1)	Tidal Flat 2 (TF2)	Low Marsh (LM)	High Marsh (HM)
d50 (µm)	5.02	5.14	8.64	8.15

4.1.1. Organic matter content

The OM content (Figure 12) is measured in the deposited sediment (Table 1). During the 26th of January survey, only a small amount of 4.96% OM was settled at TF1, which is very low especially compared to TF2, which has OM content of 52.05% of the total sediment weight (Figure 12). Due to an error in the sample analysis, it is not possible to compute the OM for LM. During the 6th of June survey, the OM content is 25.82% in TF1, 23.03% in TF2, and 28.41% in LM (Figure 12). The highest OM content in this tide was found at LM. OM content is variable between TF1 and TF2 during NTs. During the 28th of February campaign, the lowest OM content is found at TF2, with a value of 4.05%. The other station of the tidal flat, TF1 has the second lowest OM content with 7.10%. On the salt marsh, the values are higher than on the tidal flat, with 8.86% for LM and 11.93% at HM (Figure 12). For the 26th of April samples, the highest OM content is measured in TF1 with a value of 41.72%. At the remaining stations, OM content appears to increase with the distance from the channel, with values of 23.48%, 31.76 % and 34.90% for TF2, LM and HM, respectively (Figure 12**Erreur ! Source du renvoi introuvable.**). As for NTs, values are very different for the two STs. Still, without taking TF1 in account, values at TF2, LM and HM seem to show the same trend for the two STs. The OM content changes irregularly between campaigns. But it

seems that the highest stations, LM for NTs and HM for STs have higher OM content, as well as TF1 which is supplied by the channel. TF2 which is close to the creek does not have a high OM content, except for the 26th of January campaign.

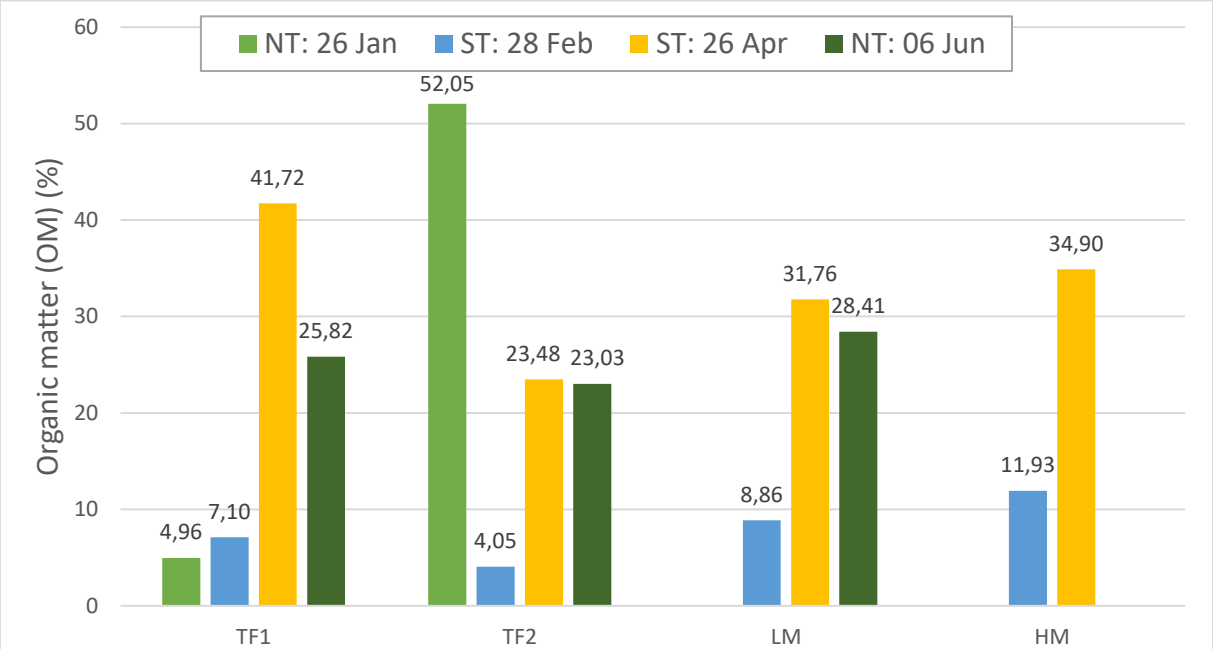

Figure 12: Organic Matter content (%) in samples collected during fieldworks

4.1. Hydrodynamic conditions recorded during fieldwork

During the NT, the two stations where the EMCM is placed (TF2 and LM) show differences in hydrodynamic characteristics (Table 3). The difference in hydroperiod is 1.06 hrs for a maximum water depth difference of 0.18 m. The mean alongshore and cross-shore velocities are higher at TF2 by 1.16 cm/s and 0.44 cm/s, respectively. The mean resultant velocity is therefore also higher at TF2 by 3.04 cm/s. The mean current direction is different by 17.65°, with a higher alongshore component at TF2. The NMF is higher at TF2 than at LM by 547.11 m^3/m^2 during the flood and by 203.06 m^3/m^2 during the ebb.

Comparing TF2 and LM during the ST (Table 3), there is a difference of 0.67 hrs with a difference in maximum water depth of 0.2 m. The mean alongshore velocity and mean cross-shore velocity are higher at LM with a difference of 2.70 cm/s for the alongshore velocity and 0.41 cm/s for the cross-shore velocity. The currents have similar average direction (difference of 2.94°). The resulting velocity of the two components has a

difference of 2.67 cm/s higher at LM than at TF2. The NMF during the flood is higher at LM by 506.70 m^3/m^2. In contrast, during the ebb, the NMF is higher at TF2 by 21.50 m^3/m^2.

Comparing the hydrodynamic conditions for the two salt marsh stations, it appears that the hydorperiod is longer at LM by 2.1 hrs for a water depth difference of 0.62 m (Table 3). The mean alongshore and cross-shore velocities are higher at LM, by 4.53 cm/s and 0.20 cm/s, respectively, with higher resultant average velocity is much at LM by 4.28 cm/s compared to HM. The difference between the mean direction of the currents is 44.83° and is the highest observed in all stations, which means that their main directions do not have the same main component. Finally, the difference between the NMF of the two stations is 1109.19 m^3/m^2 during flood and is much lower, 12.72 m^3/m^2, during ebb.

Table 3: Comparison of hydrodynamic conditions at each station for the two tide conditions

		Neap tide						Spring tide								
		TF2			LM			TF2			LM			HM		
		min	mean	max	min	mean	max	min	mean	max	min	mean	max	min	mean	max
Hydroperiod	hh:mm	7:35			6:31			7:19			6:39			4:33		
	hrs	7.58			6.52			7.32			6.65			4.55		
Maximum water depth	m	1,23			1.05			1.76			1.56			0.94		
Tidal range	m	1.80			1.80			3.20			3.20			3.20		
Alongshore velocity	cm/s	-6.01	1.57	9.03	-2.72	0.41	3.14	-3.72	2.32	10.66	-2.15	5.02	16.66	-1.17	0.49	3.11
Cross-shore velocity	cm/s	-2.55	0.77	3.96	-2.31	0.33	3.61	-1.49	1.11	4.87	-2.01	1.52	5.11	-4.29	1.38	4.04
Onshore direction	°	13.94	71.50	89.99	0.51	53.85	89.84	2.58	71.69	89.94	2.78	74.63	89.93	0.03	29.80	89.58
Resultant velocity	cm/s	0.34	5.04	9.85	0.26	2.03	4.40	0.09	3.86	11.12	0.60	6.53	17.11	0.32	2.25	4.35
NMF flood	m^3/m^2	811.15			264.04			784.59			1291.29			182.10		
NMF ebb	m^3/m^2	399.03			195.97			167.38			145.88			133.16		

The hydrodynamic measurements are described below. The different figures show the hydroperiod at the different stations (A), the direction of the current velocities in figures B determined using equation 1 (methods; chapter 3), as well as the velocity magnitude of the alongshore (C) and cross-shore (D) current components.

4.1.1. Current measurements in tidal flat (TF2)

During NT, the maximum water level reached is 1.23 m and TF2 shows a total immersion time of 7.58 hrs (Figure 13A). Values of the current direction are around 70° during the entire tide (Figure 13B). The direction is therefore alongshore, almost in the same direction as the channel, with a weak cross-shore component. The alongshore velocity is higher during the flood phase than during the ebb phase (Figure 13C). Indeed, the maximum value of the alongshore velocity during flood is 9.03 cm/s, whereas during the ebb tide it is -6.01 cm/s. The cross-shore velocity shows less difference in highest magnitudes between the two parts of the tide, with peak values of 3.96 cm/s during flood phase and of -2.55 cm/s during ebb phase (Figure 13D). At the end of the measurement period, the cross-shore current velocity turns positive, in the same direction as during the flood tide (Figure 13D). The calculated NMF during the flood tide was 811.15 m^3/m^2, and 399.03 m^3/m^2 during the ebb tide (Table 3).

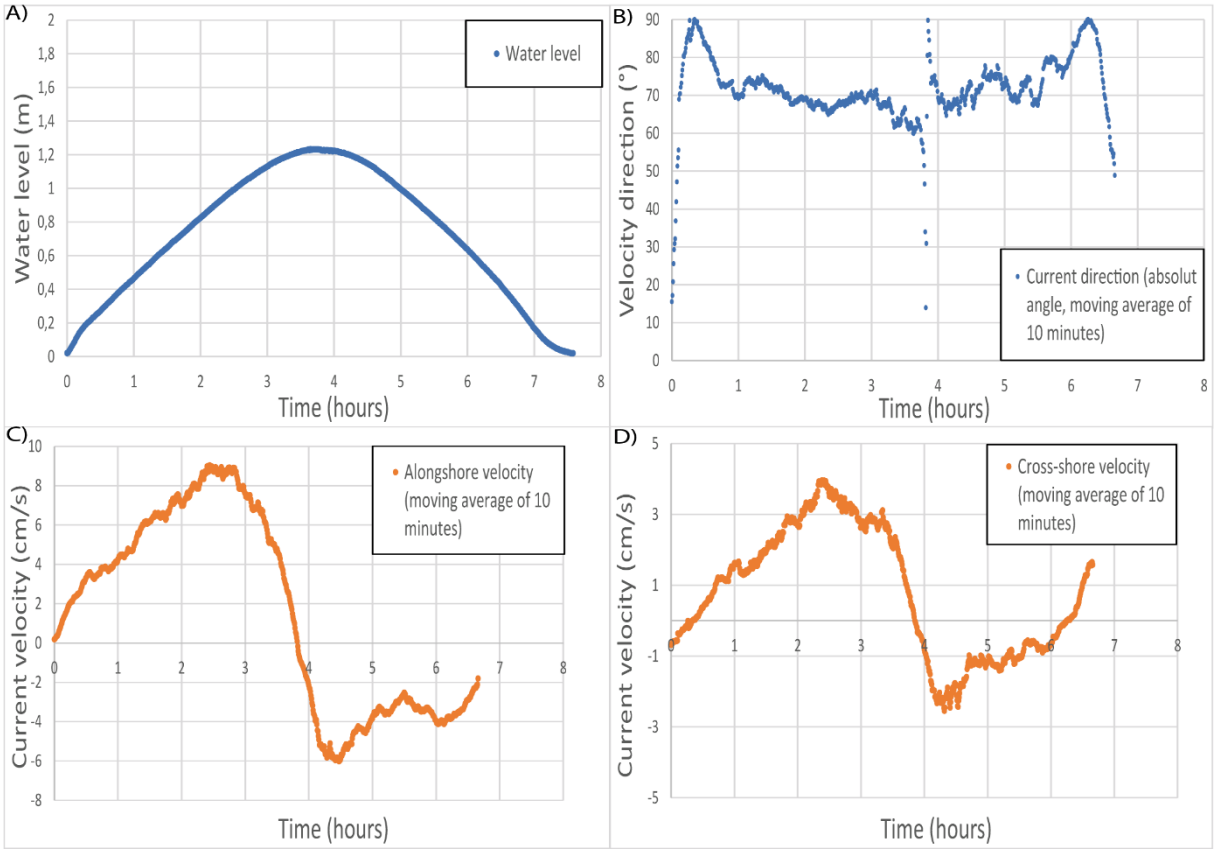

Figure 13: Current velocity characteristics at TF2 during a NT: water level (A), current direction (absolute angle) relative to cross-shore direction (B), alongshore (C) and cross-shore (D) velocity magnitude components with positive values during the flood and negative values during ebb

The ST at TF2 has a hydroperiod of 7.32 hrs with a height of 1.76 m (Figure 14A). The change between flood and ebb phases occurs around 3.60 hrs. The direction of the currents shows a weak positive trend between 60° and 80° (Figure 14B). The currents have therefore a mainly alongshore component, with a weak cross-shore component, more marked during the flood phase. During the last half hour of the tide, the direction of the currents turns towards a more pronounced cross-shore component. For the alongshore velocity (Figure 14C), the minimum value is -3.72 cm/s, and the maximum value is 10.66 cm/s. The cross-shore velocity has a minimum value of -1.49 cm/s and a maximum value of 4.87 cm/s (Figure 14D). During the ebb, some values are positive for the cross-shore velocity, like data recorded during the NT. This explains why the current direction (Figure 14B) has a more pronounced cross-shore component at the final phase of the tide. The velocity of the alongshore and cross-shore currents is higher during the flood than during the ebb. The NMF during the flood tide reached 784.59 m^3/m^2 and during the ebb, it was 167.38 m^3/m^2 (Table 3).

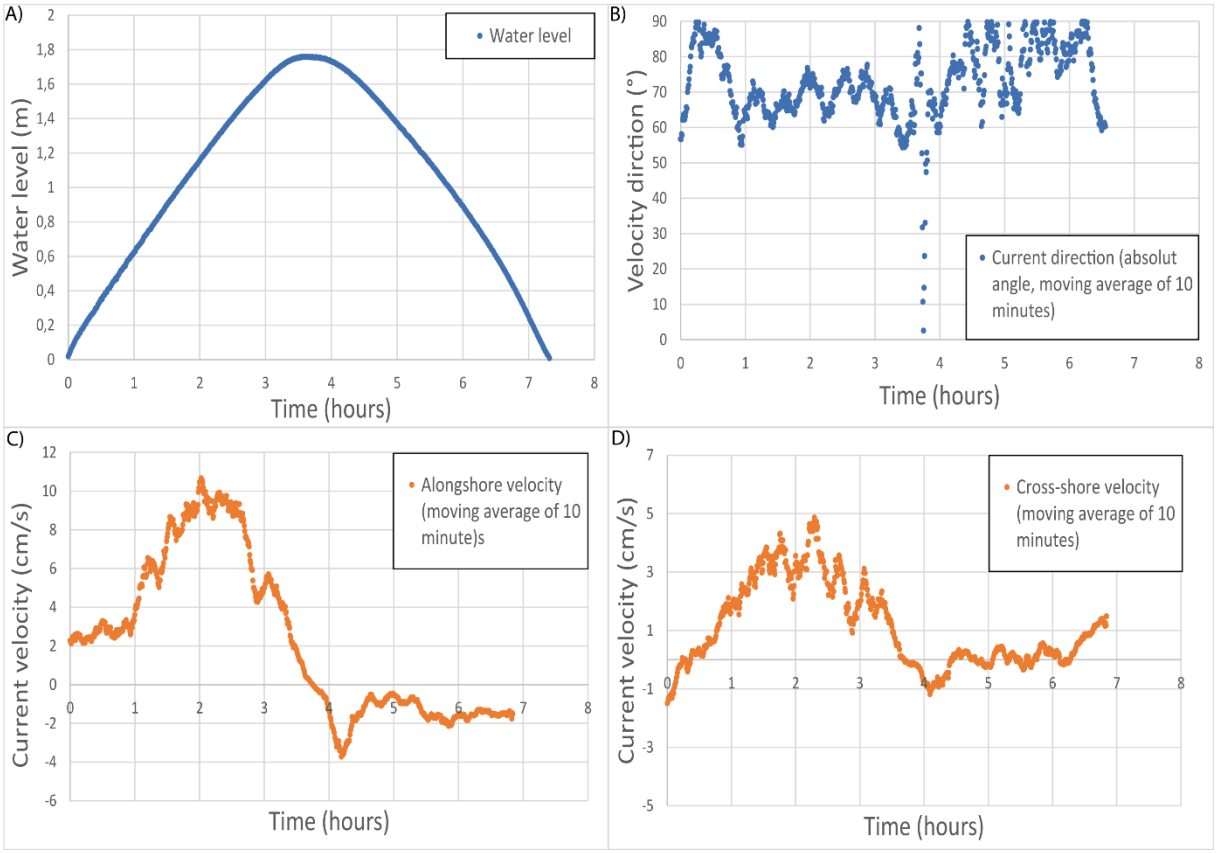

Figure 14: Current velocity characteristics at TF2 during a ST: water level (A), current direction (absolute angle) relative to cross-shore direction (B), alongshore (C) and cross-shore (D) velocity magnitude components with positive values during the flood and negative values during ebb

Comparing TF2 water levels during the two tidal conditions, it appears that the hydroperiods are almost the same (7.58 hrs during NT and 7.32 hrs during ST), with a difference of 0.26 hrs, which is considered insignificant. On the other hand, the maximum water depth is 0.53 m higher during ST at the same station (Table 3). The difference in mean current velocity direction is negligible, with values of 71.50° and 71.69° for NT and ST, respectively. As far as the velocity magnitudes are concerned, the alongshore component has a higher range of values than the cross-shore component for both tides. The maximum values during the flood are 9.03 cm/s (NT) and 10.66 cm/s (ST) for the alongshore velocity and 3.96 cm/s (NT) and 4.87 cm/s (ST) for the cross-shore velocity. Comparing velocities during ebb (Table 3), it appears that the maximum alongshore velocity magnitude is nearly twice during NT, as during ST (-6.01 cm/s, versus -3.72 cm/s). The difference is less important for the cross-shore velocity with a minimum velocity of -2.55 cm/s during NT and -1.49 cm/s during ST. The mean alongshore and cross-shore velocities are higher during ST with a difference of 0.85 cm/s and 0.34 cm/s, respectively (Table 3). The resultant velocity magnitude is slightly different, with

an average of 5.04 cm/s for NT, versus 3.86 cm/s for ST and maximum values of 9.85 cm/s for the NT and 11.12 cm/s during the ST. During the flood phase, NMF were similar, with a difference of 26.56 m^3/m^2 between the two tide conditions. During ebb tide, the difference is more pronounced, with 231.66 m^3/m^2 more during the NT (Table 3).

4.2.2. Current measurements in salt marsh (LM and HM)

Because of its elevation, the flooding time in LM is lower than TF2, with a hydroperiod of 6.52 hrs and a maximum water column height of 1.05 m, reached at 3.33 hrs (Figure 15A), during NT. At the beginning of the tide, the direction of the current is mainly alongshore (Figure 15B). After 1.23 hrs, current direction changes quickly to 30°, which means the cross-shore component becomes the main component. At the end of the ebb phase, the current returns to a more alongshore direction with a higher cross-shore component than at the beginning of the flood phase. Minimum values are -2.72 cm/s for the alongshore velocity (Figure 15C) and -2.31 cm/s for the cross-shore velocity (Figure 15D). The velocity is higher during the flood, with maximums reaching 3.14 cm/s for the alongshore velocity and 3.61 cm/s for the cross-shore velocity (Table 3). At the beginning of the record (Figure 15D), during flood, the cross-shore velocity has negative values which means that the velocity is directed offshore. During ebb, cross-shore velocity is mainly directed offshore as well (negative), except for the fluctuations noted after 4.80 hrs (near-zero values of variable direction). The NMF is lower than at TF2, with 264.04 m^3/m^2 passing through the station during the flood phase and only 195.97 m^3/m^2 during the ebb phase (Table 3).

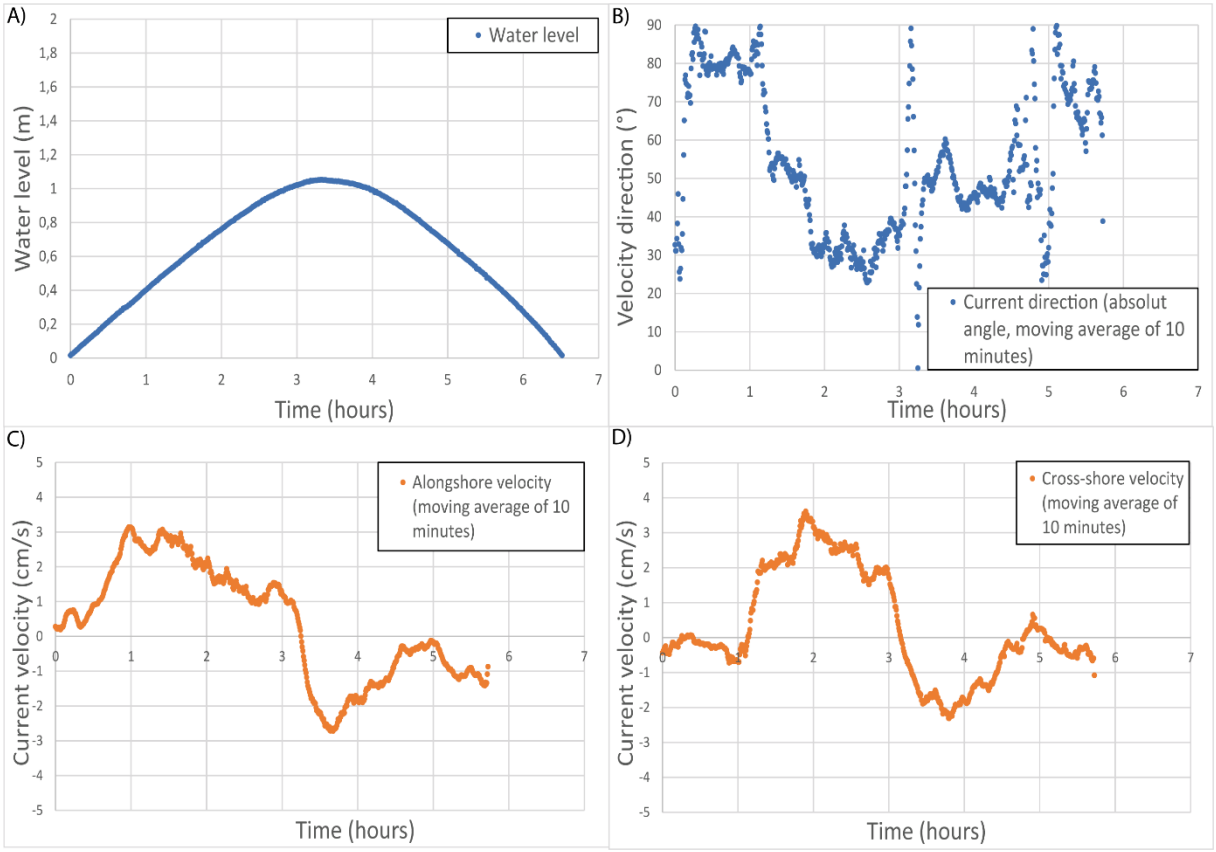

Figure 15: Current velocity characteristics at LM during a NT: water level (A), current direction (absolute angle) relative to cross-shore direction (B), alongshore (C) and cross-shore (D) velocity magnitude components with positive values during the flood and negative values during ebb

During the ST, LM has an immersion time of 6.65 hrs and the maximum water column depth is 1.56 m (Figure 16A). The change between flood and ebb phases occurs at 3.27 hrs. The direction of the currents has a positive trend during the tide (Figure 16B), showing a predominantly alongshore direction with a weak cross-shore component. The alongshore velocity magnitude (Figure 16C) is significantly higher during the flood phase than during the ebb phase. The maximum alongshore velocity magnitude is equal to 16.66 cm/s and the minimum value is -2.15 cm/s (Table 3). Regarding the cross-shore velocity (Figure 16D), it appears that, once again, the current changes its direction several time during the ebb phase. The cross-shore velocity fluctuates between 5.11 cm/s and -2.01 cm/s. The NMF during flood is equal to 1291.29 m^3/m^2, significantly higher than the one during the ebb tide, which is 145.88 m^3/m^2 (Table 3). The flux during the flood phase is the largest recorded during this study.

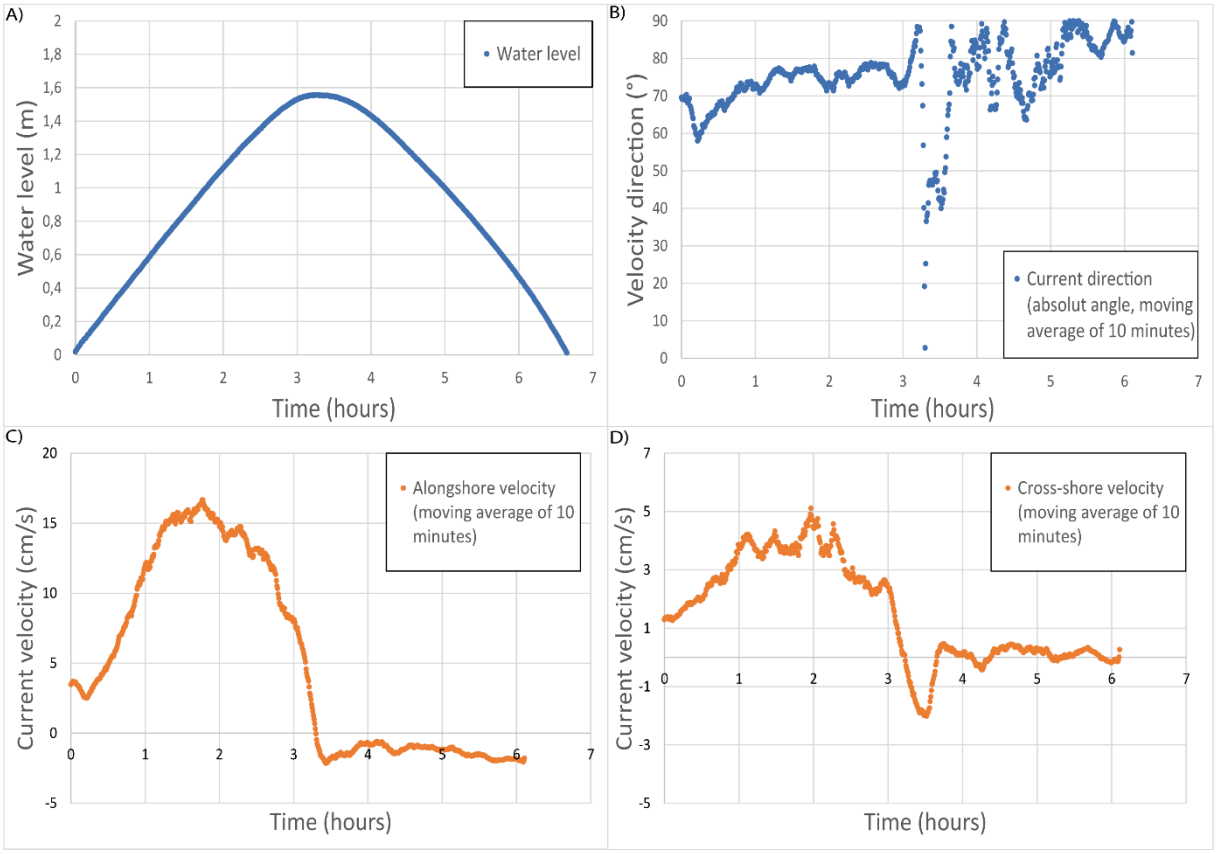

Figure 16: Current velocity characteristics at LM during a ST: water level (A), current direction (absolute angle) relative to cross-shore direction (B), alongshore (C) and cross-shore (D) velocity magnitude components with positive values during the flood and negative values during the ebb

The hydroperiod at the LM station is the same for NT and ST, with 6.52 hrs (Figure 15A) and 6.65 hrs, (Figure 16A) respectively, and with a difference of maximum water elevation of 0.51 m (Table 3). The direction of the currents at LM is different for the two types of tides. During NT, the onshore direction is 53.85°, and it is 74.63° during ST, which means that the main component of the currents is the alongshore component for both tidal conditions, but it is more pronounced during ST (Table 3). The mean alongshore velocity is much high during ST, with 4.61 cm/s more than during NT. Similarly, the mean cross-shore velocity and the mean resultant velocity are higher by 1.19 cm/s and 4.50 cm/s during ST. During the flood, the NMF is higher during ST with a difference of 1027.25 m^3/m^2. On the contrary, during the ebb, the NMF is higher during the NT with a difference of 50.09 m^3/m^2 (Table 3).

As HM is the highest station of the transect, its hydroperiod is the shortest of all stations with an immersion time of 4.55 hrs (Figure 17A). The change between flood and ebb occurs at 2.12 hrs with a maximum water height of 0.94 m. The current direction (Figure 17B) fluctuates

during the tide with a negative trend. At the beginning of the tide, the main component is alongshore, but quickly changes to cross-shore, at 0.5 hrs. Thereafter, the direction tends to fluctuate between the two components, but during ebb the main component is cross-shore (Figure 17B). The alongshore velocity (Figure 17C) does not follow the same pattern as in the other stations (TF2 and LM). Values decreases from around 1.0 cm/s to almost 0 cm/s in the first 40 minutes of measurement, to increase again after and reach a maximum value of 3.11 cm/s. During the ebb, alongshore velocities turn negative, with minimum values around -1.17 cm/s. The maximum alongshore velocity magnitude during ebb tide is, therefore, lower than during flood phase. Regarding the cross-shore velocity the change between flood and ebb is characterized by a negative spike that reaches the minimum value of -4.29 cm/s at 2.13 hrs (Figure 17D). Before and after this spike, all the data recorded are positive. The cross-shore velocity therefore maintains the same direction during most of the tide, even during its ebb phase. The NMF at this station during the flood tide is 182.10 m^3/m^2 and during the ebb tide it is 133.16 m^3/m^2 (Table 3).

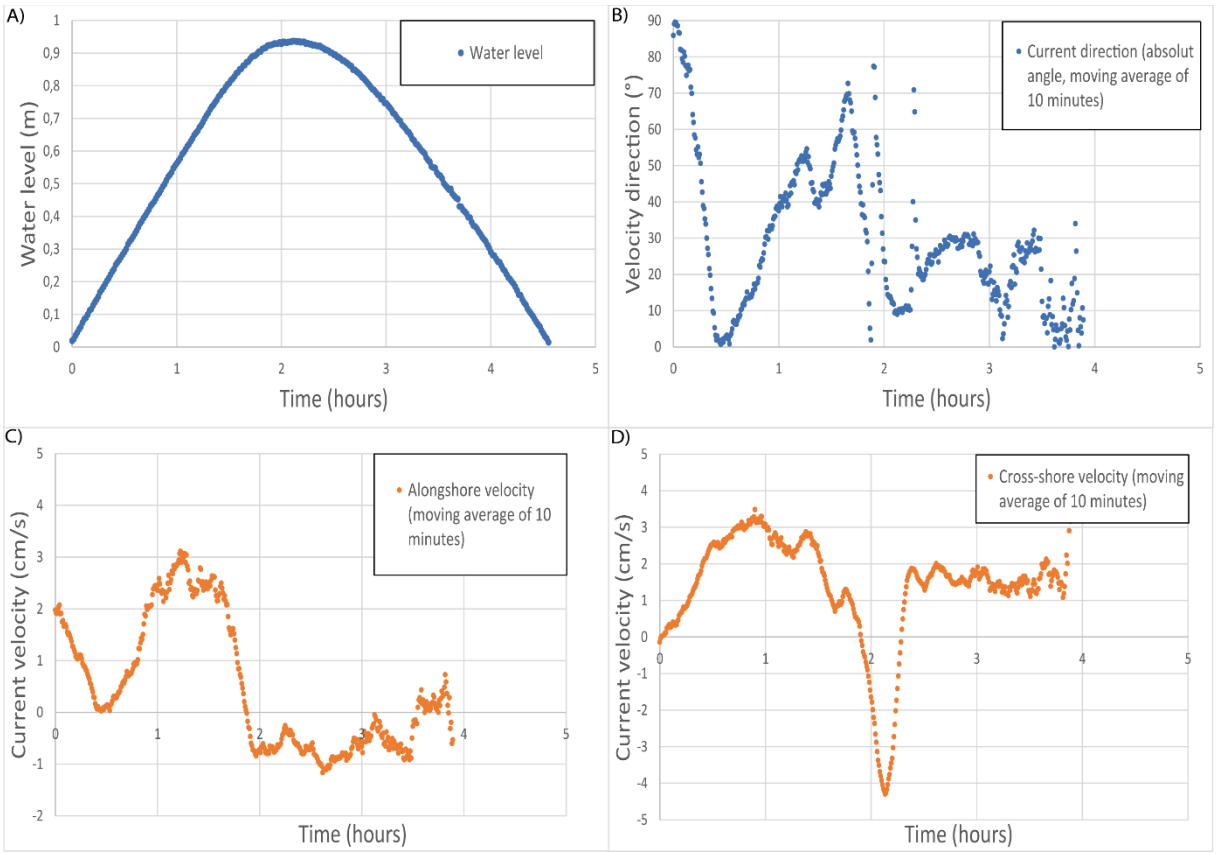

Figure 17: Current velocity characteristics at HM during a ST: water level (A), current direction (absolute angle) relative to cross-shore direction (B), alongshore (C) and cross-shore (D) velocity magnitude components with positive values during the flood and negative values during the ebb

As HM is flooded only during STs, it is not possible to compare it for the two tidal conditions. However, it has some similarities with the LM station during NT. Indeed, they have similar maximum water depths (difference of 0.11 m) and average alongshore velocities (difference of 0.08 cm/s), slightly higher differences in cross-shore velocities (higher in HM by 1.05 cm/s; Table 3), while flow at HM has a strong cross-shore component (mean direction of 29.80°). Finally, the NMF is larger at LM during NT than at HM during ST for both phases of the tide with a difference of 81.94 m^3/m^2 during the flood and 62.81 m^3/m^2 during the ebb (Table 3).

4.3. Sediment transport

4.3.1. Suspended sediment transport

The SSC samples were collected at different elevations in the water column, as described in the methods section. SSCs measured during the NT are sampled at the intake of -0.15 m and 0.65 m, with reference to MSL (Figure 18) for stations TF1 and TF2. Both stations show decreasing SSC with depth, ranging between 9.51 and 18.73 mg/l in TF1 and between 18.08 and 29.52 mg/l in TF2. At LM, the SSC at the elevation of 0.4 m from MSL was 12.32 mg/l. Along the transect, SSCs almost double at TF2, compared to TF1, located close to the channel, while at the LM SSCs drop to values close to the ones in TF1.

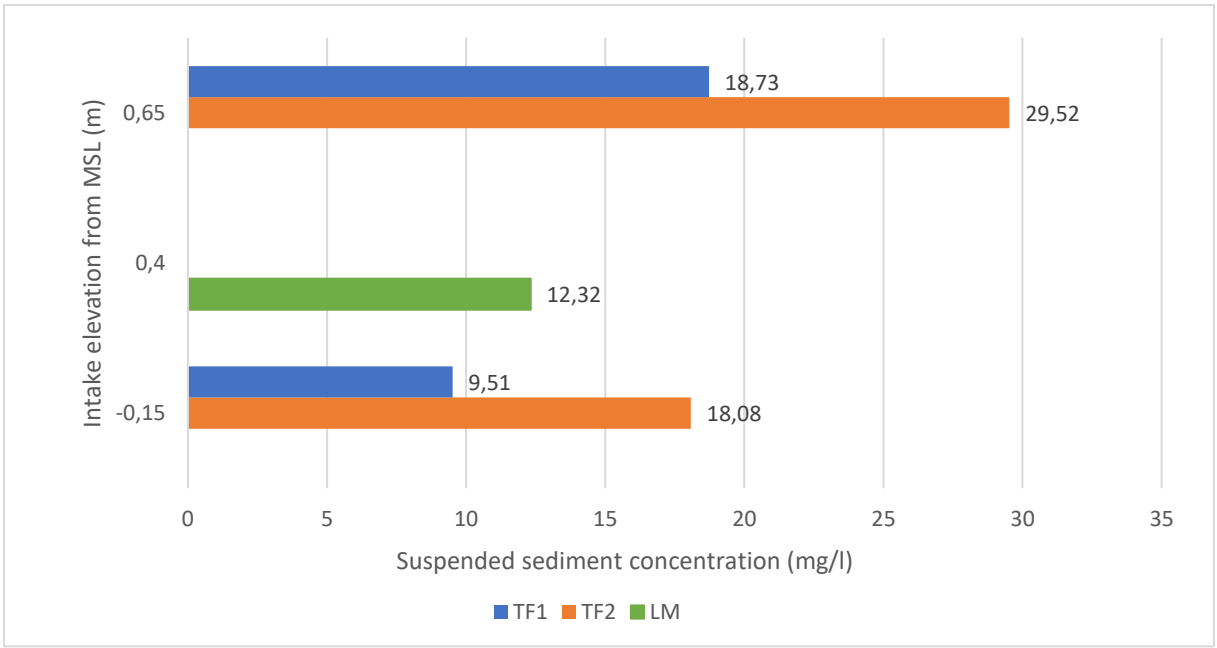

Figure 18: Variability of Suspended Sediment Concentration (SSC, in g/ml) with depth, measured during the NT conditions for TF1, TF2 (intake elevations of -0.15 m and 0.65 m from MSL, corresponding to 0.1 m and 0.9 m from the bed) and LM (intake elevation of 0.4 m from MSL corresponding to 0.4 m from the bed).

During the ST, SSCs tend to increase along the transect toward the marsh. TF1 shows near-stable concentrations with depth (6.65, 7.22 and 7.09 mg/l at -0.15, 0.65 and 1.25 m from MSL, respectively), while TF2 has higher SSCs and a peak in the middle of the column (7.85, 11.93 and 8.23, at -0.15, 0.65 and 1.25 m from MSL, respectively; Figure 19). SSCs at LM increase with depth, ranging from 12.09 at 1 m from MSL, to 24.65 mg/l near the bed (0.4 m from MSL), which is the highest SSC recorded during all field campaigns. The SSC also increases in the higher part of the water column along the transect (Figure 19) with values ranging from 8.23 mg/l in TF1 to 14.19 mg/l for HM. The highest difference of SSCs in the column appears at the LM station.

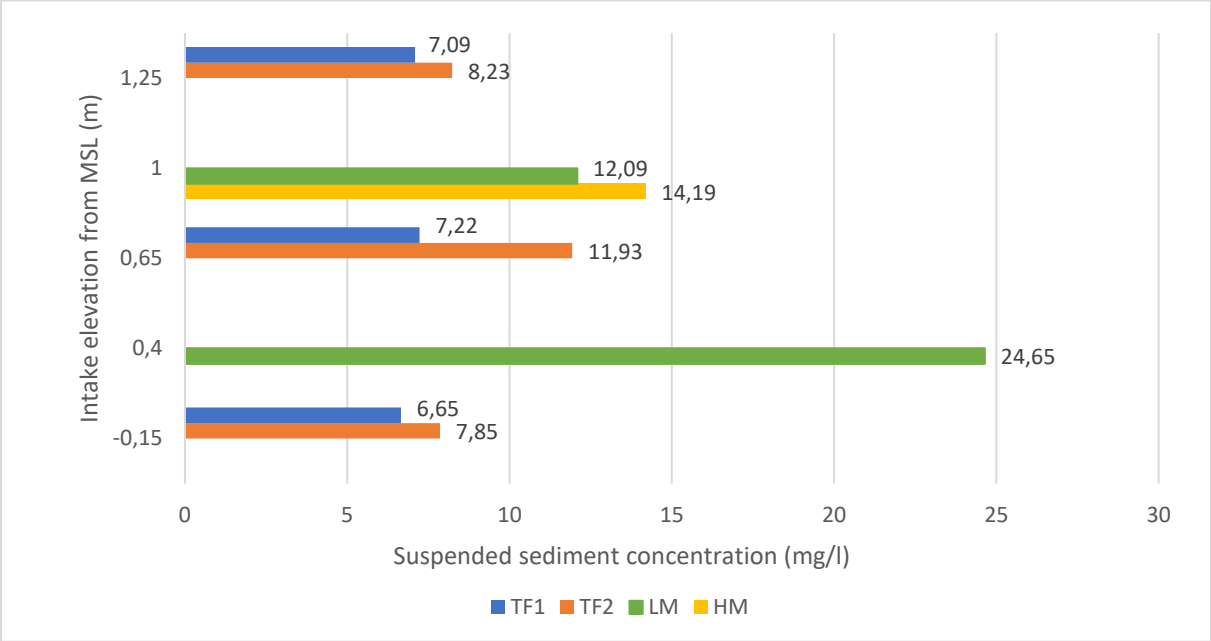

Figure 19: Variability of Suspended Sediment Concentration (SSC, in g/ml) with depth, measured during the ST conditions for TF1 and TF2 (intake elevations of -0.15 m, 0.65 m and 1.25 m from MSL, corresponding to 0.1 , 0.9 m and 1.5 m from the bed), LM (intake elevation of 0.4 m and 1 m from MSL, corresponding to 0.4 m and 1 m from the bed), and HM (intake elevation 1 m from MSL corresponding to 0.4 m from the bed)

The TSSC passing through TF1 is similar for both tides (Figure 20). They become higher at station TF2, with a difference of 3.69 g/m^2 more during NT than ST. Landwards, TSSC decreases, especially at LM for NT conditions (9.79 g/m^2 less than during ST). During the ST conditions at LM, the TSSC value has the same magnitude as the TSSCs on tidal flat stations. Finally, at HM, the TSSC has the lowest value during the ST, close to the one for LM during NT.

As the height of the water column decreases along the transect, it is expected that TSSCs also decrease.

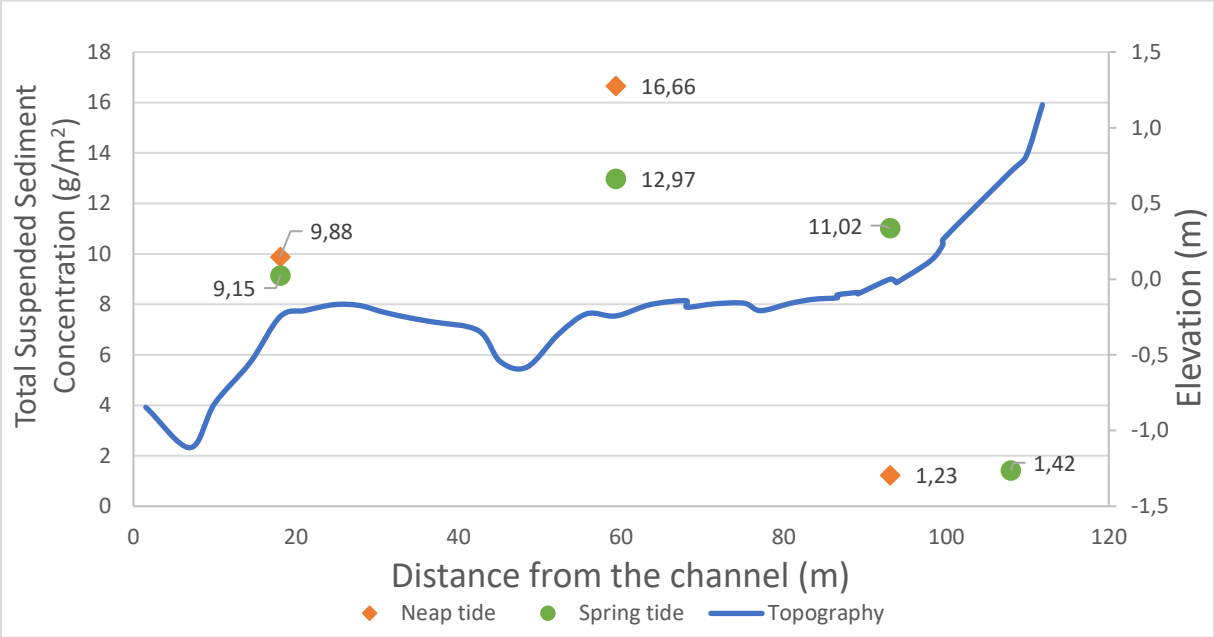

Figure 20: Total Suspended Sediment Concentration (TSSC, in g/m²) during the two tide conditions

4.1.1. Sediment bed deposition

The main difference during the two tide conditions is the tidal range, and thus the height of the water column. Tidal ranges during NTs are the same, but during STs, there are small differences. As samples on LM and HM were collected on different tides during ST, an average of the tidal ranges of these tides is made. There is a difference of 1.3 m to 1.5 m between tidal ranges from NTs and those from STs. The hydroperiod used to calculate the DR and tidal ranges of respective tides are presented in the Table 4.

Table 4: Hydroperiods of each tide used to calculate de DR and their tidal ranges

	Neap tide				Spring tide			
	26th of Jan. survey		6th of Jun. survey		28th of Feb. survey		26th of Apr. survey	
Station	Hydroperiod (hrs)	Tidal range (m)	Hydroperiod (hrs)	Tidal range (m)	Hydroperiod (hrs)	Tidal range (m)	Hydroperiod (hrs)	Tidal range (m)
Tidal Flat 1 (TF1)	6.75	1.8	7.40	1.8	7.32	3.2	8.12	3.2
Tidal Flat 2 (TF2)	6.82	1.8	7.58	1.8	7.32	3.2	8.12	3.2
Low Marsh (LM)	5.28	1.8	6.52	1.8	6.88	3.2	7.29	3.2
High Marsh (HM)					4.21	3.2	4.03	3.2

Below are the results of the laboratory analysis of the samples of deposited sediment (Figure 21). During the 26th of January survey (NT), the amount of sediment deposited decreases inland along the transect, with the maximum sediment weight of 0.095 g collected at TF1 and the minimum of 0.063 g at LM (Figure 21). During the same campaign, 0.090 g of sediment are deposited at TF2. The results of the 6th of June survey (NT) do not show the same trend as the 26th of January survey. On the 6th of June, the amount of deposited sediments are equivalent on the tidal flat with 0.110 g at TF1 and 0.109 g at TF2. The highest value measured during this campaign is at LM with 0.117 g (Figure 21). Regarding the amount of sediment deposited for ST conditions, on the 28th of February, it is higher on the tidal flat than on the salt marsh (Figure 21). There are 0.113 and 0.122 g of deposited sediment at TF1 and TF2 respectively. Salt marsh stations have almost the same amount of deposited sediment, with 0.104 g (LM) and 0.100 g (HM). For the 26th of April campaign, the highest amount of sediment deposited was 0.110 g at TF2. HM had the second highest amount of sediment with 0.098 g, and TF1 and LM received almost the same amount, with 0.094 g and 0.090 g, respectively (Figure 21).

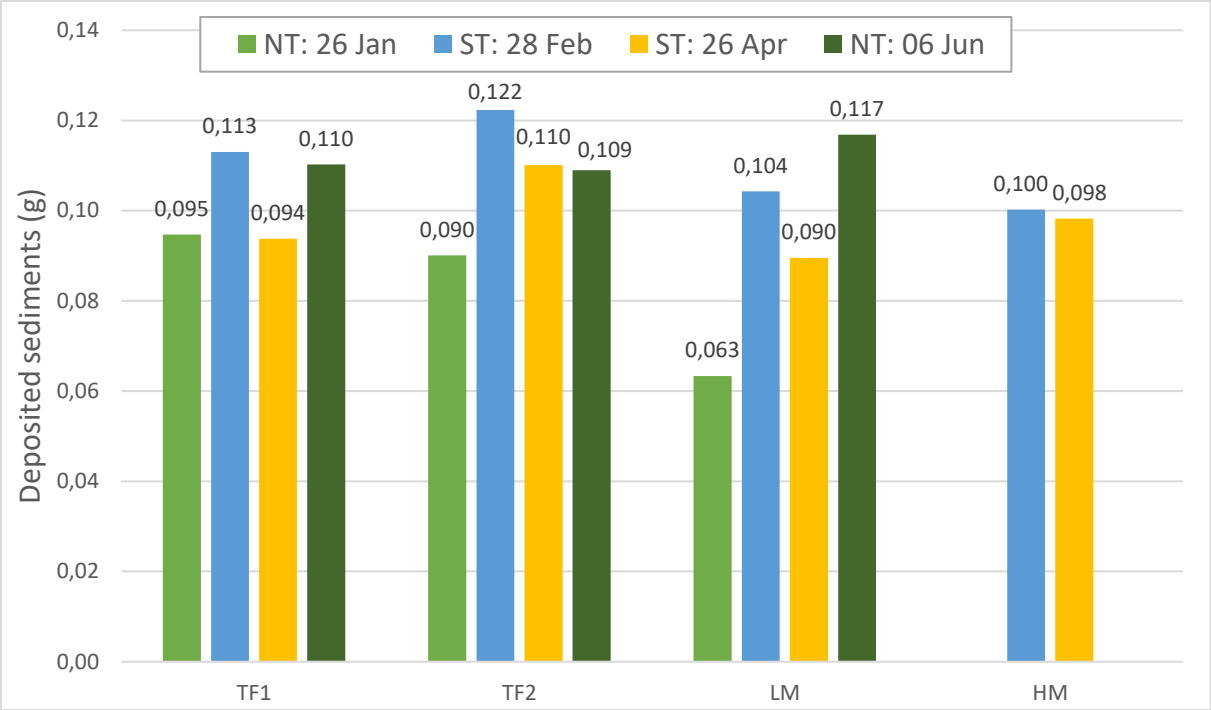

Figure 21: Amount of deposited sediments (in g) during the four campaigns

The DRs of the 26th of January campaign vary between 6.62 g/m²/hr (TF1) and 5.65 g/m²/hr (LM; Figure 22). DR values in the tidal flat station are very similar. Likewise, the lowest DR of the 6th of June campaign is at TF2 (20.34 g/m²/h), with a similar rate for TF1 (21.08 g/m²/h). The highest DR measured is 25.45 g/m²/h, at LM (Figure 22). There are notable differences in DR patterns along the transect between NT campaigns. All the DRs are higher during the 6th of June campaign. The differences in DRs are almost identical on the tidal flat with a difference of 14.46 g/m²/h on TF1 and 14.11 g/m²/h on TF2. On the ST of the 28th of February, the highest DR is 33.80 g/m²/h on HM, followed by 23.65 g/m²/h on TF2 (Figure 22). TF1 and LM have almost the same DRs with 21.86 g/m²/h and 21.52 g/m²/h, respectively. During the 26th of April campaign, HM is again the station with the highest DR (35.45 g/m²/h), while the other marsh station, LM, had a DR of 17.25 g/m²/h (Figure 22). On the tidal flat, the DR of the closest station to the channel, TF1, is 16.34 g/m²/h and that of TF2 is 19.19 g/m²/h (Figure 22). The differences in DRs between the two ST campaigns are similar between stations with differences of 0.52 g/m²/h at TF1, 4.46 g/m²/h at TF2, 4.27 g/m²/h at LM and 1.65 g/m²/h at HM. Looking at the two surveys during the ST conditions, it appears that the DRs show very similar trends, with almost uniform DR along the tidal flat to the low marsh (TF1, TF2, and LM) and with higher rates in the high marsh.

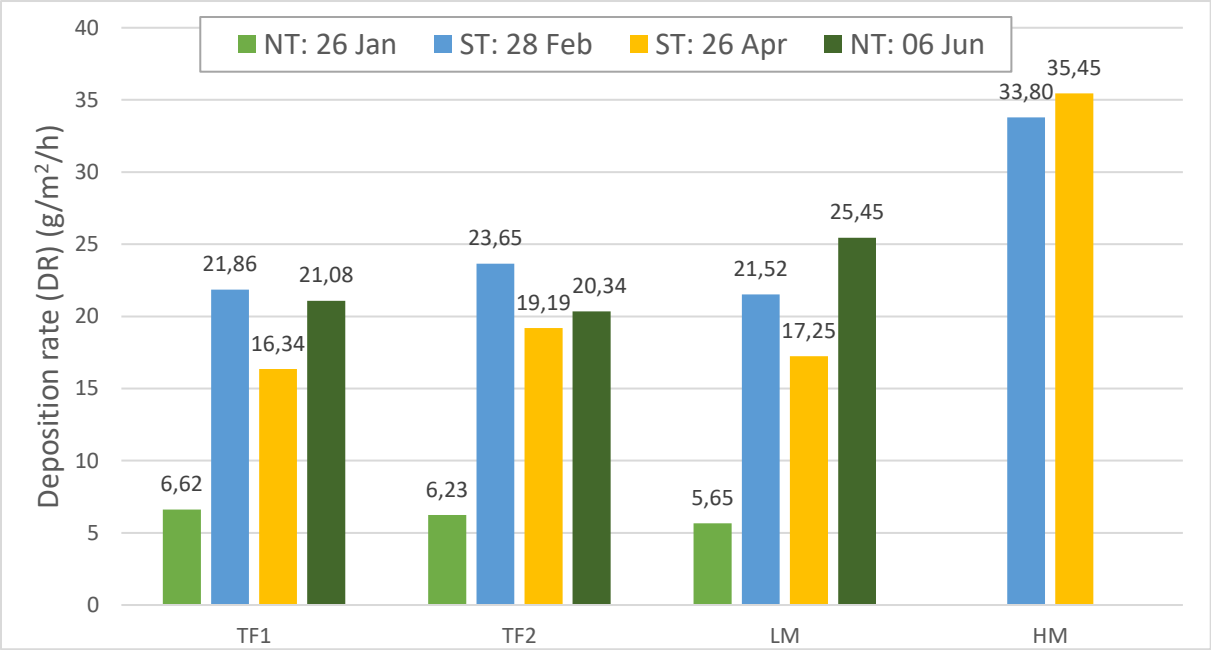

Figure 22: DR (in g/m²/h) compared between all campaigns

DRs are summarized in a boxplot, to illustrate the spatiotemporal variability between monitoring stations along the transect and between tides (Figure 23). The median of DR varies between 137.09 g/m^2/tide (LM) and 154.97 g/m^2/tide (TF2). The highest interquartile range (49.56 g/m^2/tide) is at LM, with a similar range in TF1 (46.32 g/m^2/tide) and a slightly lower value in TF2 (33.79 g/m^2/tide). The lowest interquartile range is noted in HM, with only 1.46 g/m^2/tide, partly due to the fewer samples (only 2). The maximum values are closer to the median than the minimum values. These minimum values are measured during the campaign of 26th of January.

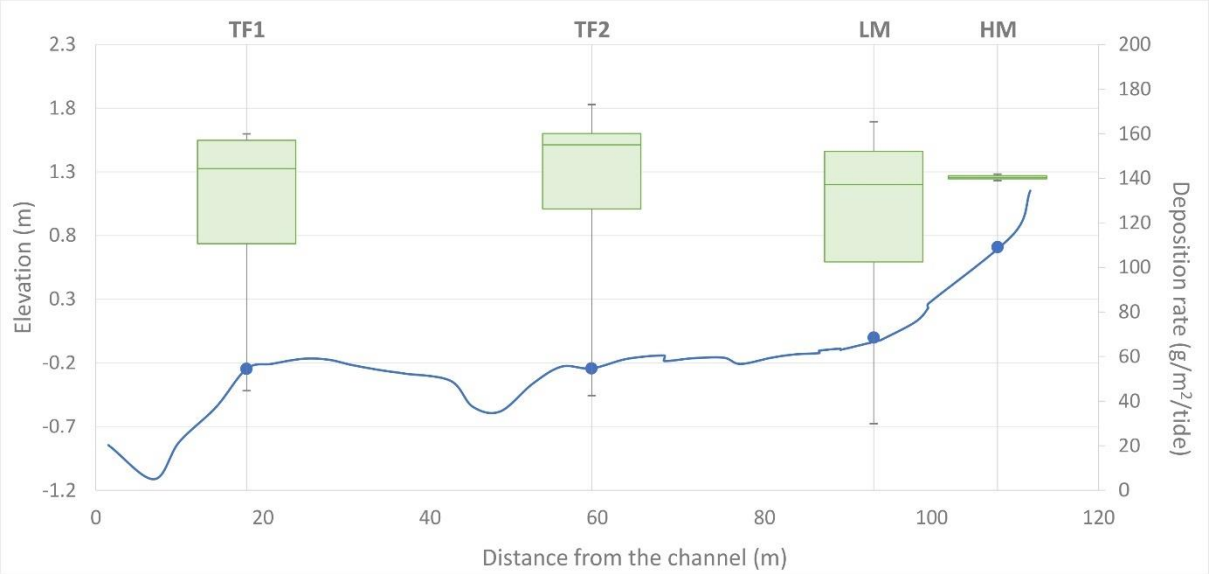

Figure 23: Whisker boxplots of DR (in g/m²/tide) of the four campaigns, with the respective position of stations

5. Discussion

5.1. Sediment transport in the coastal wetland

To characterise sediment transport in the Ria Formosa, this study considers the topography, sediment sizes, hydrodynamic conditions of the tidal flat and salt marsh (water column height, hydroperiod, current velocity and direction), and the SSC.

The topographic data shows a regular elevation during the tidal flat, while on the salt marsh (0 m compared to MSL, Figure 11), the topography elevation rises faster. The sediment size increases towards the land from the very fine silt class (tidal flat) to a fine silt class (salt marsh, Table 2). The difference in water height on the tidal flat (0.53 m) during NT and ST does not seem to be important as the TSSC values have the same magnitude (9.88 g/m^2 at TF1, 16.66 g/m^2 at TF2 during NT, and 9.15 g/m^2, 12.97 g/m^2 during ST; Figure 20). There is a higher difference in TSSC at TF2 (3.69 g/m^2 more during NT) than at TF1 (0.73 g/m^2 more during NT). This may be due to the creek located on the tidal flat which brings more water and more sediments to TF2 and to the inner part of the tidal flat. In contrast, at LM the difference in TSSC is higher with 1.23 g/m^2 during NT and 11.02 g/m^2 for ST (Figure 20), for a difference of height of the water columns of 0.51 m (Table 3). At HM, the TSSC has the same magnitude than LM during NT (1.42 g/m^2 and 1.23 g/m^2, respectively, Figure 20). The difference of tidal condition does not seem to affect sediment transport on the tidal flat but allows a higher TSSC in the low marsh during ST.

The velocity of the currents is the main factor controlling sediment transport and deposition in the Ria Formosa (Rosa et al., 2013; Sousa et al., 2019). Under both tidal conditions, currents have a major alongshore component (71.50° (NT) and 71.40° (ST) at TF2, 53.85° (NT) and 74.63° (ST) at LM and 29.80° at HM; Table 3) but by going further inland, the influence of the alongshore component decreases and the cross-shore component becomes dominant at HM (Figure 17B). There is higher velocity magnitude and NMF during the flood phase than during the ebb phase (Table 3). So, the amount of water and sediment in suspension passing through the stations during the flood (sediment imported to the system) is higher than during the ebb (sediment exported from the system). In addition, the velocity magnitude and NMF decrease towards the land (Table 3). The NMF near the bed is higher during NT than ST on the tidal flat. This means that bottom shear stresses under ST conditions are more favorable for sediment

deposition, as near-bed velocities are lower than during NT. Moreover, the hydrodynamic conditions are more favorable to sediment deposition on the salt marsh than on the tidal flat as the near-bed velocity magnitudes decrease landward (Table 3). However, there is an exception to this at LM during ST, which has the highest alongshore and cross-shore velocity magnitude during the flood (Figure 16C and Figure 16D). This is due to the presence of *Spartina maritima* which has a stiff plant shoot. This species has a positive impact on the current velocities that increase around the vegetation canopy patches (Vandenbruwaene et al., 2011).

The SSC increases with the water level since the highest SSC measured is at 0.65 m of intake during NT (Figure 18). During ST, the SSCs measured at the highest intake (7.09 mg/l for TF1, 8.23 mg/l for TF2, and 12.09 mg/l for LM) are lower than those measured at the second intake, and of the same magnitude as the SSCs measured at the lowest intake (Figure 19). The SSC therefore seems to present a peak around 0.40 m and 0.65 m from MSL in both tidal conditions (Figure 18 and Figure 19). Regarding the TSSC, the highest value measured is at TF2 for both tidal conditions (Figure 20). This station could likely be receiving more sediment input than the others, due to its proximity to the creek. Suspended sediments are brought in by the channel and by the creek which is a source of additional sediment brought directly inland of the tidal flat, allowing a higher TSSC at TF2. Furthermore, the creek likely also influences LM during ST, as the TSSC is higher than that measured at TF1 (11.02 g/m^2 at LM and for TF1 there is 9.15 g/m^2, Figure 20). Marsh stations (LM during NT and HM during ST) have the lowest values (1.23 g/m^2 at LM during NT and 1.42 g/m^2 during ST, Figure 20), as the low water column depth at these stations in these tidal conditions does not allow a significant TSSC.

Sediments are brought into suspension by currents at the study site from the Ramalhete Channel. The different tidal conditions do not influence the sediment transport on the tidal flat. Sediment arrives in suspension directly from the channel at TF1 with an origin upstream of the channel from the station as the current has an alongshore direction on the tidal flat. The other stations are influenced by the creek located on the tidal flat as the TSSC at TF2 for both tidal conditions and LM during ST are higher than that at TF1 (Figure 20). Thus, at TF2, suspended sediments originate from the channel and creek to the Northeast of the transect, as the direction of the currents is alongshore. During NT, the sediment arriving at the station originates from the channel and creek, like TF2, but with a less pronounced alongshore

direction. At LM on ST, the sediments have the same origin as those at TF2. In addition, the velocity magnitude of the currents at LM on ST is the highest in this study, which allows for a higher input of suspended sediment when compared with NT and bring sediment on higher part of the marsh. Finally, station HM receives sediments from the channel and the creek, but with a cross-shore direction (Figure 17 (B)), unlike the other stations.

The SSC measured in this thesis is twice less than the SSC measured in the Phillips Creek (Hog Island Bay, USA, Christiansen et al., 2000). This study reports SSC of 31 mg/l on the high marsh, when the flood starts (Appendix 4), while in the present work SSCs vary between 12.32 g/ml (NT) and 24.56 mg/l (ST) at LM and reach 14.19 mg/l at HM (Figure 18 and Figure 19). Even the highest SSC value (measured at LM on ST) in the Ria Formosa is lower than the one measured in Philips Creek. This marsh area is protected by a barrier island system, as is Ria Formosa. The main difference between the two studies is that in the Hog Island Bay, the marsh and transect they studied is at the edge of the stream that allows the flooding of their study site. In the Ria Formosa lagoon, the marsh is located after a tidal flat. Aside from differences in local sediment budget, the presence of the tidal flat may explain the difference in SSC measure at the marsh, as in Christiansen's study, suspended sediment does not pass through a tidal flat. Ganju et al. (2015) estimated an SSC of 54 mg/l during the flood tide for the Chesapeake Bay, (Appendix 4) in the Blackwater River, which is higher than the SSC measured in the Ria Formosa for the two locations on the marsh (LM and HM) in the two tidal conditions. They explain this SSC value thanks to the wind action which increase the SSC and the DR.

In the Netherlands, in the Rattekaai marsh and in the Sint Annaland marsh, there is an increase of the SSC on the tidal flat until the cliff edge of the marsh (Ma et al., 2018). Along their transect, Ma et al. (2018) estimated a SSC in the order of 576±137 mg/l on the Rattekaai marsh and 34±5 mg/l in the Sint Annaland marsh, during STs (Ma et al., 2018; Appendix 4. The difference in their SSC values between the two marshes in the Netherlands is explained by the wind action which is more important in the Rattekaai marsh. The average SSC in the Ria Formosa during the ST is 11.10 mg/l. Thus, the average SSC is 564.90 mg/l higher in the Rattekaai marsh than in the Ria Formosa, and it is 22.90 mg/l higher in Sint Annaland marsh than in the Ria Formosa. These differences can be explained by the characteristics of the tidal flats and the exposure of the sites. The Dutch tidal flats are more than 500m wide, whereas the Ria Formosa tidal flat is about 93 m wide (Figure 11). In addition, the tidal flats of the Dutch

marshes are non-vegetated, which allows wave and tidal action to resuspend the deposited sediments and bring them further inland towards the marsh (Ma et al., 2018). Moreover, Dutch marshes are non-protected by a barrier system. Rattekaai marsh is located in a bay, and the tidal flat is bordering directly the sea. Sint Annaland marsh is more protected than Rattekaai marsh as this coastal wetland is more enclosed inland. It is supplied with water by a channel that is several kilometres wide. The tidal flat of the Ria Formosa is covered by *Zostera noltei*, which prevents the sediment from being resuspended. At the same time, it is a much more sheltered area compared to the open-sea Dutch sites (especially that of Rattekaai), implying calmer conditions and mainly tidally driven sediment transport.

In the Kingsport marsh in the Minas Basin (Canada), an SSC of 106±66 mg/l on the low marsh and 53±24 mg/l on the high marsh were measured (Poirier et al., 2017; Appendix 4). Again, these SSC values are higher than those find in the Ria Formosa. Their study site is located on a salt marsh patch bordering a creek, with no tidal flat between them. A particularity of their study site is that it has one of the highest tidal ranges measured in the world, with 16m of tidal range (Scott & Greenberg, 1983) Suspended sediments are brought directly from the creek to the marsh. The differences between the SSC values measured in the Minas Basin and those measured in the Ria Formosa are, in part, due to the close distance from sediment sources. The suspended sediments in the Canadian marsh are partially fed by freshwater and sediment inputs from the watershed and come directly from the creek bordering the marsh. In the Ria Formosa, sediments come from the sea and feed the channel and creek which bring sediments on the tidal flat and on the marsh. The high tidal range of the Minas Basin may also have an influence on the high SSC.

In the Paulina marsh in the Netherlands, an SSC of 50 mg/l in measured on the high marsh (Temmerman et al., 2003; Appendix 4). This marsh is on the bank of the Scheldt estuary and open estuary more exposed to the influence of offshores conditions (Temmerman et al., 2003). Moreover, inputs from freshwater system have a major contribution than in Ria Formosa lagoon. In the Wanggang salt marsh (Jiangsu, China) an average SSC of 340 mg/l is measured (Wang, 2010; Appendix). This coastal system is characterized by a large tidal flat of several kilometers. Because of a wider tidal flat than in Ria Formosa, and open to the ocean, with sediment inputs from the mainland, the SSC in the Wanggang salt marsh is much higher than those presented is this study.

5.2 Sediment deposition

Sediments can only be deposited when the velocity of the currents decreases sufficiently to allow them to settle on the bed. In this study, sediment deposition depends on the magnitude of the tidal current velocity (shear stress conditions near the bed), the hydroperiod, and the total amount of sediment delivered by the SSC, and the settling velocity of the sediment grains.

Hydrodynamic conditions are assumed to be equivalent for TF1 and TF2 as these two stations are both located on the tidal flat. During NTs, the amounts of deposited sediment vary from 0.095 g to 0.110 g at TF1, from 0.090 g to 0.109 g at TF2, and from 0.063 g to 0.117 g at LM (Figure 21). The lowest values measured during the NTs were all measured during the campaign of 26th of January. During the STs, the variations in the amount of sediment deposited have smaller ranges with amounts varying between 0.094 g and 0.113 g at TF1, 0.110 g and 0.122 g at TF2, between 0.090 g and 0.104 g at LM and finally between 0.098 g and 0.100 g at HM (Figure 21). The DRs depend on the amount of sediment deposited and amounts of sediment deposited on 6th of June (NT) are of the same magnitude as those deposited during the STs. Moreover, TSSC on the 6th of June survey is on the same magnitude than those of the ST (Figure 20). These two previous arguments may explain why DRs of this campaign are of the same magnitude as those measured during the STs (Figure 25). At TF2, the sediments have two different origins, the channel and the creek. The NMF is of the same magnitude during the flood (811.15 m^3/m^2 during NT for 784.59 m^3/m^2 during ST, Table 3) which means that the amount of water which passed by TF2 is equivalent during the two tidal conditions and the difference in tidal range between NT and ST does not have any influence on the hydrodynamic conditions on the tidal flat. Furthermore, the TSSCs measured at this station are the highest of all the TSSCs measured at the different stations (16.66 g/m^2 during NT and 12.97 g/m^2 during ST; Figure 20) which clearly shows the influence of the creek on the sediment supply. The DRs of the STs campaigns are higher at this station than at TF1 (Figure 25). During the NTs campaigns, the DRs values on the tidal flat are of similar magnitude, although the DRs at TF2 are slightly lower than those at TF1 (6.62 $g/m^2/hr$ for TF1, 6.23 $g/m_2/hr$ at TF2 on 26th of January and 21.08 $g/m^2/hr$ at TF1 for 20.34 $g/m^2/hr$ at TF2on 6th of June; Figure 25). On the tidal flat*, Zostera noltei,* does not offer a strong resistance to the water flow and so the current velocity attenuation by seagrasses is relatively low as the

mean resultant velocity magnitude on the tidal flat is the highest during NT (5.04 cm/s) and during ST the mean resultant velocity magnitude is only 1.18 cm/s less than during NT (Table 3). Moreover, the SSCs at the intake of 0.65 m (7.22 mg/l to 18.73 mg/l at TF1 and 11.93 mg/l to 29.52 mg/l at TF2, Figure 18 and Figure 19) are higher than those at -0.1 m (6.65 to 9.51 mg/l at TF1 and 7.85 to 18.08 mg/l at TF2, Figure 18 and Figure 19), the increase of the velocity over the plant canopy (Ackerman & Okubo, 1993) does not allow sediments to be deposited.

The highest DR at LM was measured during the NT on 6th of June (Figure 25). The decrease in current velocity (average resultant velocity of 5.04 cm/s at TF2 for 2.03 cm/s at LM during this campaign, Table 3) and the increase in sediment size (very fine silt on the tidal flat and fine silt in the marsh, Table 2) allow sediments to settle at this station. This large amount of sediment deposition during this NT allowed a high DR (25.45 g/m^2/hr, Figure 25) at LM. Contrastingly, during the NT of 26th of January, the DR at LM is the lowest measured during the survey (5.65 g/m^2/hr). During STs, the high magnitude of the current velocity does not allow as much sediment to be deposited at LM than at TF2. Due to the increase in current velocities at LM (mean resultant velocity of 6.53 cm/s; Table 3) and the large NMF during the flood (1291.29 m^3/m^2, Table 3), sediments cannot be deposited with the same magnitude as at TF2 (0.110 g to 0.122 g of sediment deposited at TF2 for 0.090 g to 0.104 g at LM, Figure 21). Thus, the DRs are lower at LM than at TF2 (17.25 g/m^2/hr to 21.52 g/m^2/hr at LM versus 19.19 g/m^2/hr to 23.65 g/m^2/hr at TF2, Figure 25). *Spartina maritima* has a stiffer shoot morphology than *Zostera notlei,* which allows *Spartina* species to have a higher drag effect than the flexible seagrass and maximizes sediment trapping (Bouma et al., 2005). During NT, there is a decrease of the velocity between TF2 and LM as the mean resultant velocity is 5.04 cm/s at TF2 for 2.03 cm/s at LM (Table 3) in this tidal condition, which allows sediments to settle in this place, as the velocity is not high enough to keep sediments in suspension. It can be seen on the TSSC during NT with the drop of value between TF2 and LM, from 16.66 g/m^2 to 1.23 g/m^2 at LM (Figure 20). This explains the measured DR at LM during the campaign of the 6th of June (25.45 g/m^2/hr, Figure 25). During ST, on the contrary, the mean resultant velocity is high (6.53 cm/s; Table 3), which allows less sediment to settle in LM due to likely increase of the velocity around and over the plant canopy (Ackerman & Okubo, 1993; Vandenbruwaene et al., 2011) and more suspended sediment to be transported toward the

high marsh. *Spartina maritima* has different behavior during NT and ST because the NMF is different in the two tidal conditions (264.04 m^3/m^2 during NT for 1291.29 m^3/m^2 during ST, Table 3).

The high velocity at LM allowed sediments to be transported to the high marsh. At HM, the velocity decreases sharply, with an average resultant velocity of 2.25 cm/s (versus 6.53 cm/s at LM and 3.86 cm/s at TF2; Table 3) which allows sediment to be depose between LM and HM. *Sarcocornia fruticosa* and *Sarcocornia perennis* are the most rigid woody bushes identified in this study, and so are expected to reduce the current velocity significantly. These are confirmed by the TSSC of HM which is the lowest of the transect during the STs (1.42 g/m^2, Figure 20) and the high DR (33.80 $g/m^2/hr$ on 28th of February and 35.45 $g/m^2/hr$ on 26th of April, Figure 25). The amount of sediment deposited at HM is of the same magnitude during the two tides that characterize STs. These depositions are even higher than at TF1 and LM during the tide of 26th of April (0.94 g at TF1, 0.90 g at LM and 0.98g at HM, Figure 21). As the DRs are the highest measured during this study and the currents are the lowest in the transect, *Sarcocornia sp.* should have a positive impact on sedimentation thanks to its morphoplogy. Moreover, this species has a high capacity to catch OM from the tidal flat (Figure 24), which participate to the accretion on the high marsh.

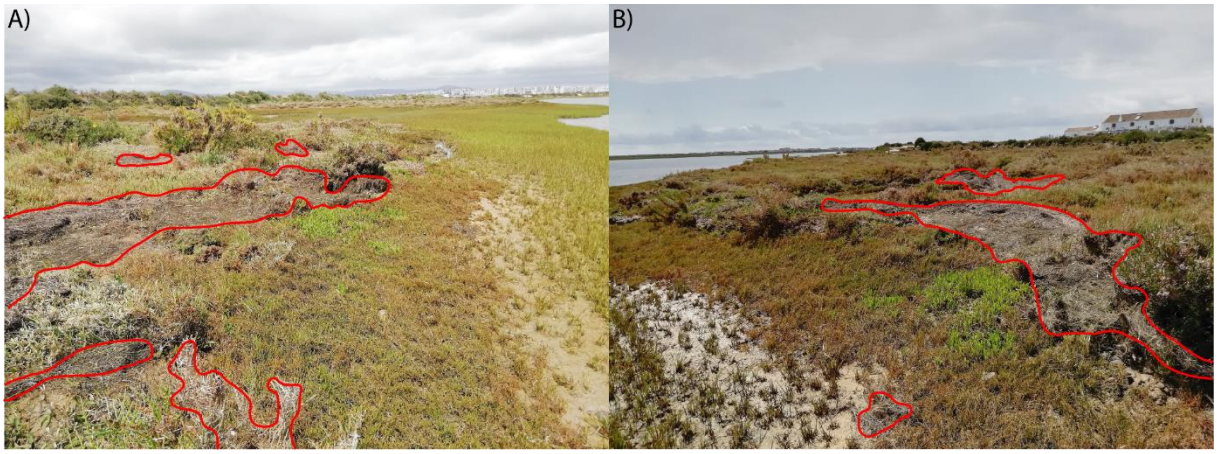

Figure 24: Deposition of Zostera noltei litter, circled in red, on the high marsh, (A) on the South-West of the transect and (B) on the North-East of the transect

The highest DRs are measured at HM. During the NT of 6th of June, the last station to be flooded, LM, is also the station with the highest DR during NT campaigns. Reduced current velocities allowed fine silt sediments to deposit. Along the transect studied, the different plant

species do not act in the same way. The higher the topography, the more rigid the plants and the greater their resistance to currents. The species most conducive to sedimentation is therefore *Sarcocornia sp*. in the high marsh, followed by *Spartina maritima* in the low marsh, and finally *Zostera noltei* which collonises the tidal flat. As the finest sediments are found on the tidal flat, it is possible to hypothesize that sediments flocculate along the transect and thus becoming heavier toward the upper parts of the transect. The DR values of 26th of January are the lowest measured during this study and do not have the same magnitude as the values of all other surveys, which may be due to misundertaken laboratory procedures (Figure 25).

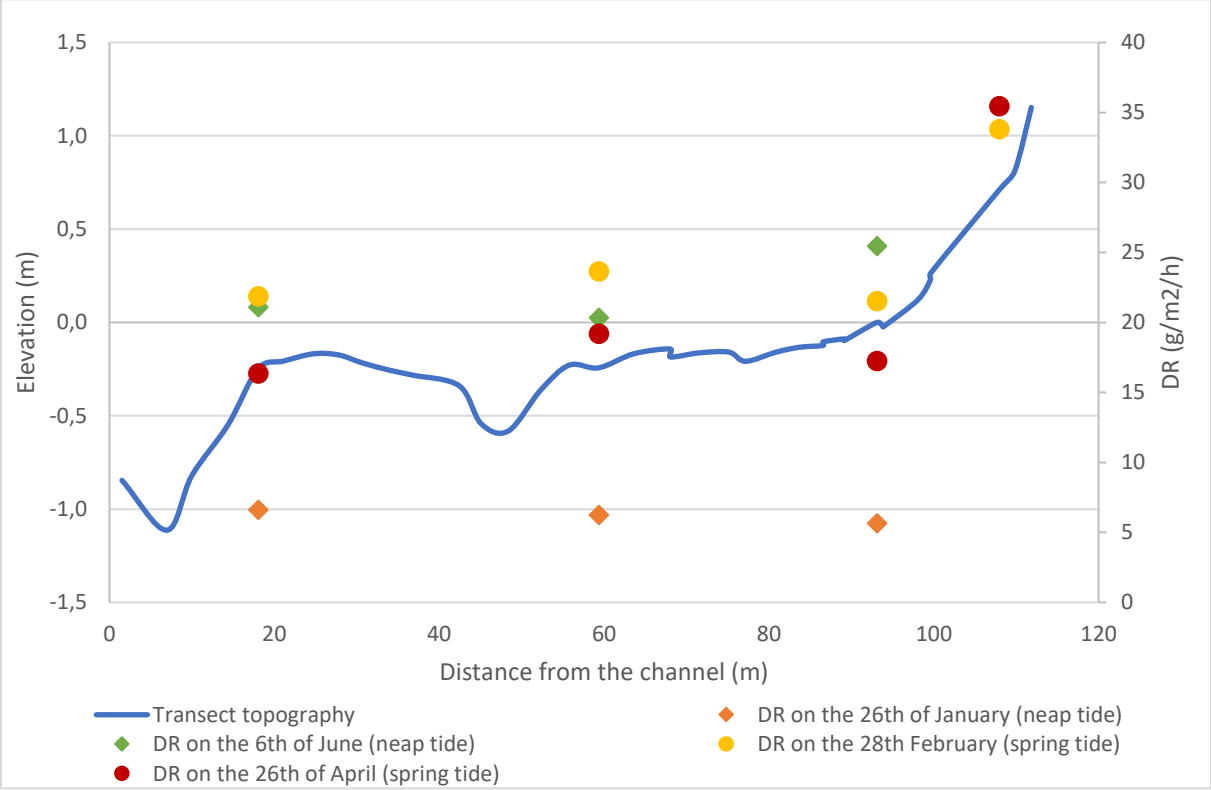

Figure 25: Deposition Rates (DRs) obtained for the four campaigns along the transect with the topography (blue line)

In the Rattekaai marsh, a DR of 53.04±11.5 g/m^2/hr and 31.38±8.75 g/m^2/hr were assessed, respectively for the low marsh and the high marsh (Ma et al., 2018, Appendix 5). In another Dutch wetland, in Sint Annaland marsh, the DR is 21.42±6.54 g/m^2/hr in the low marsh and 7.29±17.54 g/m^2/hr in the high marsh (Ma et al., 2018, Appendix 5). DRs are higher than in the Ria Formosa, which has DR values range from 5.65 g/m^2/hr to 25.45 g/m^2/hr at LM and from 33.80 g/m^2/hr to 35.45 g/m^2/hr at HM (Figure 25). The differences in vertical accretion of the Ducth marshes were attributed to storm events. The high DR of Rattekai marsh can be

explained by the large SSC measured in this marsh. In Sint Annaland marsh, the SSC is lower than in Rattekaai marsh, but DR is still higher than DRs measured during STs, on the low marsh of the Ria Formosa. On the high marsh, DRs are higher in the Ria Formosa than in the Sint Annaland marsh. These two Dutch marshes are not protected by a barrier island system like the Portuguese lagoon and therefore have a greater influence from the estuary in which they are located. Freshwater inputs are higher than in the Ria Formosa, so the amount of terrigenous sediments may have more influence than in the Portuguese lagoon. The tidal range in the inland part of the Oosterschelde estuary is 3.4 m (Ma et al., 2018), which is almost the same than in Ria Formosa (3.5 m during ST, Ferreira et al., 2016). Furthermore, as their tidal flats are not protected by vegetation, sediments are resuspended to settle further upstream towards the marsh (Ma et al., 2018). In contrast, the DRs in the upper Ria marsh are of the same magnitude as that of Rattekaai marsh and higher than that of Sint Annaland marsh. In the Ria Formosa, the DR increases with distance from the channel due to the high current velocity in the lower parts of the transect which does not allow sediment to settle, whereas in the Dutch marshes, the DR decreases inland.

In the St. Jones River in the Delaware Bay, DR values are lower than those of the Ria Formosa with a DR of 22.33 $g/m^2/hr$ in the low marsh and 3.65 $g/m^2/hr$ in the high marsh (Moskalski & Sommerfield, 2012, Appendix 5) under ST conditions. The DR measured at LM (21.52 $g/m^2/hr$) during the 28th of February campaign is almost equal to DRs measured the St. Jones River and the one measured during the 26th of April campaign is lower by just 5.08 $g/m^2/hr$ (Figure 25). These two marshes do not have the same geomorphological characteristics since the marsh studied by Moskalski and Sommerfield, (2012) borders a river, without the presence of a tidal flat. Furthermore, it is in a river estuary, whereas the Ria Formosa is a lagoon. On the marsh bordering the St. Jones River, there is no creek which brings more sediments on the highest part of their transects. These geomorphological differences do not affect DR on the lower part of the marsh. On the contrary, on the high marsh, the difference is more important, with higher DR in the Ria Formosa. They have a DR that decreases with distance from the river, as does the SSC, which decreases sharply, from 1900 mg/l near the river in the low marsh to 10 mg/l in the high marsh (Moskalski & Sommerfield, 2012). Their results have an opposite trend than those present in this thesis.

In the Kingsport marsh, the average DR are measured on the low marsh (30.90±17.70 g/m^2/tide), on the high marsh edge (15.50±5.90 g/m^2/tide) and on the high marsh surface (15.30±6.10 g/m^2/tide; Poirier et al., 2017, Appendix 5). In Ria Formosa, the DR at LM for NTs fluctuates between 29. 87 g/m^2/tide, and 165.34 g/m^2/tide. Regarding ST campaigns, the DR changes between 126.64 g/m^2/tide and 147.55 g/m^2/tide at LM and between 141.85 g/m^2/tide and 142.97 g/m^2/tide at HM. DR values of the marsh in Canada are lower than those measure in the Ria Formosa. In the Kingsport marsh, sediments flocculate in the creek and settle in the low marsh and in the creek. The SSC is higher in the Canadian marsh, but as most of the sediment was deposited in the lower parts (creek and low marsh), the sediment size is finer in the high marsh, and the hydrodynamic conditions are too high, the sediment tends to settle less in the high marsh.

Conclusion

The objective of this study was to assess sediment transport and deposition, along the transition from tidal flat to salt marsh in the Western part of the Ria Formosa lagoon, in the South of Portugal. Data on topography, sediment size, hydrodynamic conditions (tidal range, hydroperiod, sea level changes and velocities of alongshore and cross-shore currents), suspended sediment concentrations (SSC), deposition rates (DRs) and organic matter (OM) content were measured under neap tide (NT) and spring tide (ST) conditions. Data were collected at four different stations on a transect. Two of the stations were on the tidal flat (TF1 and TF2), one station located on the low marsh (LM), and the last station was on the intermediate/high marsh (HM). After laboratory analysis (filtration of the suspended sediments, OM destruction, and measurement of the amount of sediment deposited during a tidal event), the SSC and DR along the transect studied were determined. The hydrodynamic data was analysed to characterize the onshore direction and magnitude of the alongshore and cross-shore tidal velocities.

Sediments are brought to the study site by tidal currents from the Ramalhete Channel, during the flood. The local dominant currents direction is alongshore, that becomes less relevant when moving landward (towards the high marsh). The highest velocities and the highest net momentum flux (NMF) were measured on the tidal flat during NT and on the low marsh during ST. *Spartina maritima* has an amplifying effect on the velocity of the currents, however, under ST conditions current acceleration can be noted at the boundary of the low marsh. The last stations of the transect (LM during NT and HM during ST) have the lowest velocities which can be explain by the stiff of *Sarcocornia sp.* on the high marsh, the lowest NMF and the lowest height of the water column.

The topography shows that the tidal flat has an very low slope, with a creek between TF1 and TF2, while slopes are higher on the salt marsh. The sediment grain sizes increase with the topography, starting from the very fine silt on the tidal flat to the fine silt on the salt marsh. The highest total SSC (TSSC) is measured at TF2, followed by LM (only during STs), TF1, and finally the lowest TSSCs are measured at the last stations of the transect (LM during NTs and HM during STs). The high NMF and TSSC values show the influence of the creek on stations TF2, LM and HM. The analysis showed that sediments come from the north-east of the transect, from the channel for TF1 and from the channel and the creek for TF2 and LM. At HM,

the sediments also come from the channel and the creek, but with a Northwest - Southeast direction.

The highest DRs are measured at the most distant stations (LM during NTs and HM during STs) with high deposition rates at HM during STs. The decrease in velocity at these stations allows sediments to settle. TF2 has the second highest DRs over the four surveys. This station is the closest to the creek and is strongly influenced by it. During the STs, stations TF1 and LM have DRs of the same magnitude. There does not seem to be a high difference between the DRs of the NT of the 6th of June and the DRs during the STs, which means that tidal conditions do not have a high influence on the sediment dynamics on the tidal flat. The influence of the tidal conditions is higher on the salt marsh as the velocity is the highest record on the low marsh, which brings sediments on the high marsh which has the highest DR. *Sarcocornia sp.* therefore has a positive impact on sedimentation, as does *Spartina maritima*. *Zostera noltei* has a lower influence on sedimentation but protects the sediments of the tidal flat from being resuspended.

The Ria Formosa has a low SSCs, compared to other coastal wetlands, but has high deposition rates. Current velocity and SSCs are main drivers for sedimentation. Vegetation has an important role on hydrodynamics and sedimentation in the different environments analysed in this study. Further studies would provide a better understanding of the sediment dynamics in the Ria Formosa, for example by studying the flocculation of sediments in the lagoon.

References

Ackerman, J. D., & Okubo, A. (1993). Reduced Mixing in a Marine Macrophyte Canopy. *Functional Ecology*, *7*(3), 305. https://doi.org/10.2307/2390209

Andrade, C., Freitas, M. C., Moreno, J., & Craveiro, S. C. (2004). Stratigraphical evidence of Late Holocene barrier breaching and extreme storms in lagoonal sediments of Ria Formosa, Algarve, Portugal. *Marine Geology*, *210*(1–4), 339–362. https://doi.org/10.1016/j.margeo.2004.05.016

Arnaud-Fassetta, G., Bertrand, F., Costa, S., & Davidson, R. (2006). The western lagoon marshes of the Ria Formosa (Southern Portugal): Sediment-vegetation dynamics, long-term to short-term changes and perspective. *Continental Shelf Research*, *26*(3), 363–384. https://doi.org/10.1016/j.csr.2005.12.008

Backhaus, J. O., & Verduin, J. J. (2008). Simulating the interaction of seagrasses with their ambient flow. *Estuarine, Coastal and Shelf Science*, *80*(4), 563–572. https://doi.org/10.1016/j.ecss.2008.09.013

Balke, T., Stock, M., Jensen, K., Bouma, T. J., & Kleyer, M. (2016). A global analysis of the seaward salt marsh extent: The importance of tidal range. *Water Resources Research*, *52*(5), 3775–3786. https://doi.org/https://doi.org/10.1002/2015WR018318

Bertness, M. D., & Hacker, S. D. (1994). Physical Stress and Positive Associations Among Marsh Plants. *The American Naturalist*, *144*(3), 363–372. https://doi.org/10.1086/285681

Boorman, L., Garbutt, A., & Barratt, D. (1998). The role of vegetation in determining patterns of the accretion of salt marsh sediment. *Geological Society, London, Special Publications*, *139*, 389–399. https://doi.org/10.1144/GSL.SP.1998.139.01.29

Bouma, T. J., de Vries, M. B., Low, E., Kusters, L., Herman, P. M. J., Tánczos, I. C., Temmerman, S., Hesselink, A., Meire, P., & van Regenmortel, S. (2005). Flow hydrodynamics on a mudflat and in salt marsh vegetation: Identifying general relationships for habitat characterisations. *Hydrobiologia*, *540*(1–3), 259–274. https://doi.org/10.1007/s10750-004-7149-0

Bouma, T. J., de Vries, M. B., Low, E., Peralta, G., Tánczos, I. C., van de Koppel, J., & Herman, P. M. J. (2005). Trade-offs related to ecosystem engineering: A case study on stiffness of emerging macrophytes. *Ecology*, *86*(8), 2187–2199. https://doi.org/10.1890/04-1588

Bouma, T. J., Friedrichs, M., Klaassen, P., van Wesenbeeck, B. K., Brun, F. G., Temmerman, S., van Katwijk, M. M., Graf, G., & Herman, P. M. J. (2009). Effects of shoot stiffness, shoot size and current velocity on scouring sediment from around seedlings and propagules. *Marine Ecology Progress Series*, *388*, 293–297. https://doi.org/10.3354/meps08130

Bouma, T. J., van Belzen, J., Balke, T., van Dalen, J., Klaassen, P., Hartog, A. M., Callaghan, D. P., Hu, Z., Stive, M. J. F., Temmerman, S., & Herman, P. M. J. (2016). Short-term mudflat

dynamics drive long-term cyclic salt marsh dynamics. *Limnology and Oceanography*, *61*(6), 2261–2275. https://doi.org/https://doi.org/10.1002/lno.10374

Carrasco, A. R., Ferreira, O., & Roelvink, D. (2016). Coastal lagoons and rising sea level: A review. *Earth-Science Reviews*, *154*, 356–368. https://doi.org/10.1016/j.earscirev.2015.11.007

Carrasco, A. R., Kombiadou, K., Amado, M., & Matias, A. (2021). Past and future marsh adaptation: Lessons learned from the Ria Formosa lagoon. *Science of the Total Environment*, *790*, 148082. https://doi.org/10.1016/j.scitotenv.2021.148082

Chmura, G. L., Anisfeld, S. C., Cahoon, D. R., & Lynch, J. C. (2003). Global carbon sequestration in tidal, saline wetland soils. *Global Biogeochemical Cycles*, *17*(4). https://doi.org/https://doi.org/10.1029/2002GB001917

Chmura, G. L., & Hung, G. A. (2004). Controls on salt marsh accretion: A test in salt marshes of eastern Canada. In *Estuaries* (Vol. 27, Issue 1). https://doi.org/10.1007/BF02803561

Christiansen, T., Wiberg, P. L., & Milligan, T. G. (2000). Flow and sediment transport on a tidal salt marsh surface. *Estuarine, Coastal and Shelf Science*, *50*(3), 315–331. https://doi.org/10.1006/ecss.2000.0548

Costa, J. C., Lousã, M., & Espírito-Santo, M. D. (1996). A vegetação do Parque Natural da Ria Formosa (Algarve, Portugal). *Studia Botanica*, *15*(0), 69–157.

Craft, C., Clough, J., Ehman, J., Joye, S., Park, R., Pennings, S., Guo, H., & Machmuller, M. (2009). Forecasting the effects of accelerated sea-level rise on tidal marsh ecosystem services. In *Frontiers in Ecology and the Environment* (Vol. 7, Issue 2). https://doi.org/https://doi.org/10.1890/070219

Cui, B., He, Q., Gu, B., Bai, J., & Liu, X. (2016). China's Coastal Wetlands: Understanding Environmental Changes and Human Impacts for Management and Conservation. *Wetlands*, *36*, 1–9. https://doi.org/10.1007/s13157-016-0737-8

D'Alpaos, A., & Marani, M. (2016). Reading the signatures of biologic-geomorphic feedbacks in salt-marsh landscapes. *Advances in Water Resources*, *93*, 265–275. https://doi.org/10.1016/j.advwatres.2015.09.004

Davy, A. J., Brown, M. J. H., Mossman, H. L., & Grant, A. (2011). Colonization of a newly developing salt marsh: disentangling independent effects of elevation and redox potential on halophytes. *Journal of Ecology*, *99*(6), 1350–1357. https://doi.org/https://doi.org/10.1111/j.1365-2745.2011.01870.x

Duarte, C., Losada, I. J., Hendriks, I., Mazarrasa, I., & Marba, N. (2013). The role of coastal plant communities for climate change mitigation and adaptation. *Nature Climate Change*, *3*, 961–968. https://doi.org/10.1038/nclimate1970

Elellterills, L. N., Eleuterills, C. K., The, M., & Although, Y. (1979). *TIDE LEVELS AND SALT MARSH ZONATION Coastal salt marshes have evolved under the controlling influence of*

the sea . Tidal amplitude in relation to the slope and elevation of the shore define the area for the development and maintenance of salt marsh . A di. *29*(3), 394–400.

Evans, D. (2006). THE HABITATS OF THE EUROPEAN UNION HABITATS DIRECTIVE. *Biology and Environment: Proceedings of the Royal Irish Academy*, *106B*(3), 167–173. http://www.jstor.org/stable/20728591

Fagherazzi, S., Kirwan, M. L., Mudd, S. M., Guntenspergen, G. R., Temmerman, S., D'Alpaos, A., van de Koppel, J., Rybczyk, J. M., Reyes, E., Craft, C., & Clough, J. (2012). Numerical models of salt marsh evolution: Ecological, geomorphic, and climatic factors. In *Reviews of Geophysics* (Vol. 50, Issue 1). https://doi.org/https://doi.org/10.1029/2011RG000359

Fagherazzi, S., Mariotti, G., Leonardi, N., Canestrelli, A., Nardin, W., & Kearney, W. S. (2020). Salt Marsh Dynamics in a Period of Accelerated Sea Level Rise. In *Journal of Geophysical Research: Earth Surface* (Vol. 125, Issue 8). https://doi.org/10.1029/2019JF005200

Fagherazzi, S., Torres, R., Hopkinson, C., & van Proosdij, D. (2005). Salt marsh geomorphology: Physical and ecological effects on landform. *Eos, Transactions American Geophysical Union*, *86*(6), 57–58. https://doi.org/https://doi.org/10.1029/2005EO060002

Ferreira, Ó., Matias, A., & Pacheco, A. (2016). The East Coast of Algarve: a Barrier Island Dominated Coast. In *Thalassas: An International Journal of Marine Sciences* (Vol. 32, Issue 2). https://doi.org/10.1007/s41208-016-0010-1

Folk, R., & Ward, W. (1957). Brazos River Bar: A Study in the Significance of Grain Size Parameters. *Journal of Sedimentary Petrology*, *27*, 3–26. https://doi.org/10.1306/74D70646-2B21-11D7-8648000102C1865D

Fonseca, M. S., & Koehl, M. A. R. (2006). Flow in seagrass canopies: The influence of patch width. *Estuarine, Coastal and Shelf Science*, *67*(1–2), 1–9. https://doi.org/10.1016/j.ecss.2005.09.018

French, J. R. (1993). Numerical simulation of vertical marsh growth and adjustment to accelerated sea-level rise, North Norfolk, U.K. *Earth Surface Processes and Landforms*, *18*(1), 63–81. https://doi.org/https://doi.org/10.1002/esp.3290180105

French, J. R., & Stoddart, D. R. (1992). Hydrodynamics of salt marsh creek systems: Implications for marsh morphological development and material exchange. *Earth Surface Processes and Landforms*, *17*(3), 235–252. https://doi.org/https://doi.org/10.1002/esp.3290170304

Friedrichs, C. T., & Perry, J. E. (2001). Tidal Salt Marsh Morphodynamics: A Synthesis. *Journal of Coastal Research*, 7–37. http://www.jstor.org/stable/25736162

Gacia, E., Granata, T. C., & Duarte, C. M. (1999). An approach to measurement of particle flux and sediment retention within seagrass (Posidonia oceanica) meadows. *Aquatic Botany*, *65*(1–4), 255–268. https://doi.org/10.1016/S0304-3770(99)00044-3

Ganju, N. K., Kirwan, M. L., Dickhudt, P. J., Guntenspergen, G. R., Cahoon, D. R., & Kroeger, K. D. (2015). Sediment transport-based metrics of wetland stability. *Geophysical Research Letters*, *42*(19), 7992–8000. https://doi.org/10.1002/2015GL065980

Garzon, J. L., Maza, M., Ferreira, C. M., Lara, J. L., & Losada, I. J. (2019). Wave Attenuation by Spartina Saltmarshes in the Chesapeake Bay Under Storm Surge Conditions. *Journal of Geophysical Research: Oceans*, *124*(7), 5220–5243. https://doi.org/10.1029/2018JC014865

Gedan, K. B., Silliman, B. R., & Bertness, M. D. (2009). Centuries of human-driven change in salt marsh ecosystems. In *Annual review of marine science* (Vol. 1). https://doi.org/10.1146/annurev.marine.010908.163930

Ghisalberti, M. (2002). Mixing layers and coherent structures in vegetated aquatic flows. *Journal of Geophysical Research*, *107*(C2). https://doi.org/10.1029/2001jc000871

Ghisalberti, M., & Nepf, H. (2009). Shallow flows over a permeable medium: The hydrodynamics of submerged aquatic canopies. *Transport in Porous Media*, *78*(2), 309–326. https://doi.org/10.1007/s11242-008-9305-x

Guillou, S., Thiebot, J., Romuald Verjus, J. C., Besq, A., Hau, D., & Se, K. (2011). The Filling Dynamics of an Estuary: From the Process to the Modelling. *Sediment Transport in Aquatic Environments*, *September*. https://doi.org/10.5772/19933

Houwing, E., Houwing, E.-J., van Duin, W. E., Waaij, Y. S. der, Dijkema, K. S., & Terwindt, J. H. J. (1999). Biological and abiotic factors influencing the settlement and survival of Salicornia dolichostachya in the intertidal pioneer zone. *Mangroves and Salt Marshes*, *3*(4), 197–206. https://doi.org/10.1023/A:1009919008313

Johnston, M. E., Cavatorta, J. R., Hopkinson, C. S., & Valentine, V. (2003). Importance of Metabolism in the Development of Salt Marsh Ponds. *The Biological Bulletin*, *205*(2), 248–249. https://doi.org/10.2307/1543278

Johnston, R. J., Magnusson, G., Mazzotta, M. J., & Opaluch, J. J. (2002). Combining Economic and Ecological Indicators to Prioritize Salt Marsh Restoration Actions. *American Journal of Agricultural Economics*, *84*(5), 1362–1370. http://www.jstor.org/stable/1245072

Kirwan, M. L., & Guntenspergen, G. R. (2010). Influence of tidal range on the stability of coastal marshland. *Journal of Geophysical Research: Earth Surface*, *115*(F2). https://doi.org/https://doi.org/10.1029/2009JF001400

Kirwan, M. L., & Murray, A. B. (2007). A coupled geomorphic and ecological model of tidal marsh evolution. *Proceedings of the National Academy of Sciences*, *104*(15), 6118 LP – 6122. https://doi.org/10.1073/pnas.0700958104

Kombiadou, K., & Krestenitis, Y. (2013). *Modelling Cohesive Sediment Dynamics in the Marine Environment* (pp. 213–246). https://doi.org/10.5772/51061

Kumar, M., Boski, T., González-Vila, F. J., de la Rosa, J. M., & González-Pérez, J. A. (2020). Discerning natural and anthropogenic organic matter inputs to salt marsh sediments of

Ria Formosa lagoon (South Portugal). *Environmental Science and Pollution Research*, *27*(23), 28962–28985. https://doi.org/10.1007/s11356-020-09235-9

Ladd, C. J. T., Duggan-Edwards, M. F., Bouma, T. J., Pagès, J. F., & Skov, M. W. (2019). Sediment Supply Explains Long-Term and Large-Scale Patterns in Salt Marsh Lateral Expansion and Erosion. *Geophysical Research Letters*, *46*(20), 11178–11187. https://doi.org/10.1029/2019GL083315

Leonard, L. A., & Luther, M. E. (1995). Flow hydrodynamics in tidal marsh canopies. *Limnology and Oceanography*, *40*(8), 1474–1484. https://doi.org/https://doi.org/10.4319/lo.1995.40.8.1474

Ma, Z., Ysebaert, T., van der Wal, D., & Herman, P. M. J. (2018). Conditional effects of tides and waves on short-term marsh sedimentation dynamics. In *Earth Surface Processes and Landforms* (Vol. 43, Issue 10). https://doi.org/10.1002/esp.4357

Mariotti, G., & Carr, J. (2014). Dual role of salt marsh retreat: Long-term loss and short-term resilience. *Water Resources Research*, *50*(4), 2963–2974. https://doi.org/https://doi.org/10.1002/2013WR014676

Mariotti, G., & Fagherazzi, S. (2010). A numerical model for the coupled long-term evolution of salt marshes and tidal flats. *Journal of Geophysical Research: Earth Surface*, *115*(F1). https://doi.org/https://doi.org/10.1029/2009JF001326

Mariotti, G., & Fagherazzi, S. (2013). Critical width of tidal flats triggers marsh collapse in the absence of sea-level rise. *Proceedings of the National Academy of Sciences*, *110*(14), 5353 LP – 5356. https://doi.org/10.1073/pnas.1219600110

McKinley, E., Pagès, J. F., Alexander, M., Burdon, D., & Martino, S. (2020). Uses and management of saltmarshes: A global survey. *Estuarine, Coastal and Shelf Science*, *243*(June). https://doi.org/10.1016/j.ecss.2020.106840

Morris, J. T., Sundareshwar, P. v, Nietch, C. T., Kjerfve, B., & Cahoon, D. R. (2002). RESPONSES OF COASTAL WETLANDS TO RISING SEA LEVEL. *Ecology*, *83*(10), 2869–2877. https://doi.org/https://doi.org/10.1890/0012-9658(2002)083[2869:ROCWTR]2.0.CO;2

Moskalski, S. M., & Sommerfield, C. K. (2012). Suspended sediment deposition and trapping efficiency in a Delaware salt marsh. *Geomorphology*, *139–140*, 195–204. https://doi.org/10.1016/j.geomorph.2011.10.018

Mudd, S. M., D'alpaos, A., & Morris, J. T. (2010). How does vegetation affect sedimentation on tidal marshes? Investigating particle capture and hydrodynamic controls on biologically mediated sedimentation. *J. Geophys. Res*, *115*, 3029. https://doi.org/10.1029/2009JF001566

Murray, A. B., Knaapen, M. A. F., Tal, M., & Kirwan, M. L. (2008). Biomorphodynamics: Physical-biological feedbacks that shape landscapes. *Water Resources Research*, *44*(11), 1–18. https://doi.org/10.1029/2007WR006410

Mwamba, M. J., & Torres, R. (2002). Rainfall effects on marsh sediment redistribution, North Inlet, South Carolina, USA. *Marine Geology*, *189*(3), 267–287. https://doi.org/https://doi.org/10.1016/S0025-3227(02)00482-6

Neckles, H. A., Lyons, J. E., Guntenspergen, G. R., Shriver, W. G., & Adamowicz, S. C. (2015). Use of Structured Decision Making to Identify Monitoring Variables and Management Priorities for Salt Marsh Ecosystems. *Estuaries and Coasts*, *38*(4), 1215–1232. https://doi.org/10.1007/s12237-014-9822-5

Newton, A., & Mudge, S. M. (2003). Temperature and salinity regimes in a shallow, mesotidal lagoon, the Ria Formosa, Portugal. *Estuarine, Coastal and Shelf Science*, *57*(1–2), 73–85. https://doi.org/10.1016/S0272-7714(02)00332-3

Pasternack, G. B., Hilgartner, W. B., & Brush, G. S. (2000). Biogeomorphology of an upper Chesapeake Bay river-mouth tidal freshwater marsh. *Wetlands*, *20*(3), 520–537. https://doi.org/10.1672/0277-5212(2000)020<0520:BOAUCB>2.0.CO;2

Poirier, E., van Proosdij, D., & Milligan, T. G. (2017). The effect of source suspended sediment concentration on the sediment dynamics of a macrotidal creek and salt marsh. *Continental Shelf Research*, *148*(July), 130–138. https://doi.org/10.1016/j.csr.2017.08.017

Raposa, K. B., Wasson, K., Smith, E., Crooks, J. A., Delgado, P., Fernald, S. H., Ferner, M. C., Helms, A., Hice, L. A., Mora, J. W., Puckett, B., Sanger, D., Shull, S., Spurrier, L., Stevens, R., & Lerberg, S. (2016). Assessing tidal marsh resilience to sea-level rise at broad geographic scales with multi-metric indices. *Biological Conservation*, *204*, 263–275. https://doi.org/https://doi.org/10.1016/j.biocon.2016.10.015

Reed, D. J. (1989). Patterns of sediment deposition in subsiding coastal salt marshes, Terrebonne Bay, Louisiana: The role of winter storms. *Estuaries*, *12*(4), 222–227. https://doi.org/10.2307/1351901

Reed, D. J. (1990). The impact of sea-level rise on coastal salt marshes. *Progress in Physical Geography: Earth and Environment*, *14*(4), 465–481. https://doi.org/10.1177/030913339001400403

Reed, D. J., Spencer, T., Murray, A. L., French, J. R., & Leonard, L. (1999). Marsh surface sediment deposition and the role of tidal creeks: Implications for created and managed coastal marshes. *Journal of Coastal Conservation*, *5*(1), 81–90. https://doi.org/10.1007/BF02802742

Ribeiro, J., Monteiro, C. C., Monteiro, P., Bentes, L., Coelho, R., Gonçalves, J. M. S., Lino, P. G., & Erzini, K. (2008). Long-term changes in fish communities of the Ria Formosa coastal lagoon (southern Portugal) based on two studies made 20 years apart. *Estuarine, Coastal and Shelf Science*, *76*(1), 57–68. https://doi.org/10.1016/j.ecss.2007.06.001

Rosa, F., Rufino, M. M., Ferreira, Ó., Matias, A., Brito, A. C., & Gaspar, M. B. (2013). The influence of coastal processes on inner shelf sediment distribution: The Eastern Algarve

shelf (Southern Portugal). *Geologica Acta*, *11*(1), 59–73. https://doi.org/10.1344/105.000001755

Sadat, M., Rosa Pinto, J., & Pinto, J. E. (2011). *Roteiro Ecológico da Ria Formosa. VI - Flora*. Ed. CIMA; Universidade do Algarve.

Samper-Villarreal, J., Lovelock, C. E., Saunders, M. I., Roelfsema, C., & Mumby, P. J. (2016). Organic carbon in seagrass sediments is influenced by seagrass canopy complexity, turbidity, wave height, and water depth. *Limnology and Oceanography*, *61*(3), 938–952. https://doi.org/10.1002/lno.10262

Sánchez, J. M., SanLeon, D. G., & Izco, J. (2001). Primary colonisation of mudflat estuaries by Spartina maritima (Curtis) Fernald in Northwest Spain: vegetation structure and sediment accretion. *Aquatic Botany*, *69*(1), 15–25. https://doi.org/https://doi.org/10.1016/S0304-3770(00)00139-X

Schuerch, M., Spencer, T., & Evans, B. (2019). Coupling between tidal mudflats and salt marshes affects marsh morphology. *Marine Geology*, *412*(March), 95–106. https://doi.org/10.1016/j.margeo.2019.03.008

Scott, D. B., & Greenberg, D. A. (1983). Relative sea-level rise and tidal development in the Fundy tidal system. *Canadian Journal of Earth Sciences*, *20*(10), 1554–1564. https://doi.org/10.1139/e83-145

Simas, T., Nunes, J. P., & Ferreira, J. G. (2001). Effects of global climate change on coastal salt marshes. In *Ecological Modelling* (Vol. 139, Issue 1). https://doi.org/10.1016/S0304-3800(01)00226-5

Sly, P. G. (1989). Sediment dispersion: part 1, fine sediments and significance of the silt/clay ratio. *Hydrobiologia*, *176–177*(1), 99–110. https://doi.org/10.1007/BF00026547

Sousa, C., Boski, T., & Pereira, L. (2019). Holocene evolution of a barrier island system, Ria Formosa, South Portugal. *Holocene*, *29*(1), 64–76. https://doi.org/10.1177/0959683618804639

Stock, M. (2014). *TMAP Typology of Coastal Vegetation in the Wadden Sea Area WADDEN SEA ECOSYSTEM No. 32 - 2014* (Issue 32).

Strachan, K. L., Finch, J. M., Hill, T. R., Barnett, R. L., Morris, C. D., & Frenzel, P. (2016). Environmental controls on the distribution of salt-marsh foraminifera from the southern coastline of South Africa. *Journal of Biogeography*, *43*(5), 887–898. https://doi.org/https://doi.org/10.1111/jbi.12698

Taramelli, A., Valentini, E., Cornacchia, L., Monbaliu, J., & Sabbe, K. (2018). Indications of Dynamic Effects on Scaling Relationships Between Channel Sinuosity and Vegetation Patch Size Across a Salt Marsh Platform. *Journal of Geophysical Research: Earth Surface*, *123*(10), 2714–2731. https://doi.org/10.1029/2017JF004540

Temmerman, S., Bouma, T. J., Govers, G., Wang, Z. B., de Vries, M. B., & Herman, P. M. J. (2005). Impact of vegetation on flow routing and sedimentation patterns: Three-

dimensional modeling for a tidal marsh. *Journal of Geophysical Research: Earth Surface*, *110*(4), 1–18. https://doi.org/10.1029/2005JF000301

Temmerman, S., Govers, G., Wartel, S., & Meire, P. (2003). Spatial and temporal factors controlling short-term sedimentation in a salt and freshwater tidal marsh, scheldt estuary, Belgium, SW Netherlands. *Earth Surface Processes and Landforms*, *28*(7), 739–755. https://doi.org/10.1002/esp.495

TINER, R. W. (2013). *Tidal Wetlands Primer*. University of Massachusetts Press. http://www.jstor.org/stable/j.ctt5vk8qw

Titus, J. G., Park, R. A., Leatherman, S. P., Weggel, J. R., Greene, M. S., Mausel, P. W., Brown, S., Gaunt, C., Trehan, M., & Yohe, G. (1991). Greenhouse effect and sea level rise: The cost of holding back the sea. *Coastal Management*, *19*(2), 171–204. https://doi.org/10.1080/08920759109362138

van der Wal, D., Wielemaker-Van den Dool, A., & Herman, P. M. J. (2008). Spatial patterns, rates and mechanisms of saltmarsh cycles (Westerschelde, The Netherlands). *Estuarine, Coastal and Shelf Science*, *76*(2), 357–368. https://doi.org/https://doi.org/10.1016/j.ecss.2007.07.017

van Regteren, M., Amptmeijer, D., de Groot, A. v., Baptist, M. J., & Elschot, K. (2020). Where does the salt marsh start? Field-based evidence for the lack of a transitional area between a gradually sloping intertidal flat and salt marsh. In *Estuarine, Coastal and Shelf Science* (Vol. 243, Issue June). https://doi.org/10.1016/j.ecss.2020.106909

van Regteren, M., ten Boer, R., Meesters, E. H., & de Groot, A. v. (2017). Biogeomorphic impact of oligochaetes (Annelida) on sediment properties and Salicornia spp. seedling establishment. *Ecosphere*, *8*(7), e01872. https://doi.org/https://doi.org/10.1002/ecs2.1872

Vandenbruwaene, W., Temmerman, S., Bouma, T. J., Klaassen, P. C., de Vries, M. B., Callaghan, D. P., van Steeg, P., Dekker, F., van Duren, L. A., Martini, E., Balke, T., Biermans, G., Schoelynck, J., & Meire, P. (2011). Flow interaction with dynamic vegetation patches: Implications for biogeomorphic evolution of a tidal landscape. *Journal of Geophysical Research: Earth Surface*, *116*(1). https://doi.org/10.1029/2010JF001788

Wang, A. (2010). A simplified conception model for salt marsh sedimentation rate calculation: Response to changing suspended sediment concentration-A case study of Wanggang salt marsh, Jiangsu Province, China. *Frontiers of Earth Science in China*, *4*(4), 403–409. https://doi.org/10.1007/s11707-010-0123-4

Wang, C., & Temmerman, S. (2013). Does biogeomorphic feedback lead to abrupt shifts between alternative landscape states?: An empirical study on intertidal flats and marshes. *Journal of Geophysical Research: Earth Surface*, *118*(1), 229–240. https://doi.org/https://doi.org/10.1029/2012JF002474

Wiberg, P. L., Carr, J. A., Safak, I., & Anutaliya, A. (2015). Quantifying the distribution and influence of non-uniform bed properties in shallow coastal bays. *Limnology and Oceanography: Methods*, *13*(12), 746–762. https://doi.org/https://doi.org/10.1002/lom3.10063

Winterwerp, J. C., & van Kesteren, W. G. M. (2004). *Introduction to the physics of cohesive sediment dynamics in the marine environment*. Elsevier.

Yang, S. L., Li, H., Ysebaert, T., Bouma, T. J., Zhang, W. X., Wang, Y. Y., Li, P., Li, M., & Ding, P. X. (2008). Spatial and temporal variations in sediment grain size in tidal wetlands, Yangtze Delta: On the role of physical and biotic controls. *Estuarine, Coastal and Shelf Science*, *77*(4), 657–671. https://doi.org/https://doi.org/10.1016/j.ecss.2007.10.024

Appendices

Appendix 1

Species name n°1: *Sueda vera*

Figure 26: Photos of Sueda vera, pictures A and B have been taken on the 3rd of March and pictures C have been taken on the 28th of February

Location: high marsh

Elevation (with respect to mean sea level): more than 0.70 m

Plant characteristics: woody bush who can measure up to 60 cm of high but usually more around 20 cm of high. Leaves are small and green but have some shades of yellow to red. They have a lenticular shape with a pointed end. They grow by isolated patch. They have also a high capacity to capture other plants brought by tides and are not too much influenced by water flow. They are located on the high marsh, near *Sarcoconia fructicosa*, they are flooded only during STs, when the water reaches the high marsh. They bloom

between March to June (Sadat et al., 2011) with small blue-violet flowers.

Family: Chenopodiaceae

Species n°2: *Cistanche phelypaea*

Figure 27: Photos of Cistanche pehlypaea took on the 3rd of March, A is a photo of one specimen, B photo of several specimen

Location: High marsh

Elevation (with respect to mean sea level): more than 0.70 m

Plant characteristics: This plant has only one broad stem, having short leaves that surround the branch at their bases. They can be up to 30 cm long and end in several rows of yellow bell-shaped flowers. This species can grow in wetland environment. They develop next to estuaries and in the upper part of salt marsh (Costa et al., 1996). This species is listed as a pest species (Costa et al., 1996; Sadat et al., 2011). Flowers grow between Marsh to April (Sadat et al., 2011).

Family: Orobanchaceae Vent.

Species n°3: *Limoniastrum monopetalum*

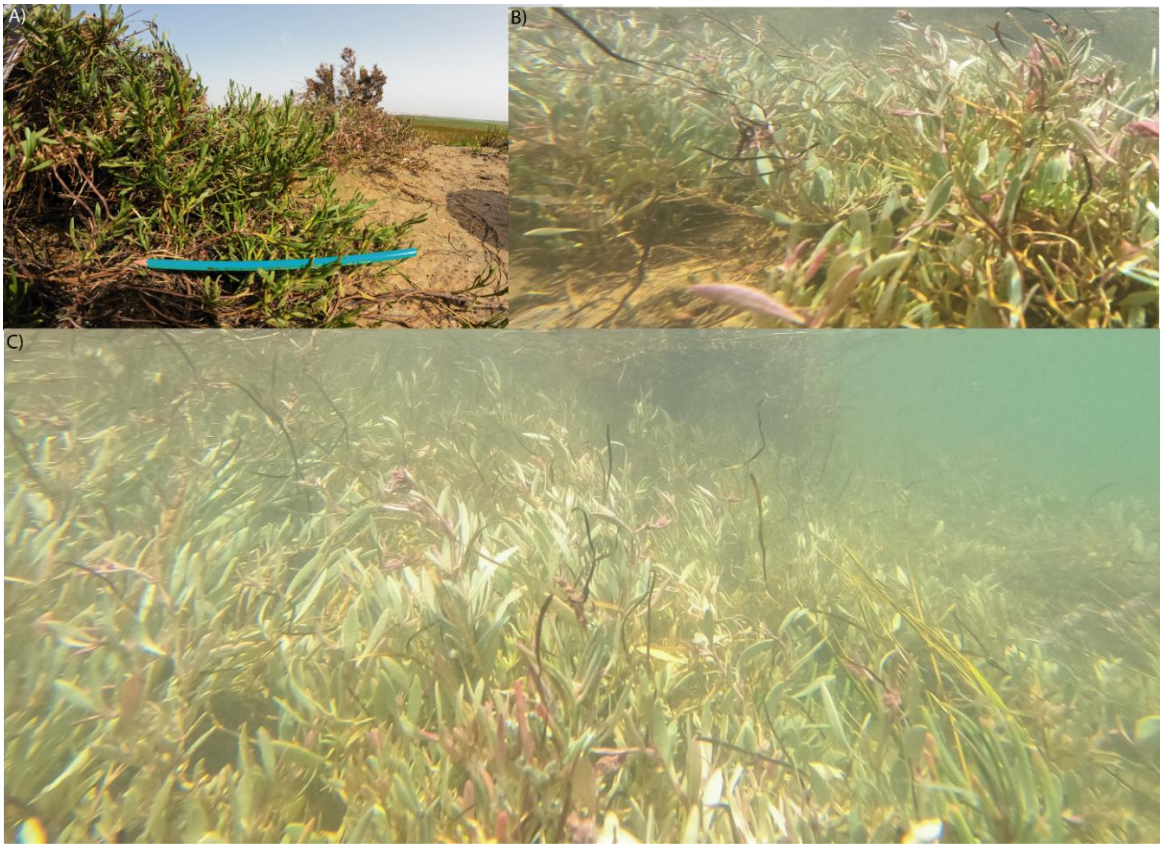

Figure 28: Pictures of Limoniastrum monopletalum, the picture A have been taken on the 3rd of march and B and C on the 23rd of April

Location: high marsh

Elevation (with respect to mean sea level): more than 0.70 m

Plant characteristics: small woody bush bearing numerous thick, leathery stem leaves. The bush can be high as 20 cm and leaves can be long as 3cm. They extend more horizontally than laterally. Pink flowers with glabrous calyx. They look more flexible than the two previous species and follow the movement of the water flow. They grow on the high part of the salt marsh, or on the slope of the marsh, flooded only during spring tides (Costa et al., 1996). They bloom between April to November (Sadat et al., 2011)

Family: Plumbaginaceae Juss.

Species n°4: *Limbarda crithmoides*

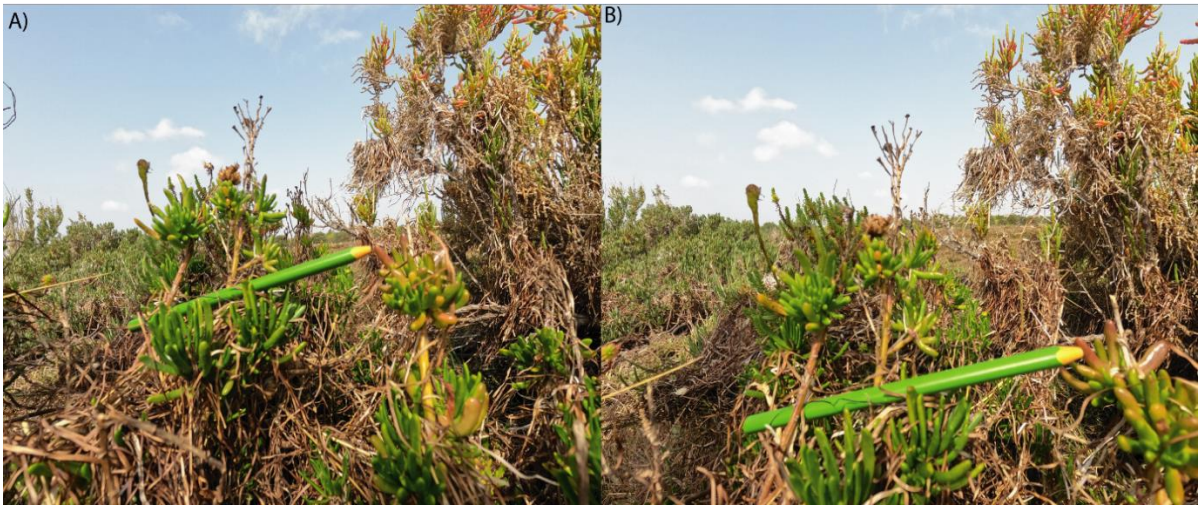

Figure 29: Pictures of Limbarda crithmoides took on the 3rd of March

Location: high marsh

Elevation (with respect to mean sea level): more than 0.70 m

Plant characteristics: woody bush who can be 40cm high. Leaves may be long as more than 5cm with branches of 0.5cm. Leaves have a swollen cylindrical shape. The flower is yellow. They look less flexible *Limoniastrum monopetalum*. They are halophytic plants. They bloom from August to September.

Familly: Asteraceae Dumort

Species n°5: *Spergularia marina*

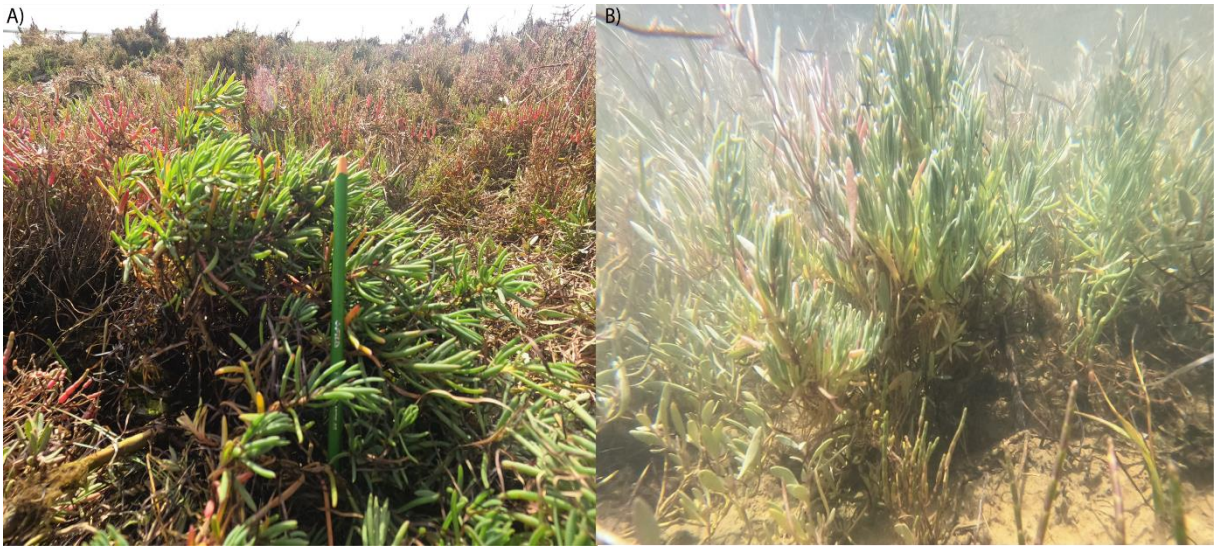

Figure 30: Pictures of Spergularia marina, photo A has been taken on the 3rd of Marsh and picture B has been taken on the 23rd of April

Location: High marsh

Elevation (with respect to mean sea level): more than 0.70 m

Plant characteristics: woody bush who can be tall as 30 cm of high, it can extend more horizontally than vertically. Stems are robust, evergreen, hard and often bare at the base. Leaves have elongated half cylindrical shape, swollen, and finish with a spike shape. They are mostly green, but some leaves may have red part. Flowers are pink. They are halophytic plants located on the high marsh and marsh slope. They can also be finding on disturbed environments. Their bloom occurs from May to August.

Family: Caryophyllaceae Juss.

Species name n°6: *Sarcocornia sp.*

Figure 31 : Pictures of Sarcocornia sp., pictures A and B have been taken on the 3rd of March, the picture C have been taken on the 28th of February, and pictures D, E and F have been taken on the 23rd of April. Photos A, B and D show Sarcocornia fruticosa and photos C, E and F show Sarcornia perennis

Location: high marsh

Elevation (with respect to mean sea level): 0.70 m

Plant characteristics: woody bush with cylindrical green to reddish-brown leaves. The bush can measure more than 75 cm with branches between 0.5 cm to 1 cm of diameter and the leaves can be up to 10 cm long. Leaves have a spiciform shape. This kind of plant can grow by isolated patch, but they may cover a large area over the ground. In the Ria Formosa, they are the major species find in the high marsh (Kumar et al., 2020). They have a high capacity

to capture other plants brought by tides (as we can see on Figure 31 A and B, where some seagrasses remain on it). As they are bush, their movements are not too much influenced by water flow.

Ecologic characteristics: they are halophilous plants who are usually located in high marshes. They need to be flood with a lowest frequency than plants find on low marsh and tidal flat. The are flooded only during spring tides. This species blooms between September and November (Sadat et al., 2011)

Family: Chenopodiaceae

Species n°7: *Limonium vulgare*

Figure 32: Pictures of Limonium vulgare, pictures A and D have been taken on the 3rd of March, and pictures B and C on the 28th of February

Location: middle and high marsh

Elevation (with respect to mean sea level): 0.30 m to 0.70 m

Plant characteristics: this plant grows scattered from the other, with a dozen leaves on every individual. The leaves generally measure between 5 and 10 cm with a maximum width of 3

cm. All leaves are green. They may have violet blue-flower. They grow on salt marsh slope. Flower blooms occur between July to September.

Familly: Plumbaginaceae Juss.

Species n°8: *Ulva sp.*

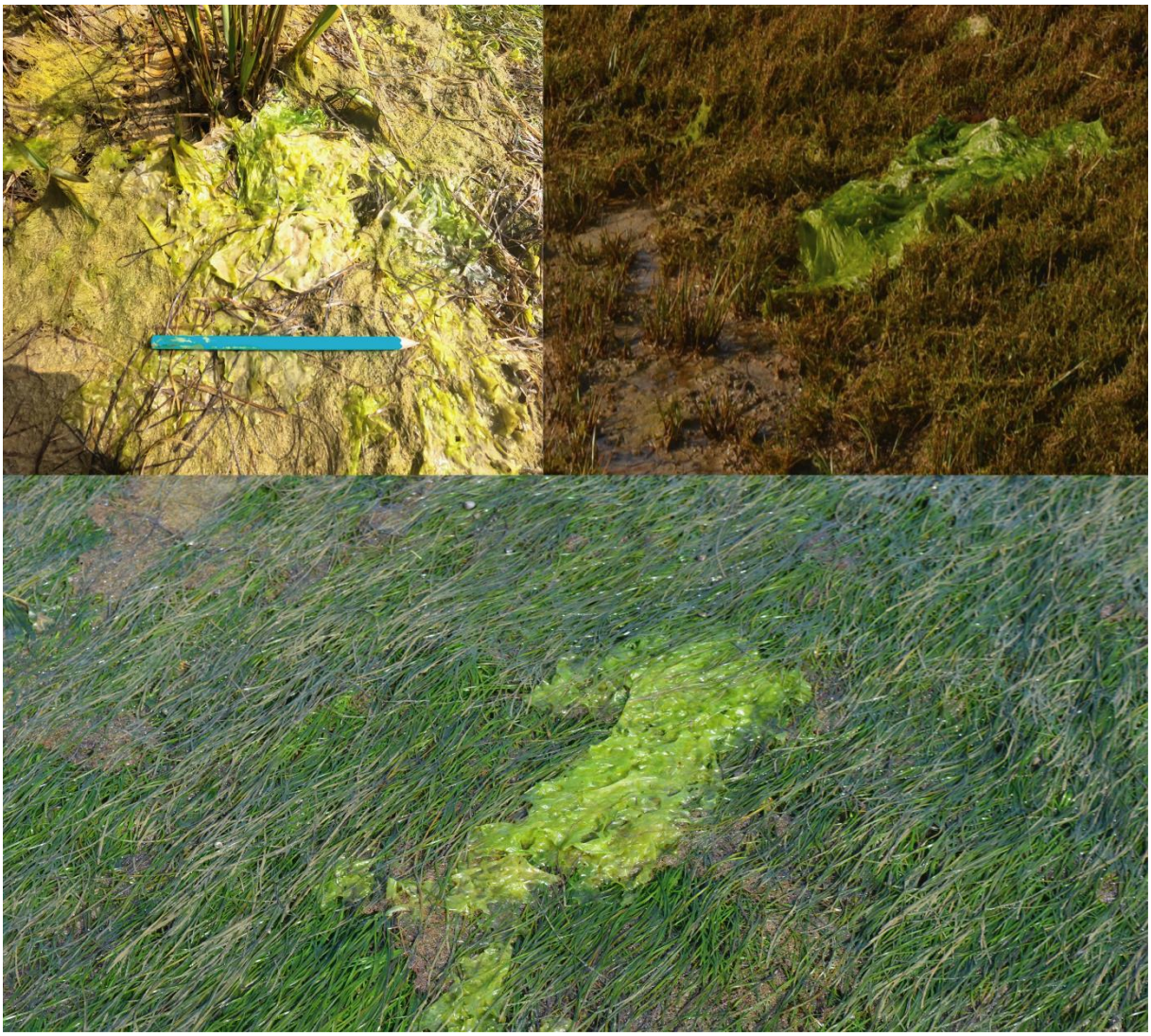

Figure 33: Ulva species, (A) taken on the low marsh on the 3rd of March, (B) taken on the high marsh on the 28th of February, and (C) taken on the tidal flat on the 3rd of March

Location: everywhere

Elevation (with respect to mean sea level): depends on the location

Plant characteristics: patch of green algae who are deposed by tides. As watching photos, it can be seen that this kind of algae can be found next to *Sarcocornia fructicosa*, *Spartina maritima,* and *Zostera noltei,* who characterized three different environments. They are light with a thickness less than 1mm. They can measure 10 to 15 cm. They are usually fix on rocks, but they can be ripped out of their substrate. They do not live to long, only a few months,

but several blooms occur during the year, due to generation who succeed each other.

Familly: Ulvacea

Species n°9: *Spartina maritima*

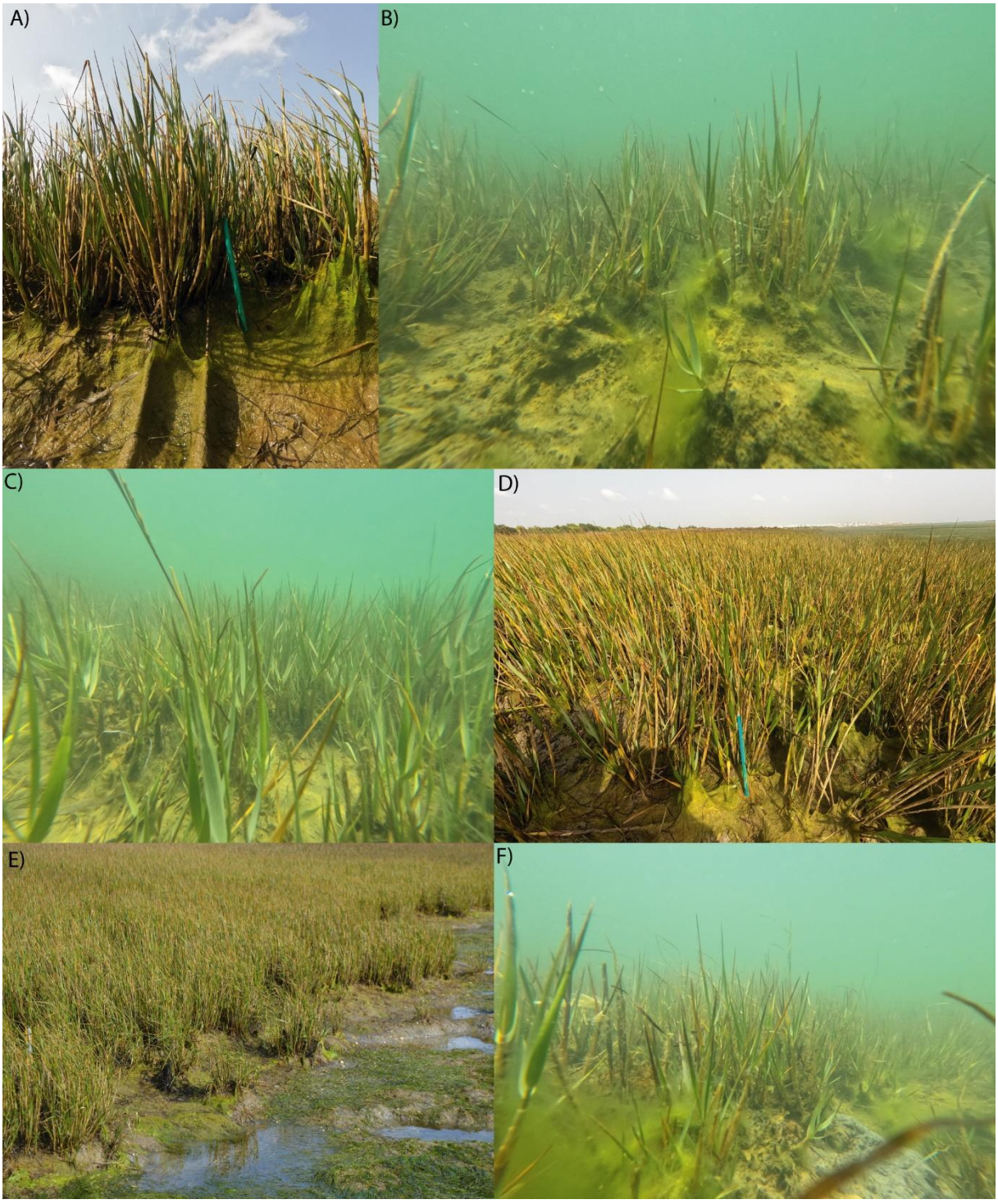

Figure 34: Spartina maritima, (A) and (D) taken on the 3rd of March, (B) (C) and (F) on the 23rd of April and (E) on the 28th of February

Location: low marsh

Elevation (with respect to mean sea level) : 0 to 0.70 m

Plant characteristics : green grass with a cylindrical stem at the base of the plant, and have several leaves who start around 20 cm of high. Plants make around 45 cm of high. Leaves have an elongated shape. Their stems are not flexible, but their leaves can follow the water movements. This species serve as pioneer species for the other plants. Thanks to their location, they are they are the pionner species (Costa et al., 1996).

Familly: Poaceae

Species n°10: *Zostera Noltei*

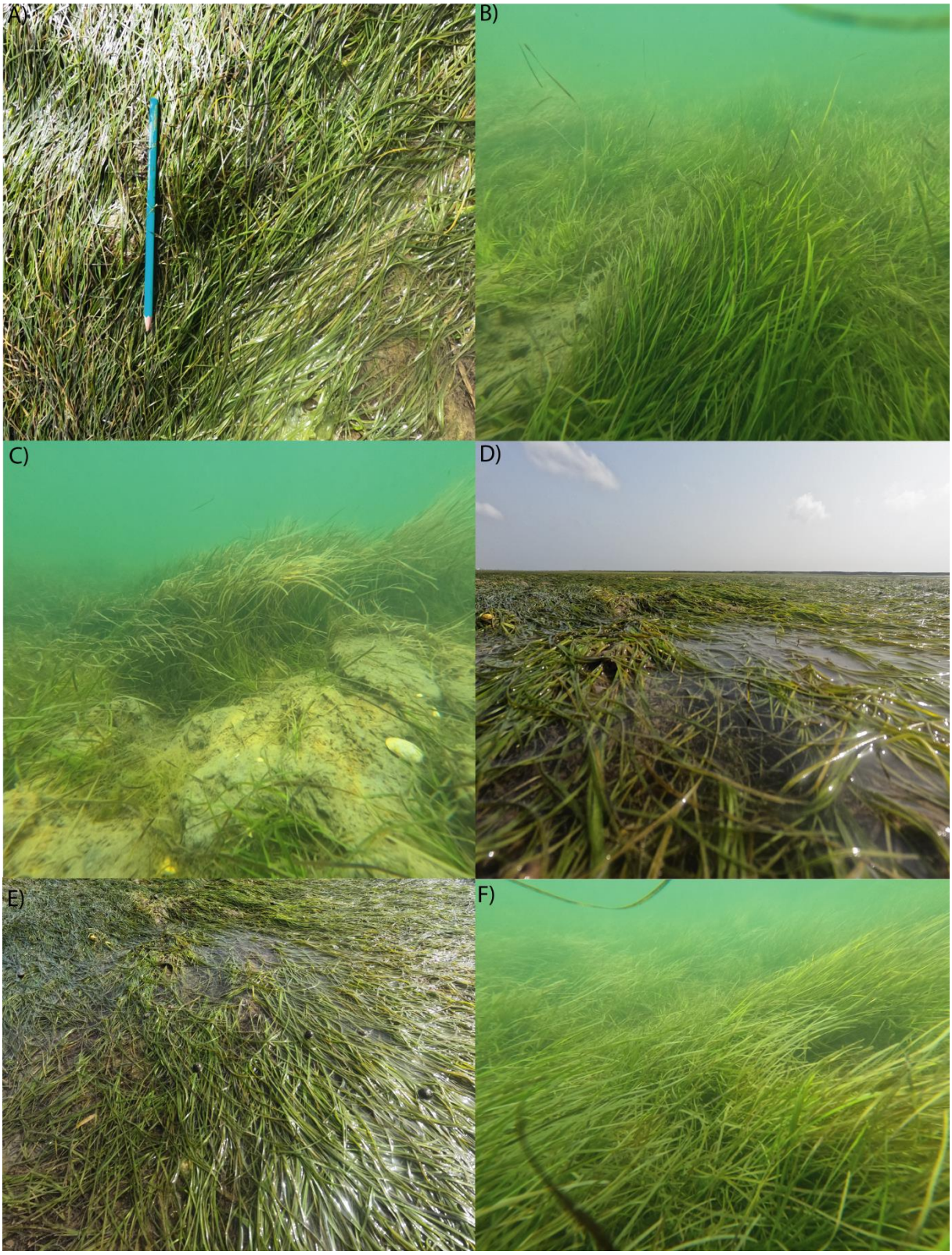

Figure 35: Zostera noltei, (A) (D) and (E) on the 3rd of March, and (B) (C) and (D) on the 23rd of April.

Location: Tidal flat

Elevation (with respect to mean sea level): below 0 m

Plant characteristics: seagrass long and narrow, who cover the entire tidal flat. They are green and don’t have shades. They are long as 30 cm. They are the flexiest plants presented in this thesis. As they are located on the tidal flat, they have the longest hydroperiod of all plants presented before. They grow in the subtidal zone. They cover a large area and are an underwater meadow.

Familly: Zosteraceae

Appendix 2

Table 5: Tidal range table for the January, February and March of the year 2021 at Faro

HORAS DO FUSO 0 (TU) — **2021**

JANEIRO

	Hora		Altura		Hora		Altura
	h	m	m		h	m	m
1 SEX	03	47	3.3	16 SÁB	04	36	3.4
	09	44	0.7		10	34	0.7
	16	07	3.1		16	55	3.0
	21	51	0.8		22	39	0.8
2 SÁB	04	27	3.3	17 DOM	05	15	3.3
	10	24	0.7		11	12	0.8
	16	48	3.0		17	34	2.9
	22	32	0.8		23	17	1.0
3 DOM	05	09	3.2	18 SEG	05	54	3.1
	11	08	0.8		11	50	1.0
	17	33	3.0		18	14	2.8
	23	17	0.9		23	56	1.1
4 SEG	05	55	3.2	19 TER	06	35	2.9
	11	56	0.9		12	32	1.2
	18	24	2.9		18	59	2.7
5 TER	00	08	1.0	20 QUA	00	42	1.3
	06	47	3.1		07	21	2.8
	12	50	1.0		13	20	1.3
	19	22	2.8		19	52	2.6
6 QUA	01	07	1.1	21 QUI	01	38	1.4
	07	47	3.0		08	18	2.6
	13	53	1.0		14	21	1.4
	20	27	2.8		20	59	2.5
7 QUI	02	16	1.2	22 SEX	02	54	1.5
	08	56	2.9		09	27	2.5
	15	04	1.1		15	37	1.5
	21	38	2.8		22	11	2.5
8 SEX	03	33	1.2	23 SÁB	04	20	1.5
	10	07	2.9		10	38	2.5
	16	17	1.0		16	48	1.4
	22	45	2.9		23	15	2.6
9 SÁB	04	48	1.1	24 DOM	05	27	1.4
	11	14	3.0		11	38	2.6
	17	21	1.0		17	42	1.3
	23	46	3.0				
10 DOM	05	52	0.9	25 SEG	00	08	2.8
	12	15	3.1		06	18	1.2
	18	18	0.9		12	29	2.7
					18	27	1.2
11 SEG	00	43	3.2	26 TER	00	53	2.9
	06	50	0.8		07	00	1.1
	13	11	3.2		13	13	2.9
	19	10	0.8		19	07	1.0
12 TER	01	35	3.3	27 QUA	01	35	3.1
	07	42	0.6		07	39	0.9
	14	03	3.2		13	54	3.0
	19	58	0.7		19	45	0.9
13 QUA	02	25	3.4	28 QUI	02	15	3.2
	08	30	0.6		08	16	0.8
	14	51	3.2		14	34	3.1
	20	42	0.7		20	23	0.7
14 QUI	03	11	3.5	29 SEX	02	54	3.4
	09	14	0.5		08	53	0.6
	15	35	3.2		15	13	3.2
	21	23	0.7		21	01	0.6
15 SEX	03	55	3.5	30 SÁB	03	33	3.5
	09	56	0.6		09	31	0.5
	16	16	3.1		15	53	3.2
	22	02	0.7		21	39	0.6
				31 DOM	04	13	3.5
					10	09	0.5
					16	34	3.3
					22	19	0.6

FEVEREIRO

	Hora		Altura		Hora		Altura
	h	m	m		h	m	m
1 SEG	04	54	3.5	16 TER	05	18	3.2
	10	50	0.5		11	09	0.9
	17	16	3.2		17	33	2.9
	23	01	0.7		23	17	1.0
2 TER	05	37	3.4	17 QUA	05	51	3.0
	11	33	0.6		11	42	1.0
	18	02	3.1		18	08	2.8
	23	47	0.8		23	54	1.1
3 QUA	06	24	3.2	18 QUI	06	27	2.8
	12	21	0.8		12	19	1.2
	18	52	3.0		18	49	2.7
4 QUI	00	38	1.0	19 SEX	00	39	1.3
	07	18	3.1		07	12	2.6
	13	16	1.0		13	07	1.4
	19	51	2.8		19	45	2.5
5 SEX	01	41	1.1	20 SÁB	01	40	1.5
	08	23	2.9		08	18	2.5
	14	24	1.2		14	15	1.5
	21	02	2.8		21	06	2.5
6 SÁB	03	01	1.2	21 DOM	03	15	1.6
	09	42	2.8		09	46	2.4
	15	48	1.2		15	51	1.5
	22	21	2.8		22	30	2.5
7 DOM	04	34	1.2	22 SEG	04	53	1.5
	11	01	2.8		11	05	2.5
	17	09	1.2		17	10	1.5
	23	33	2.9		23	36	2.7
8 SEG	05	50	1.0	23 TER	05	55	1.3
	12	09	2.9		12	04	2.7
	18	13	1.1		18	04	1.3
9 TER	00	35	3.1	24 QUA	00	28	2.9
	06	49	0.9		06	40	1.1
	13	07	3.0		12	51	2.8
	19	05	0.9		18	47	1.1
10 QUA	01	29	3.3	25 QUI	01	12	3.1
	07	39	0.7		07	19	0.9
	13	56	3.1		13	34	3.0
	19	50	0.8		19	27	0.8
11 QUI	02	15	3.4	26 SEX	01	54	3.3
	08	22	0.6		07	57	0.6
	14	38	3.2		14	14	3.2
	20	30	0.7		20	06	0.6
12 SEX	02	57	3.5	27 SÁB	02	34	3.5
	09	00	0.6		08	34	0.5
	15	17	3.2		14	54	3.4
	21	07	0.6		20	44	0.5
13 SÁB	03	36	3.5	28 DOM	03	14	3.6
	09	35	0.6		09	11	0.3
	15	53	3.2		15	34	3.5
	21	41	0.6		21	22	0.4
14 DOM	04	11	3.4				
	10	07	0.6				
	16	27	3.1				
	22	13	0.7				
15 SEG	04	45	3.3				
	10	38	0.7				
	17	00	3.0				
	22	44	0.8				

MARÇO

	Hora		Altura		Hora		Altura
	h	m	m		h	m	m
1 SEG	03	54	3.7	16 TER	04	14	3.3
	09	49	0.3		10	03	0.7
	16	14	3.5		16	27	3.2
	22	01	0.4		22	13	0.8
2 TER	04	35	3.6	17 QUA	04	44	3.2
	10	28	0.4		10	31	0.8
	16	55	3.4		16	57	3.0
	22	42	0.5		22	44	0.9
3 QUA	05	17	3.5	18 QUI	05	13	3.0
	11	08	0.5		11	00	1.0
	17	39	3.3		17	28	2.9
	23	25	0.6		23	17	1.1
4 QUI	06	03	3.3	19 SEX	05	45	2.8
	11	53	0.8		11	33	1.2
	18	26	3.1		18	03	2.8
					23	57	1.3
5 SEX	00	14	0.9	20 SÁB	06	24	2.6
	06	55	3.0		12	13	1.4
	12	45	1.0		18	48	2.6
	19	23	2.9				
6 SÁB	01	16	1.1	21 DOM	00	51	1.4
	08	01	2.8		07	20	2.5
	13	53	1.3		13	11	1.5
	20	37	2.8		20	00	2.5
7 DOM	02	45	1.3	22 SEG	02	17	1.6
	09	27	2.6		08	54	2.4
	15	33	1.4		14	48	1.6
	22	06	2.7		21	40	2.5
8 SEG	04	35	1.3	23 TER	04	13	1.5
	10	58	2.7		10	29	2.4
	17	06	1.3		16	33	1.5
	23	26	2.8		22	59	2.6
9 TER	05	50	1.1	24 QUA	05	23	1.3
	12	08	2.8		11	35	2.6
	18	08	1.2		17	35	1.3
					23	56	2.9
10 QUA	00	28	3.0	25 QUI	06	10	1.1
	06	43	0.9		12	24	2.9
	13	00	2.9		18	21	1.0
	18	56	1.0				
11 QUI	01	17	3.2	26 SEX	00	43	3.1
	07	26	0.8		06	51	0.8
	13	42	3.1		13	08	3.1
	19	36	0.8		19	03	0.8
12 SEX	01	59	3.3	27 SÁB	01	27	3.3
	08	03	0.6		07	30	0.6
	14	19	3.2		13	49	3.3
	20	11	0.7		19	43	0.6
13 SÁB	02	36	3.4	28 DOM	02	09	3.5
	08	36	0.6		08	09	0.3
	14	53	3.2		14	30	3.5
	20	44	0.6		20	22	0.4
14 DOM	03	11	3.4	29 SEG	02	50	3.7
	09	07	0.6		08	47	0.2
	15	25	3.2		15	11	3.6
	21	15	0.6		21	01	0.3
15 SEG	03	43	3.4	30 TER	03	32	3.7
	09	36	0.6		09	25	0.2
	15	57	3.2		15	52	3.6
	21	44	0.7		21	41	0.3
				31 QUA	04	14	3.7
					10	04	0.3
					16	34	3.5
					22	22	0.4

Table 6: Tidal range table for April, May, and July of the year 2021 at Faro

HORAS DO FUSO 0 (TU) **2021**

ABRIL						MAIO						JUNHO					
	Hora		Altura		Hora		Altura		Hora		Altura		Hora		Altura		Hora		Altura
	h	m	m		h	m	m		h	m	m		h	m	m		h	m	m
1 QUI	04	57	3.5	16 SEX	04	43	3.0	1 SÁB	05	32	3.1	16 DOM	04	57	2.8	1 TER	00	48	1.0	16 QUA	06	19	2.7
	10	45	0.5		10	27	1.0		11	13	0.9		10	38	1.1		07	18	2.7		12	02	1.2
	17	18	3.3		16	58	3.0		17	54	3.2		17	15	2.9		13	00	1.3		18	42	2.9
	23	07	0.6		22	50	1.0		23	50	0.9		23	15	1.1		19	42	2.9				
2 SEX	05	45	3.2	17 SÁB	05	16	2.8	2 DOM	06	30	2.9	17 SEG	05	39	2.7	2 QUA	02	00	1.2	17 QUI	00	50	1.1
	11	30	0.8		10	59	1.1		12	08	1.2		11	21	1.2		08	24	2.6		07	19	2.7
	18	06	3.1		17	32	2.8		18	55	3.0		18	00	2.8		14	14	1.4		13	04	1.3
	23	58	0.9		23	30	1.2										20	48	2.8		19	43	2.9
3 SÁB	06	40	3.0	18 DOM	05	54	2.6	3 SEG	01	03	1.1	18 TER	00	08	1.2	3 QUI	03	11	1.2	18 SEX	01	54	1.1
	12	22	1.1		11	39	1.3		07	39	2.7		06	33	2.6		09	34	2.6		08	26	2.7
	19	06	2.9		18	15	2.7		13	24	1.4		12	16	1.4		15	30	1.4		14	14	1.3
									20	07	2.8		19	00	2.7		21	55	2.8		20	50	2.9
4 DOM	01	05	1.1	19 SEG	00	23	1.4	4 TER	02	36	1.2	19 QUA	01	16	1.3	4 SEX	04	15	1.2	19 SÁB	03	03	1.1
	07	50	2.7		06	48	2.5		09	02	2.5		07	46	2.5		10	37	2.7		09	34	2.8
	13	35	1.4		12	34	1.5		15	01	1.5		13	31	1.5		16	34	1.3		15	27	1.2
	20	22	2.8		19	20	2.6		21	28	2.8		20	15	2.7		22	54	2.8		21	57	2.9
5 SEG	02	47	1.3	20 TER	01	41	1.5	5 QUA	04	01	1.2	20 QUI	02	37	1.3	5 SÁB	05	07	1.2	20 DOM	04	09	1.0
	09	20	2.6		08	14	2.4		10	24	2.6		09	07	2.5		11	27	2.8		10	36	2.9
	15	26	1.5		14	02	1.6		16	21	1.4		14	58	1.4		17	26	1.2		16	34	1.1
	21	52	2.7		20	53	2.6		22	42	2.8		21	32	2.8		23	43	2.9		23	00	3.0
6 TER	04	29	1.2	21 QUA	03	24	1.4	6 QUI	05	04	1.1	21 SEX	03	51	1.2	6 DOM	05	50	1.1	21 SEG	05	08	0.9
	10	52	2.6		09	49	2.5		11	25	2.7		10	17	2.7		12	10	2.9		11	33	3.1
	16	53	1.4		15	46	1.5		17	19	1.3		16	12	1.3		18	10	1.1		17	34	0.9
	23	12	2.8		22	16	2.7		23	38	2.9		22	38	2.9						23	57	3.2
7 QUA	05	36	1.1	22 QUI	04	40	1.2	7 SEX	05	51	1.0	22 SÁB	04	51	1.0	7 SEG	00	25	2.9	22 TER	06	02	0.7
	11	56	2.8		10	59	2.7		12	09	2.8		11	14	2.9		06	28	1.0		12	26	3.2
	17	51	1.2		16	57	1.3		18	04	1.1		17	11	1.0		12	49	3.0		18	28	0.7
					23	19	2.9						23	33	3.1		18	49	1.0				
8 QUI	00	10	3.0	23 SEX	05	33	1.0	8 SÁB	00	22	3.0	23 DOM	05	42	0.8	8 TER	01	05	3.0	23 QUA	00	52	3.3
	06	24	0.9		11	51	2.9		06	29	0.9		12	04	3.1		07	03	1.0		06	53	0.6
	12	41	2.9		17	48	1.0		12	46	3.0		18	02	0.8		13	27	3.0		13	18	3.3
	18	35	1.0						18	43	1.0						19	25	1.0		19	21	0.6
9 SEX	00	55	3.1	24 SÁB	00	09	3.1	9 DOM	01	01	3.1	24 SEG	00	24	3.3	9 QUA	01	43	3.0	24 QUI	01	45	3.3
	07	02	0.8		06	18	0.8		07	03	0.9		06	29	0.6		07	36	0.9		07	42	0.6
	13	18	3.0		12	37	3.1		13	21	3.1		12	52	3.3		14	03	3.1		14	10	3.5
	19	12	0.9		18	33	0.8		19	17	0.9		18	50	0.6		20	00	0.9		20	12	0.5
10 SÁB	01	33	3.2	25 DOM	00	55	3.3	10 SEG	01	37	3.1	25 TER	01	13	3.4	10 QUI	02	20	3.0	25 SEX	02	38	3.3
	07	36	0.7		07	00	0.5		07	35	0.8		07	14	0.4		08	07	0.9		08	30	0.6
	13	52	3.1		13	21	3.3		13	55	3.2		13	39	3.5		14	39	3.1		15	00	3.5
	19	46	0.8		19	16	0.5		19	50	0.8		19	36	0.4		20	34	0.9		21	02	0.5
11 DOM	02	08	3.3	26 SEG	01	40	3.5	11 TER	02	11	3.1	26 QUA	02	02	3.5	11 SEX	02	56	3.0	26 SÁB	03	28	3.3
	08	07	0.7		07	41	0.3		08	04	0.8		07	58	0.4		08	39	0.9		09	16	0.6
	14	25	3.2		14	04	3.5		14	29	3.2		14	26	3.5		15	14	3.2		15	50	3.5
	20	17	0.7		19	58	0.3		20	21	0.8		20	22	0.4		21	08	0.9		21	51	0.5
12 SEG	02	41	3.3	27 TER	02	25	3.6	12 QUA	02	45	3.1	27 QUI	02	51	3.5	12 SÁB	03	31	3.0	27 DOM	04	17	3.2
	08	36	0.7		08	21	0.2		08	33	0.8		08	43	0.4		09	12	0.9		10	02	0.7
	14	57	3.2		14	47	3.6		15	01	3.2		15	13	3.5		15	49	3.1		16	38	3.4
	20	47	0.7		20	40	0.3		20	52	0.8		21	09	0.4		21	44	0.9		22	39	0.6
13 TER	03	13	3.3	28 QUA	03	09	3.7	13 QUI	03	17	3.1	28 SEX	03	39	3.4	13 DOM	04	07	2.9	28 SEG	05	05	3.1
	09	03	0.7		09	02	0.3		09	01	0.8		09	27	0.5		09	48	1.0		10	47	0.9
	15	28	3.2		15	31	3.6		15	33	3.2		16	01	3.5		16	25	3.1		17	26	3.3
	21	16	0.7		21	22	0.3		21	23	0.8		21	57	0.5		22	22	0.9		23	27	0.8
14 QUA	03	44	3.2	29 QUI	03	55	3.6	14 SEX	03	49	3.0	29 SÁB	04	29	3.3	14 SEG	04	46	2.8	29 TER	05	53	2.9
	09	30	0.8		09	43	0.4		09	31	0.9		10	13	0.7		10	27	1.0		11	34	1.0
	15	58	3.2		16	15	3.5		16	05	3.1		16	51	3.4		17	05	3.0		18	15	3.2
	21	46	0.8		22	07	0.4		21	56	0.9		22	48	0.6		23	05	1.0				
15 QUI	04	14	3.1	30 SEX	04	41	3.4	15 SÁB	04	22	2.9	30 DOM	05	21	3.1	15 TER	05	29	2.8	30 QUA	00	16	1.0
	09	58	0.9		10	26	0.6		10	03	1.0		11	01	0.9		11	11	1.1		06	43	2.8
	16	28	3.1		17	02	3.4		16	38	3.0		17	43	3.2		17	50	3.0		12	24	1.2
	22	16	0.9		22	55	0.6		22	33	1.0		23	44	0.9		23	53	1.1		19	05	3.0
												31 SEG	06	17	2.9								
													11	56	1.1								
													18	40	3.1								

Appendix 3

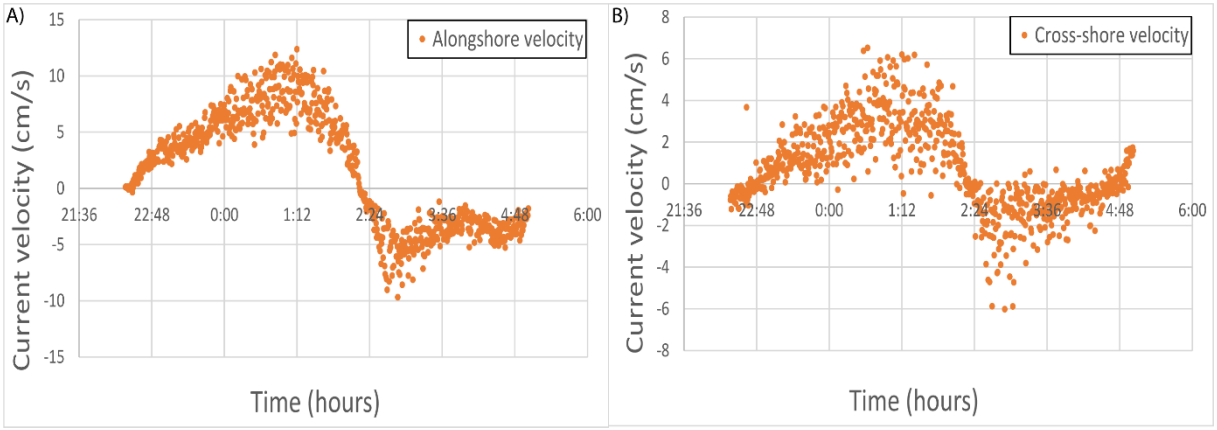

Figure 36: Alongshore velocity recorded (A) and cross-shore velocity recorded, during the Neap tide (NT) at TF2

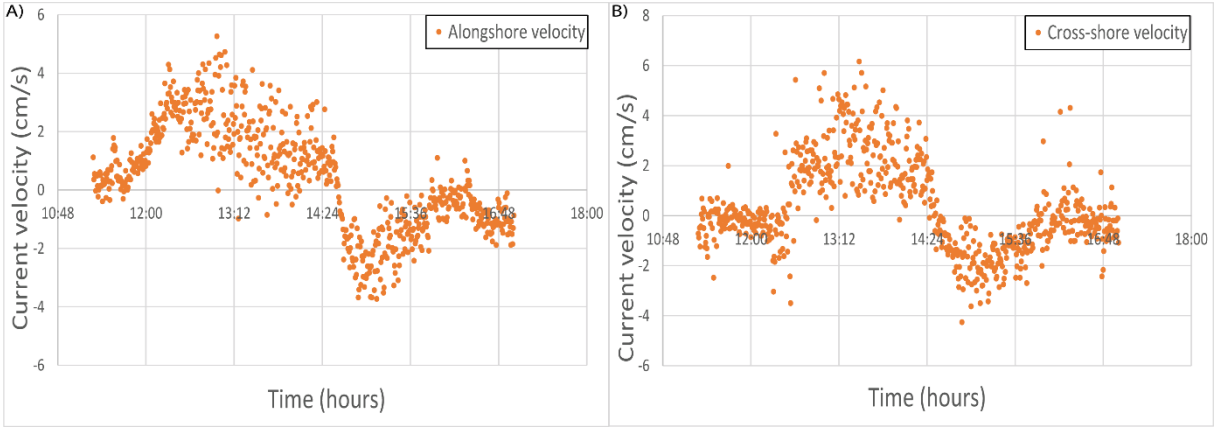

Figure 37: Alongshore velocity recorded (A) and cross-shore velocity recorded, during the Neap tide (NT) at LM

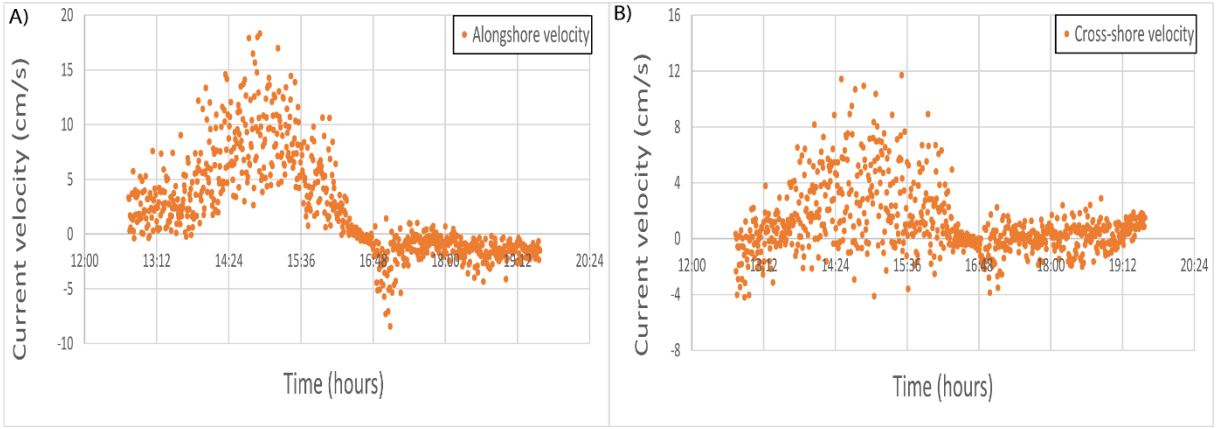

Figure 38: Alongshore velocity recorded (A) and cross-shore velocity recorded, during the Spring Tide (ST) at TF2

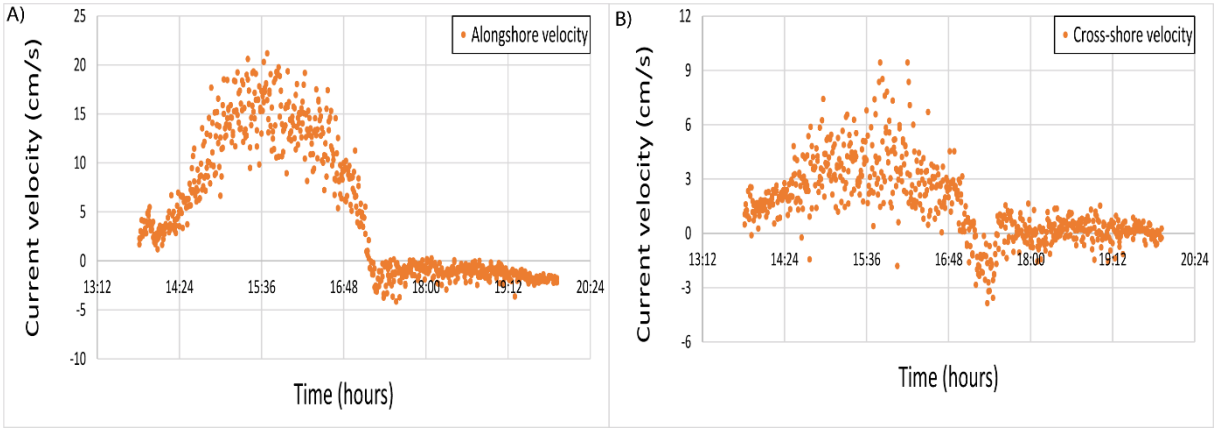

Figure 39: Alongshore velocity recorded (A) and cross-shore velocity recorded, during the Spring Tide (ST) at LM

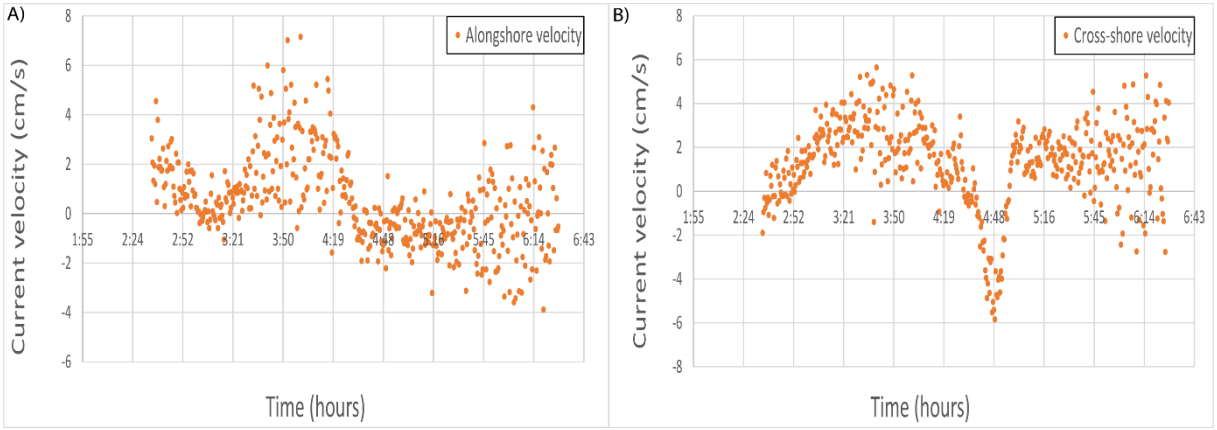

Figure 40: Alongshore velocity recorded (A) and cross-shore velocity recorded, during the Spring Tide (ST) at HM

Appendix 4

Table 7: Comparison of suspended sediment concentrations from other studies

Authors	Location	Suspended Sediment Concentration (SSC; mg/l)	Details/observations
MSc Anicet	Ria Formosa, Portugal	Low marsh SSC=24.56 g/ml SSC=12.09 mg/l	Spring tide conditions (28th of February) Intake: first on at 0.40 m and second one at 1.25 m Vegetation: *Spartina maritima*
MSc Anicet	Ria Formosa, Portugal	High marsh SSC=14.19 mg/l	Spring tide conditions (28th of February) Intake: 1.25 m Vegetation: *Sarcocornia sp.*
MSc Anicet	Ria Formosa, Portugal	Low marsh SSC=12.32 mg/l	Neap tide conditions (6th of June) Intake: 0.40 m Vegetation: *Spartina maritima*
(Christiansen et al., 2000)	Phillips creek, Hog Island Bay, USA	High marsh SSC=31 mg/l	suspended sediment concentration on the beginning of the tide results read on a graph Vegetation: *Spartina Alterniflora*
(Ganju et al., 2015)	Blackwater River, Chesapeake Bay, USA	Low marsh SSC=54mg/l	Mean SSC of the flood Vegetation: *Spartina patens* and *Schoenoplectus americanus*
(Ma et al., 2018)	Rattekaai marsh, Netherland	meanSSC= 576 ± 137 mg/l	MeanSSC is the SSC average for all stations of the transect Only spring tide condition Vegetation: *Spartina anglica, Halimione portulacoides, Elymus athericus* and *Puccinellia maritima*
(Ma et al., 2018)	Sint Annaland, Netherland	MeanSSC=34 ± 5 mg/l	MeanSSC is the SSC average for all stations of the transect

			Vegetation: *Halimione portulacoides, Elymus athericus* and *Festuca rubra*
(Moskalski & Sommerfield, 2012)	St. Jones River, Delawar, USA	Marsh surface SSC=10 mg/l to 1900 mg/l	SSC decreases from the water source Only spring tide condition Vegetation: *Spartina sp* and *Phragmites australis*
(Poirier et al., 2017)	Kingsport marsh, Minas Basin, Canada	Low marsh SSC=106±66 mg/l	Average of 62 tides (May 2012 to June 2013) Vegetation: *Spartina alterniflora*
(Poirier et al., 2017)	Kingsport marsh, Minas Basin, Canada	High marsh SSC=53±24 mg/l	Average of 62 tides (May 2012 to June 2013) Vegetation: *Spartina patens*
(Temmerman et al., 2003)	Paulina marsh, SW Netherlands	High marsh: SSC=50 mg/l	Sedimentation rates are summarized by neap/spring tidal cycle SSC measured between April 2000 and May 2001 Vegetation: *Puccinellia Towsendii, Aster Tripolium, Atriplex Portulacoides, Elytrigia Pungens*
(A. Wang, 2010)	Wanggang, China	High marsh: ASSC=340 mg/l	Average over the year Average Suspended Sediment Concentration (ASSC) Vegetation: *Suaeda salsa, Spartina angelica* and *Spartina alterniflora*

Appendix 5

Table 8: Comparison of deposition rates in other studies

Authors	Location	Deposition rate (DR; $g/m^2/h$)	Details/observations
Anicet Pétillon, 2021	Ria Formosa, Portugal	Low marsh DR=5.65 $g/m^2/h$	Neap tide conditions Vegetation: *Spartina maritima*
Anicet Pétillon, 2021	Ria Formosa, Portugal	Low marsh DR=21.52 $g/m^2/h$	Spring-tide conditions Vegetation: *Spartina maritima*
Anicet Pétillon, 2021	Ria Formosa, Portugal	High marsh DR=33.80 $g/m^2/h$	Spring-tide conditions Vegetation: *Sarcocornia sp*
Anicet Pétillon, 2021	Ria Formosa, Portugal	Low marsh DR=17.25 $g/m^2/h$	Spring-tide conditions Vegetation: *Spartina maritima*
Anicet Pétillon, 2021	Ria Formosa, Portugal	High marsh DR=35.45 $g/m^2/h$	Spring-tide conditions Vegetation: *Sarcocornia sp*
Anicet Pétillon, 2021	Ria Formosa, Portugal	Low marsh DR=25.45 $g/m^2/h$	Neap tide conditions Vegetation: *Spartina maritima*
(Ma et al., 2018)	Rattekaai marsh, Netherland	Low marsh DR=53.04±11.5 $g/m^2/h$	Only spring tide condition Vegetation: *Spartina anglica, Halimione portulacoides, Elymus athericus* and *Puccinellia maritima*
(Ma et al., 2018)	Rattekaai marsh, Netherland	High marsh : DR=31.38±8.75 $g/m^2/h$	Only spring tide condition Vegetation: *Spartina anglica, Halimione portulacoides, Elymus athericus* and *Puccinellia maritima*
(Ma et al., 2018)	Sint Annaland, Netherland	Low marsh : DR=21.42±6.54 $g/m^2/h$	Only spring tide condition Vegetation: *Halimione portulacoides, Elymus*

			athericus and *Festuca rubra*
(Ma et al., 2018)	Sint Annaland, Netherland	High marsh DR=7.29±17.54 g/m^2/h	Only spring tide condition Vegetation: *Halimione portulacoides, Elymus athericus* and *Festuca rubra*
(Moskalski & Sommerfield, 2012)	St. Jones River, Delawar, USA	Low marsh: DR=22.33 g/m^2/h	Spring tide condition Average calculated thanks to the table 1 of the Moskalski & Sommerfield's study
(Moskalski & Sommerfield, 2012)	St. Jones River, Delawar, USA	High marsh: DR=3.65 g/m^2/h	Spring tide condition Average calculated thanks to the table 1 of the Moskalski & Sommerfield's study
(Poirier et al., 2017)	Kingsport marsh, Minas Basin, Canada	Low marsh DR=30.9±17.7 g/m^2/tide	Average of 62 tides (May 2012 to June 2013) Vegetation Low marsh: *Spartina alterniflora*
(Poirier et al., 2017)	Kingsport marsh, Minas Basin, Canada	High marsh edge DR=15.5±5.9 g/m^2/tide	Average of 62 tides (May 2012 to June 2013) Vegetation Marsh edge: *Spartina patens*
(Poirier et al., 2017)	Kingsport marsh, Minas Basin, Canada	High marsh DR=15.3±6.1 g/m^2/tide	Average of 62 tides (May 2012 to June 2013) Vegetation Marsh surface: *Spartina patens*